



Effect of internal leaf structures on gas exchange of leaves

Roland Pieruschka



Forschungszentrum Jülich GmbH
Institut für Chemie und Dynamik der Geosphäre III: Phytosphäre

Effect of internal leaf structures on gas exchange of leaves

Roland Pieruschka

Schriften des Forschungszentrums Jülich
Reihe Umwelt/Environment

Band/Volume 56

ISSN 1433-5530 ISBN 3-89336-403-X

Bibliographic information published by Die Deutsche Bibliothek.
Die Deutsche Bibliothek lists this publication in the Deutsche
Nationalbibliografie; detailed bibliographic data are available in the
Internet <<http://dnb.ddb.de>>.

Publisher and
Distributor: Forschungszentrum Jülich GmbH
Zentralbibliothek
52425 Jülich
Phone +49 (0)2461 61-5368 · Fax +49 (0)2461 61-6103
e-mail: zb-publikation@fz-juelich.de
Internet: <http://www.fz-juelich.de/zb>

Cover Design: Grafische Medien, Forschungszentrum Jülich GmbH

Printer: Grafische Medien, Forschungszentrum Jülich GmbH

Copyright: Forschungszentrum Jülich 2005

Printed on environmentally friendly paper.

Schriften des Forschungszentrums Jülich
Reihe Umwelt/Environment Band/Volume 56

D 61 (Diss., Düsseldorf, Univ., 2005)

ISSN 1433-5530
ISBN 3-89336-403-X

Neither this book nor any part of it may be reproduced or transmitted in any form or by any means, electronic or mechanical, including photocopying, microfilming, and recording, or by any information storage and retrieval system, without permission in writing from the publisher.

Acknowledgment

Without direct and indirect involvement of the following persons, this dissertation would have not been made possible. I would like therefore to convey my sincere gratitude and thankfulness to:

My advisor, Professor Dr. Ulrich Schurr, for giving me the chance of being involved in plant research at the Institute Phytosphere (ICG III), Research Centre Jülich, for his continuous support, encouragement, and expertise. PD Dr. Dirk Gansert, for being on my committee and for reading this thesis.

Dr. Siegfried Jahnke deserves some very special thanks. He has accompanied my scientific development since my first steps during the study and conveyed to me the joy of plant science through his own enthusiasm.

Colleagues from Phytosphere Institute (ICG III): Andrés (for great mathematical support), Maja, Frank, Ingar, Shizue (for valuable discussions), Andreas, Bernd, Peter, Kerstin, vandy, Uwe, Roland, Gerhard, Hanno, Beate (for having green fingers), Achim, Wilfried. Many thanks go to the tabletop soccer-team for creative diversion from work.

Prof. Dr. Guido-Benno Feige, Dr. Herfried Kutzelnigg, Prof. Dr. Nosratollah Ale-Agha, Dr. Manfred Jensen, Kerstin, Imke, Michael, Freddy from University Duisburg-Essen where a large part of the work was performed. I appreciated the good working atmosphere and valuable discussions.

Bernd, Institut für Laser- und Plasmaphysik, University Duisburg-Essen for automation of the gas exchange system.

A great thank goes to my parents and family for inestimable support.

Düsseldorf 2005

Contents

Abstract	5
Zusammenfassung	6
Chapter 1 Introduction.....	7
Chapter 2 Materials and methods	13
2.1 Plant material.....	13
2.2 Growth conditions	14
2.3 Gas exchange measurements	15
2.3.1 Gas exchange system.....	15
2.3.2 Leaf chambers.....	17
2.3.3 Automation of the gas exchange system	18
2.3.4 Calculations and control measurements	19
2.4 Measurement of lateral diffusion inside leaves.....	19
2.4.1 Experimental protocol	19
2.4.2 Calculation of lateral gas conductance and conductivity	20
2.4.3 Data analysis.....	22
2.5 Dark respiration measurement	22
2.6 Gas exchange measurement in light	23
2.6.1 Analysis of CO ₂ response curves	24
2.6.2 Shading of the leaf part outside the leaf chamber	25
2.7 Gas exchange measurements under overpressure.....	25
2.7.1 Influence of air pressure on gas diffusion – theoretical considerations	27
2.8 Photosynthesis of partly shaded leaves.....	28
2.8.1 Measurement of chlorophyll fluorescence	28
2.8.1.1 Experimental conditions	29
2.8.1.2 Experimental protocol	29
2.8.2 Combined measurements of chlorophyll fluorescence and gas exchange	30
2.8.2.1 The experimental protocol.....	30
2.8.2.2 Data analysis.....	31
2.8.2.3 Estimation of measurement errors.....	33

Chapter 3 Results..... 35

3.1	Diffusion inside leaves	35
3.1.1	Biometric parameters of the investigated leaves.....	35
3.1.2	Gas conductance and conductivity of the intercellular air space	36
3.1.3	Summary of diffusion inside leaves	40
3.2	Influence of lateral diffusion on gas exchange measurement.....	40
3.2.1	Measurement of dark respiration.....	40
3.2.2	Measurement of photosynthesis.....	42
3.2.3	Shading of the leaf part outside the leaf chamber	46
3.2.4	Summary of the impact of lateral diffusion on gas exchange measurements	48
3.3	Gas exchange measurement under overpressure in the leaf chamber	49
3.3.1	Measurement of dark respiration.....	49
3.3.2	Photosynthetic gas exchange under overpressure	51
3.3.3	Transpiration and overpressure	54
3.3.4	Summary of the impact of overpressure on gas exchange measurement.....	55
3.4	Chlorophyll fluorescence of partly shaded leaves	56
3.4.1	Well watered plants.....	56
3.4.2	Plants under drought stress.....	58
3.4.3	Quantification of the effect of lateral diffusion on photochemical and non-photochemical quenching.....	60
3.4.4	Re-watering of drought stressed plants	61
3.4.5	Summary of chlorophyll fluorescence of partly shaded leaves.....	62
3.5	Photosynthesis of leaves illuminated with lightflecks	63
3.5.1	Experiments with <i>Vicia faba</i>	64
3.5.2	Experiments with <i>Glycine max</i>	70
3.5.3	Summary of photosynthesis of leaves illuminated with lightflecks.....	76

Chapter 4 Discussion 79

4.1	Carbon fluxes in and out of leaves.....	79
4.1.1	Influence of elevated CO ₂ on respiration – direct effect.....	79
4.1.2	Measurement artefacts.....	80
4.1.3	Gas conductance and conductivity in lateral and vertical direction.....	80
4.1.4	Gas fluxes in lateral direction.....	81
4.2	Influence of lateral diffusion on gas exchange measurement.....	82
4.2.1	Screening for species with different leaf anatomy	83
4.2.2	Influence of lateral diffusion on gas exchange in light	84
4.2.2.1	Lateral gradients within homobaric leaves caused by shading	86
4.3	Gas exchange measurement and overpressure.....	87
4.3.1	CO ₂ exchange under overpressure in homobaric leaves	88
4.3.2	Impact of air pressure on transpiration.....	89

4.4	Influence of leaf anatomy on gas exchange measurement - conclusion.....	90
4.5	Visualisation of lateral CO₂ diffusion	92
4.5.1	Stomatal conductance and lateral flux of CO ₂ inside leaves	93
4.6	Lightflecks	94
4.6.1	Photosynthesis under drought stress.....	95
4.6.2	Reduction of drought stress symptoms by lateral CO ₂ diffusion	98
4.7	Impact of lateral diffusion on photosynthesis - conclusion.....	100
4.8	Ecology of plants with homobaric leaves.....	101
References		103
Abbreviations		113
Appendix		117
Geometrical correction of conductance and conductivity		117

Abstract

Gas exchange of leaves is generally considered as the interchange of gaseous compounds between the leaf interior and ambient air. Once inside the leaf, CO₂ can diffuse along its concentration gradients mainly regarded in the vertical direction of the blade towards the assimilating tissues. Lateral gas diffusion within intercellular air spaces may be much more effective than has been considered so far which depends on anatomical features of leaves. In heterobaric leaves, lateral diffusion is restricted by bundle-sheath extensions and the mesophyll is composed of closed compartments. Homobaric leaves, however, lack such extensions and the leaves have large interconnected intercellular air spaces. The specific internal gas diffusion properties of the leaves were characterized by gas conductivities. Gas conductivity was larger in lateral than in the vertical direction of homobaric leaf blades. However, there was a large variability of the size and property of the intercellular air space among different species. When 'clamp-on' leaf chambers were used it was found that lateral diffusion inside leaves seriously affected gas exchange measurements. The impact of lateral CO₂ diffusion on gas exchange measurement was substantial when exchange rates were low. Homobaric leaves showed internal lateral gas fluxes when an overpressure was applied to the leaf chamber which has been used in commercial gas exchange systems to minimise the effects of leaks in the leaf chamber. It was found here that overpressure affected CO₂ and H₂O exchange rates of homobaric leaves substantially larger than the theoretical direct impact of air pressure on gas exchange processes. Gas gradients inside leaves emerged when a leaf part was shaded and the adjacent area of the leaf blade illuminated. Respiratory CO₂ evolved in the shaded region diffused to the illuminated area where it was fixed by photosynthesis. These processes obviously increased the photosynthetic efficiency along the light/shade borderline as was visualized by chlorophyll fluorescence imaging techniques. The recycling of respiratory CO₂ from distant shaded areas was found to be larger when stomatal conductance was low as is the case under drought stress. Thus, when a homobaric leaf was illuminated by lightflecks, additional CO₂ increased the carbon gain, water use efficiency, and reduced light stress. It was hypothesized that homobaric leaf anatomy is a trait which has evolved under certain environmental conditions.

Zusammenfassung

Gaswechsel von Blättern wird im Allgemeinen als der Austausch von Gaskomponenten zwischen dem Blatt und der Atmosphäre betrachtet. CO₂ breitet sich im Blatt entlang des Gasgradienten zum photosynthetisch aktiven Gewebe aus, meistens in vertikaler Richtung. Allerdings kann auch laterale Gasdiffusion in Interzellularräumen in beträchtlichem Ausmaß auftreten, was von bestimmten anatomischen Blattmerkmalen abhängt. In heterobaren Blättern wird laterale Diffusion von Bündelscheiderweiterungen eingeschränkt und das Mesophyll besteht aus kleinen, geschlossenen Kompartimenten. Homobare Blätter weisen keine Bündelscheiderweiterungen auf und die Blätter haben große, verbundene Interzellularräume. Die Gasdiffusionseigenschaften des Blattmesophylls wurden durch spezifische Leitfähigkeit charakterisiert. In homobaren Blättern war die spezifische Gasleitfähigkeit größer in lateraler als in vertikaler Richtung. Eine große Variabilität in Bezug auf die Größe und die Eigenschaften des Interzellularraums wurde bei unterschiedlichen Spezies beobachtet. Wenn 'clamp-on' Blattkammern zur Gaswechsellmessung benutzt wurden, führte laterale Diffusion im Blattmesophyll zu starken Messartefakten, die sich auf die Messung kleiner CO₂-Austauschraten besonderes stark auswirkten. Die blattinterne Gaswegsamkeit führte auch zu lateralen Gasflüssen, wenn es einen Überdruck in der Blattkammer gab, was häufig dazu verwendet wird, Undichtigkeiten in der Blattkammer zu minimieren. In homobaren Blättern beeinflusste der Überdruck CO₂- und H₂O-Austauschprozesse stärker, als die theoretisch abgeleitete Auswirkung des Atmosphärendrucks auf Gasaustauschprozesse. Gasgradienten in Blättern entstehen auch, wenn ein Blattteil beschattet wird, während die angrenzende Blattfläche belichtet ist. Respiratorisches CO₂, das in der beschatteten Region gebildet wurde, diffundierte zu dem belichteten Flächen, wo es durch Photosyntheseprozesse fixiert wurde. Diese Prozesse erhöhten die Photosyntheseeffizienz entlang der Licht/Schatten-Grenze, was mit Hilfe von bildgebenden Chlorophyll-Fluoreszenz Messverfahren visualisiert wurde. Das 'Recycling' von respiratorischen CO₂ aus beschatteten Blattbereichen war größer, unter niedriger stomatärer Leitfähigkeit, wie z.B. unter Trockenstress. Wenn ein Blatt mit einem Lichtfleck belichtet wurde, dann führte zusätzliches CO₂ zur Erhöhung der Kohlenstoffaufnahme, des Wasserausnutzungskoeffizienten und zur Reduktion von Lichtstress. Eine Hypothese wurde aufgestellt, dass Anatomie homobarer Blätter sich unter bestimmten Umweltbedingungen entwickelte.

Chapter 1 Introduction

Plant functional traits are directly responsible for the acquisition of resources required for growth (light, water, nutrients, CO₂ etc.) and the regulation of conditions that influence metabolism (e.g. temperature, turgor pressure). Functional traits vary across a wide range of spatial and temporal scales among cells, leaves, shoots, individuals, populations, and ecosystems (Ackerly 2003). Leaves play the decisive role in photosynthetic CO₂ fixation, which is stored in organic compounds (Niklas 2000). Leaf anatomy influences net leaf photosynthesis to a large degree under variable environmental conditions (Bolhár-Nordenkamp & Draxler 1993). The substrates for photosynthesis, CO₂ and H₂O, have to be distributed throughout the leaf and CO₂ has to reach chloroplasts to be assimilated. CO₂ is mainly supplied by diffusion from the surrounding air through stomata. Intercellular openings, stomatal pores, formed by two kidney-shaped cells, the guard cells, control the gas fluxes from and into the leaf in order to optimise CO₂ uptake and to minimise water loss (Meidner & Mansfield 1968; Cowan 1977; Farquhar & Sharkey 1982). Extensive gas spaces beneath stomata and within leaves allow gas diffusion to the assimilating parenchyma. Another dominating structure of leaves are the leaf veins, which form a venation system in leaf lamina for sufficient water supply (Bolhár-Nordenkamp et al. 1993; Esau 1977). These veins called vascular bundles are generally surrounded by bundle sheaths, and in some leaves, bundle sheath extensions can be found ranging from the upper to the lower epidermis. Such leaves are named heterobaric (Fig. 1 a; page 8). Whereas leaves without these bundle sheath extensions are named homobaric (Fig. 1 b; page 8). Both terms, homo- and heterobaric, were introduced by Neger (1912; 1918). He performed infiltration experiments and found different infiltration patterns depending of the internal structure of the leaves. Heterobaric leaves showed distinct patches over the leaf blade after infiltration of water and Neger concluded that mesophyll tissue in the patches are isolated from each other and might be under different (heterobaric) pressure. Homobaric leaves, however, were uniformly infiltrated which indicated uniform (homobaric) pressure inside leaves due to large interconnected intercellular air space.

The different anatomic traits investigated by Neger were rarely mentioned in literature afterwards. Williams (1948) concluded that the leaf anatomy allows lateral fluxes over very large distances, which was observed with a double chamber porometer. Changes of the air

pressure in one of the porometer chamber had an influence on the air pressure measured in the other chamber even when the chambers were separated by major veins. Anatomical studies revealed that intercellular space systems of leaves may be connected with each other even across main veins (Williams 1948).

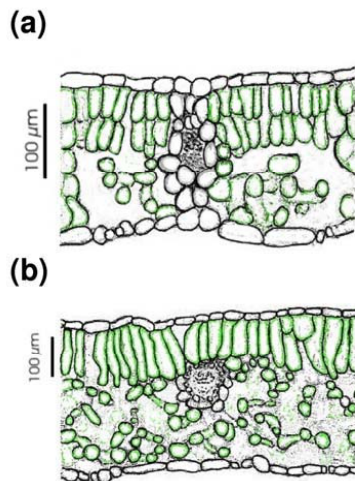


Figure 1. Drawing of a cross section (a) of a heterobaric leaf of *Glycine max* and (b) of a homobaric leaf of *Vicia faba*. The green cells show photosynthetic active mesophyll tissue and the white cells on the adaxial and abaxial leaf side demonstrate the epidermis. The grey area in the middle of the cross sections represents vascular tissue surrounded by vascular bundle and bundle sheath extension a in heterobaric leaf (a) whereas in a homobaric leaf no bundle sheath extension is present (b). Drawing after own microscopical cross-sections of leaves.

Wylie (1952) presented a survey on 348 plant species with respect to the occurrence of bundle sheath extensions. Approximately 40 % of the investigated species had homobaric leaves and most of the species were from subtropical regions while plants with heterobaric leaves were mostly from northern areas. A large variation among different species was found for plant growing under similar climatic conditions. In Mediterranean region some species showed leaves with extensions accompanying the veins throughout their length. In others the extensions showed different patterns of vascular bundles with or without bundle sheath extensions with varying distances between the bundles encircled by the extensions, while in some of them the extensions were completely absent (Esau 1969; Fahn 1982). Thus, an extremely variable interconnectivity of the intercellular air space in leaves was found for different species but also within one species in different developmental stages (Jahnke & Krewitt 2002).

Homobaric and heterobaric leaf anatomy was first associated with leaf physiology by Terashima et al. (1988; 1992). When stomatal closure was unevenly distributed across the

leaf surface in heterobaric leaves, mesophyll compartmentation resulted in patches of different intercellular CO₂ concentrations. Such patchiness was not found in homobaric leaves due to lateral gas diffusion. However, the regarded distances of gas movement were between neighbouring stomata. The response of stomatal density to elevated CO₂ was found to be different in variegated homobaric leaves from variegated heterobaric leaves (Beerling & Woodward 1995). It was speculated that leaf structure may play an important role in determining the magnitude of stomatal density. Küppers et al. (1999) found that cotyledons of *Fagus sylvatica* had homobaric leaves whereas primary and secondary leaves were heterobaric. They concluded that shade leaves tend to be more homobaric than sun leaves due to larger intercellular air spaces.

The homobaric leaf anatomy can also substantially influence gas exchange measurements. After careful characterisation of artefacts in gas exchange measurement (Jahnke 2001), lateral gas diffusion was found to be effective over large distance in homobaric leaves and was responsible for artefacts in measured respiration rates (Jahnke et al. 2002). Gas diffusion inside leaves has been regarded mainly as a (linear) transport of gaseous compounds from the surrounding air through stomata, intercellular air space, cell walls and membranes to chloroplasts (Evans & von Caemmerer 1996). Gas diffusion inside leaves, however, is a 3-dimensional process because CO₂ not only spreads to the place of CO₂ fixation but in all directions (cf. Parkhurst 1994). Published studies on lateral gas diffusion within leaves have up to now focussed on gas transport between neighbouring stomata, i.e., fairly small distances (Terashima 1992; Parkhurst 1994). However, gas fluxes in lateral direction may be substantial over large distances and create general problems for gas exchange measurements performed on homobaric leaves (Jahnke et al. 2002). Recent development in gas exchange techniques has tended towards miniaturisation and small 'clamp-on' leaf chambers have become very common to measure plant performance in the field. Such leaf chambers generally enclose only parts of a leaf. Gas gradients in gas concentration may cause then a flux between the chamber and the surrounding air leading to erroneous results.

The open internal anatomy of homobaric leaves allows gas diffusion under atmospheric pressure inside and outside a leaf chamber. When pressure differences between the leaf chamber and the atmosphere is not zero lateral fluxes within the mesophyll occur (cf. Williams 1948). However, it has not been studied so far whether these pressure driven fluxes influence gas exchange measurement. The question is of practical interest since overpres-

sure has been used in some gas exchange systems to avoid leakiness between the leaf surface and the gasket (Küppers & Häder 1999). However, there is no detailed description about the overpressures provided in the respective gas exchange systems in literature. The impact of air pressure on plants has been studied so far with respect to declining pressure with higher altitude (Gale 1972a; Körner 1999; Körner, Farquhar, & Wong 1991). As total atmospheric pressure decreases with altitude, the partial pressures of CO₂ and O₂ became smaller, which influences the photosynthetic efficiency (Körner et al. 1991; Terashima et al. 1995). A decrease in air pressure with altitude enhances also the potential transpiration by increasing the leaf to air water vapour gradient and by increasing the diffusivity of water vapour in the air (Gale 1972b).

One goal of the present work was to quantify the influence of lateral fluxes caused by respective gas and pressure gradient on gas exchange measurement. Therefore, (1) gas conductance and conductivity as a specific measure of gas diffusion properties of leaves were calculated in heterobaric or homobaric leaves in lateral and vertical directions of leaf blades; (2) gas exchange measurement was performed to screen different plant species to be characterised as heterobaric or homobaric; (3) the impact of lateral diffusion on CO₂ response curves (A/c_i curves) and the derived parameters were evaluated, (4) CO₂ and H₂O exchange rates of leaves were measured under overpressure in the leaf chamber in order to prove whether the impact of overpressure matches theoretical consideration given by Terashima et al. (1995) and Gale (1972a, 1972b); (5) the impact of pressure driven fluxes in homobaric leaves on gas exchange rates was quantified in light and darkness; (6) the effect of stomatal conductance on pressure driven fluxes inside leaves was characterised.

The efficiency how plants can capture light depends on the amount and spatial distribution of radiation as well as the architectural arrangement of leaves within the canopy. The plant canopy architecture determines the leaf orientations relative to the sources of light and the degree of self-shading from leaf overlap in a plane orthogonal to the light source. The role of leaf orientation in light interception by individual leaves and plant canopies has been well investigated (Niinemets 1998; Nobel, Forseth, & Long 1993; Pearcy et al. 2004). Except in the unusual case of some forest herbs producing only a few leaves, all plant species exhibit substantial self shading. Only the upper five 'layers' of a canopy are above light compensation and layers below would respire more than they are assimilating (Nobel et al. 1993). In such cases, partial illumination with sunflecks plays an important role in provid-

ing light for photosynthesis. Utilisation of sunflecks has been investigated in numerous studies for rainforest plants (Allen & Pearcy 2000; Leakey et al. 2002; Valladares, Allen, & Pearcy 1997; Watling et al. 1997); cultivated plants (Fay & Knapp 1993; Jifon & Syvertsen 2003; Pons & Pearcy 1992); or deciduous forest plants (Johnson et al. 1997; Schulte, Offer, & Hansen 2003; Tognetti, Johnson, & Michelozzi 1997). Up to 60% of daily carbon gain is attributable to sunflecks that provide up to 90% of total daily photon flux (Küppers et al. 1996; Pearcy et al. 1994; Pfitsch & Pearcy 1989). However, potential processes along the light/shade borderline have not been studied so far. Shaded areas may be effective as CO₂ source because respiratory processes dominate whereas in adjacent illuminated areas photosynthetic CO₂ uptake creates CO₂ sinks. Thus, a gradient is present and a lateral flux may emerge leading to re-fixation of respiratory CO₂ from shaded leaf parts. This recycling of respiratory CO₂ may render to be useful under conditions when stomatal conductance is low and the plant is under drought stress. Stomatal conductance decreases under drought stress which reduces intercellular CO₂ concentration and affects photosynthesis (Flexas & Medrano 2002; Lawlor 2002; Medrano et al. 2002). Reduced CO₂ availability under drought stress is prevalently accompanied by excess light energy which may cause photoinhibitory damage of the photosynthetic apparatus (Cornic & Fresneau 2002; Ort 2001; Ort & Baker 2002; Osmond et al. 1997). Therefore, plants developed several mechanisms to avoid excess light. Change of leaf orientation relative to direct solar irradiance affects the amount of absorbed light by the leaf and thus its photosynthetic activity, transpiration rate and temperature (Cornic & Massacci 1996). Non-photochemical quenching of absorbed light associated with light induced formation of zeaxanthin is thought to be essential in protecting leaves from light induced damage (Demmig-Adams & Adams III 1992; Horton, Ruban, & Walters 1996). Additionally, re-fixation of respiratory CO₂ from remote shaded leaf parts may reduce the light stress and increase net-carbon gain, especially in plants under drought stress exposed to sunflecks.

The second aim of the present work was to explore whether lateral gas diffusion in homobaric leaves may have an impact on plant physiology, and under which environmental conditions the impact is prevailing. Therefore: (1) potential lateral CO₂ flux along the light/shade borderline was visualised using chlorophyll fluorescence imaging technique; (2) the impact of stomatal conductance on lateral fluxes along the light/shade borderline was studied with plants under drought stress; (3) additional carbon gain and reduction of light stress due to CO₂ re-fixation from shaded leaf areas was investigated using combined

measurement of gas exchange and chlorophyll fluorescence on leaves illuminated with lightflecks with plants under different water status.

Chapter 2 Materials and methods

2.1 Plant material

In the time between July and October 2003, a screening of different plant species was executed with arbitrarily chosen plants from different locations in order to characterise the leaves of the plants as hetero- or homobaric (Tab. 1; page 13).

Table 1. Plant species used for a screening and their locations in order to characterise leaf anatomy.

Plant species	Location
<i>Acanthus mollis</i> L.	Botanical Garden, University Duisburg-Essen ²
<i>Arum maculatum</i> L.	Segerothpark, Essen ¹
<i>Beta vulgaris</i> L.	Cropland, Jülich ¹
<i>Calendula arvensis</i> L.	Botanical Garden, University Duisburg-Essen ¹
<i>Capsicum frutescens</i> L.	Botanical Garden, University Duisburg-Essen ¹
<i>Chenopodium album</i> L.	Segerothpark, Essen ¹
<i>Cichorium intybus</i> L.	Campus Essen, University Duisburg-Essen ¹
<i>Cirsium arvense</i> (L.) Scop.	Campus Essen, University Duisburg-Essen ¹
<i>Citrus spec.</i> L.	Botanical Garden, University Duisburg-Essen ²
<i>Cyclamen persicum</i> L.	Botanical Garden, University Duisburg-Essen ²
<i>Dianthus barbatus</i> L.	Botanical Garden, University Duisburg-Essen ¹
<i>Euphorbia amygdaloides</i> L.	Botanical Garden, University Duisburg-Essen ²
<i>Fallopia aubertii</i> (Henry) Holub	Campus Essen, University Duisburg-Essen ¹
<i>Hedera helix</i> L.	Campus Essen, University Duisburg-Essen ¹
<i>Ilex aquifolium</i> L.	Campus Essen, University Duisburg-Essen ¹
<i>Ligustrum vulgare</i> L.	Campus Essen, University Duisburg-Essen ¹
<i>Lupinus spec.</i> Rydb.	Segerothpark, Essen ¹
<i>Mentha spec.</i> L.	Botanical Garden, University Duisburg-Essen ¹
<i>Mimulus guttatus</i> DC.	Botanical Garden, University Duisburg-Essen ¹
<i>Nerium oleander</i> L.	Botanical Garden, University Duisburg-Essen ²
<i>Phragmites australis</i> (Cav.) Trin. ex Steud.	Campus Essen, University Duisburg-Essen ¹
<i>Picris hieracioides</i> L.	Segerothpark, Essen ¹
<i>Plantago lanceolata</i> L.	Segerothpark, Essen ¹
<i>Pulmonaria officinalis</i> L.	Botanical Garden, University Duisburg-Essen ²
<i>Rumex crispus</i> L.	Segerothpark, University Duisburg-Essen ¹
<i>Skimmia japonica</i> Nakai	Botanical Garden, University Duisburg-Essen ²
<i>Smilax spec.</i> L.	Botanical Garden, University Duisburg-Essen ²
<i>Taraxacum officinale</i> F.H.Wigg.	Campus Essen, University Duisburg-Essen ¹
<i>Zea mays</i> L.	Cropland, Essen-Werden ¹

¹Field plants were dug out and potted in a large 5 L pot to perform the experiments.

²Plants were grown in pots

Plants of *Glycine max* (L.) Merr. cv. Williams, *Nicotiana tabacum* L. cv. Samsun, *Phaseolus vulgaris* L. cv. Saxa and *Vicia faba* L. cv. Hangdown Grünkernig were grown from seeds in 1 L pots.

2.2 Growth conditions

The growing conditions differed between the experimental sites at University Duisburg-Essen and Research Centre Jülich.

University Duisburg-Essen

The plants were grown in soil (Einheitserde Typ P, Balster-Feuerfest GmbH, Germany) mixed with perlite (4:1 v/v) in 1 L pots. Periodical irrigation was performed with a nutrient solution (2 mM KNO₃, 4 mM Mg(NO₃)₂·6H₂O, 0.8 mM KH₂PO₄, 0.5 mM MgSO₄·2H₂O, 1.1 mM CaSO₄·2H₂O, 11 µM Fe-EDTA (Fetrilon, BASF), 7.5 µM H₃BO₃, 1.75 µM MnSO₄·H₂O, 0.08 µM CuSO₄·5H₂O, 0.13 µM ZnSO₄·7H₂O, 0.04 µM H₂MoO₄, 0.003 µM CoCl₂·6H₂O) adjusted to pH 5.8. A photon flux density (PFD) of 400–550 mmol (photons) m⁻² s⁻¹ was at the upper leaf level of the plants. Growing conditions were as described in Jahnke (2001).

Research Centre Jülich

The plants were grown in a green house. For germination, the seeds were put into small pots (ca. 25cm³). After 4-6 day, the plants were potted in soil (Einheitserde Typ ED 73, Balster-Feuerfest GmbH, Germany). Periodical irrigation was performed with tap water (0.7 mM NO₃⁻, 2.9 mM Cl⁻, 1.3 µM PO₄⁻³, 0.6 mM SO₄⁻², 0.1 mM K⁺, 1.2 mM Na⁺, 1.3 mM Mg²⁺, 3mM Ca⁺², 2.3 µM Fe, 0.2 µM Mn, 4µm B; according to chemical water analysis, Hygiene Institut Dr. Berg, from 27.03.2002). Additionally, every plant was watered once a week with 100 mL of nutrient solution Hakaphos grün (for concentration of nutrients see: http://www.compo-profi.de/produkte/naehrsalze_hakaphos_gruen.html; COMPO GmbH & KG, Münster, Germany). The light intensity in the greenhouse corresponded approximately to field conditions because the glass panels in the green house were highly translucent by passing more then 95% of the whole light spectrum including UV (for details see: <http://www.fz-juelich.de/icg/icg-iii/index.php?index=112>). When the light intensity dropped below 6000 Lux (approximately 110 µmol photons m⁻² s⁻¹; cf. Larcher 1995)

artificial light was switched on (SON-T, 400W, Philips, Germany; HQI-Lamps, 400W Osram, München, Germany) which provided PFD of 400-450 $\mu\text{mol m}^{-2} \text{s}^{-1}$ at 30 cm above the pots. During the winter months the day/night regime was 12/12 h, temperature was controlled by a 21/19 °C reaching maxima of 30°C during sunny summer days. The air humidity was not controlled and ranged between 50-70% r.h.

2.3 Gas exchange measurements

2.3.1 Gas exchange system

Gas exchange of leaves was measured by open gas exchange systems at two different sites. A detailed description of the gas exchange system used at the University Duisburg-Essen is given by Jahnke (2001). This measurement system was transferred in 2004 to the Research Centre Jülich and was rebuilt with some modifications (cf. Fig. 2; page 16). Flexible gas tubings (Polyamide 12; Deutsche Tecalet, Bielefeld, Germany) were used in the system. H₂O and CO₂ free air was delivered by a gas generator (CO₂RP140, Domnick Hunter, Willel, Germany). Different CO₂ concentrations ([CO₂]) were produced by mixing CO₂ free air with CO₂ from a pressure cylinder by using mass flow controllers (MFC; Bronkhorst, model F-201C and F-200C, Mättig Mess- und Regeltechnik Vertriebs GmbH, Unna, Germany). Alternatively, air composition was performed by mixing N₂, O₂ and CO₂ with mass flow controllers. Moisture was adjusted by a custom made humidifier (HM) and a dew point condenser (DP) in which a small overpressure was kept at approximately +0.1 kPa above ambient air pressure. Air conduction was provided by three different parallel gas lines (Line 1-3 in Fig. 2; page 16). When the gas in line 1 was vented to the leaf chamber, air of different composition was already prepared in the second line. The gas line feeding the leaf chamber was chosen by switching the solenoid valve (MV1). The third line was used to provide the air into the external chamber of double gasket chambers (cf. chapter 2.3.2) or to provide calibration gases to the gas analyser. Part of the incoming air was vented to the reference cell of the differential infrared gas analyser (IRGA; LICOR 7000, LICOR Corporate, Lincoln, Nebraska, USA). The gas flow entering the leaf chamber was measured by a mass flow meter (MFM; Bronkhorst, model F-101D) and kept constant by the pressure pump GP1 (WISA-300, ASF Thomas Industries, Puchheim, Germany). A differential pressure transducer (PD2; CTEM7N025GMO, Sensortronics, Puchheim,

Germany) controlled the suction pump (GP2) to keep the pressure difference between the leaf chamber and atmosphere small. Process controllers (Sipart DR20, Siemens, Essen, Germany) were used for the control circuits. Additionally, a bypass pump GP3 (GK-M 12/07, ASF Thomas Industries GmbH, Memmingen, Germany) was connected to the leaf chamber in order to increase the wind speed inside the leaf chamber and reduce the boundary layer of the leaf surface. The air humidity was measured either by IRGA or with humidity sensors (H1, H2; HMP 133, Vaisala, Hamburg, Germany) by activating or deactivating the solenoid valves (MV2, MV3). When the outcoming air was vented through the dewpoint trap (DP2), the gas had the similar vapour pressure as the incoming gas that passed the dewpoint trap DP1 (Fig. 2; page 16). Activating the solenoid valve MV4 resulted in supply of the same air into the reference and sample cell of the IRGA, which was used the match this two cells every time $[CO_2]$ was changed (cf. LI-COR 2005). The system had several vents to avoid any negative influence of overpressure. All these vents were controlled by differential pressure transducers (PD; CTEM7N025GMo; Sensortronics, Puchheim, Germany) to keep slight overpressure in order to avoid diffusive contamination from the air outside the system.

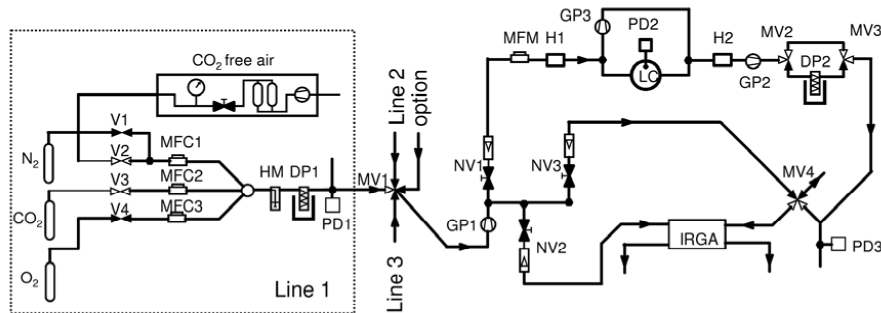


Figure 2. Scheme of the gas flow of the gas exchange system. Air of required gas composition including the water partial pressure was prepared by mixing different gases (Line 1). The CO_2 and H_2O concentration was measured by an infrared gas analyser (IRGA). The flow was measured with a mass flow meter (MFM) and constant flux was controlled by the pressure pump (GP1). Inside the leaf chamber the pressure difference to the atmosphere was measured (PD2) and controlled by the suction pump (GP2). CO_2 , N_2 and O_2 was supplied by pressure cylinders with the corresponding gas; CO_2 free air was provided by a gas generator producing dry CO_2 free air; V1-V4, valves; MFC, mass flow controller; HM, humidifier; DP dewpoint trap; MV, solenoid valve; GP pump; NV, needle valve; MFM, mass flow meter; H, humidity sensor; PD differential pressure transducer; details in text.

2.3.2 Leaf chambers

Different leaf chambers were used for various purposes. (1) A large single-gasket leaf chamber (LLC) with a circular outline, an inner diameter of 7 cm and gasket width of 8 mm which was taken to clamp apical parts of leaves enclosing an average leaf area of approximately 25 cm² (cf. Jahnke et al. 2002). Atmospheric CO₂ concentration inside LLC was denoted $c_{a,i}$ whereas [CO₂] in the experimental growth cabinet during experiments (i.e. outside the leaf chamber) was denoted $c_{a,o}$. (2) A double-gasket leaf chamber (LC) with rectangular outlines and gasket width of 6 mm was used. The inner leaf chamber (LC_i) enclosed an area of 6 cm² (2 x 3 cm) while the area between the inner and the outer gaskets (i.e. the outer leaf chamber LC_o; Fig. 3; page 17) was 15 cm². Atmospheric CO₂ concentrations inside LC_i and LC_o are denoted $c_{a,i}$ and $c_{a,o}$, respectively. Gas exchange measurements were performed inside LC_i whilst LC_o was used to quickly change [CO₂] at the outer edge of LC_i (Fig. 3, page 17; cf. Pieruschka, Schurr, & Jahnke 2005). Both, LLC and LC are clamp-on leaf chambers.

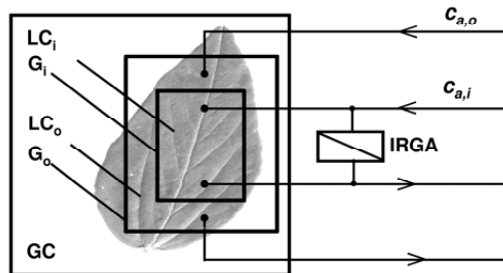


Figure 3. Scheme of the double-gasket leaf chamber (LC) used in an open gas exchange system. G_i, inner gaskets; G_o, outer gaskets; GC, growth cabinet in which the experiments were performed and (external) CO₂ concentration was controlled; IRGA, differential infrared gas analyser; LC_i, inner leaf chamber in which the inner atmospheric CO₂ concentration ($c_{a,i}$) was varied; LC_o, outer leaf chamber in which the outer atmospheric CO₂ concentration ($c_{a,o}$) was varied.

(3) A new leaf chamber was constructed in order to enclose a whole leaf (XLC, Fig. 4; page 18). The leaf chamber was build up from a stainless steel frame. A highly light-translucent teflon-transparent (Nowofol Kunststoffprodukte GmbH & Co. KG, Siegsdorf, Germany) was stuck on the bottom and on the lid of the chamber with adhesive tape (Kap-

ton CMC 70752, CMC Klebetechnik GmbH, Germany). A natural rubber (Meteor, Gummiwerke K.H. Bädje, Bockenem, Germany) with circular cross section of 4 mm was glued with Terokal-2444 (Henkel Teroson GmbH, Düsseldorf, Germany) in a seal groove in order to tightly close the chamber. The incoming and outgoing air was led by an inert tube with a series of holes to provide excellent gas mixing. The leaf was inserted into the chamber with the petiole in an aperture and the leaf blade was between two nets. To avoid leakiness through the aperture, the leaf petiole was sealed with silicon-based putty (Optosil P Plus; Heraeus Kulzer, Dormagen, Germany). This putty was also used to seal the thermocouples used to measure leaf and air temperature. The pressure difference to the atmosphere was measured with a pressure transducer (PD) in order to control atmospheric pressure inside the chamber (cf. Fig. 2; page 16).

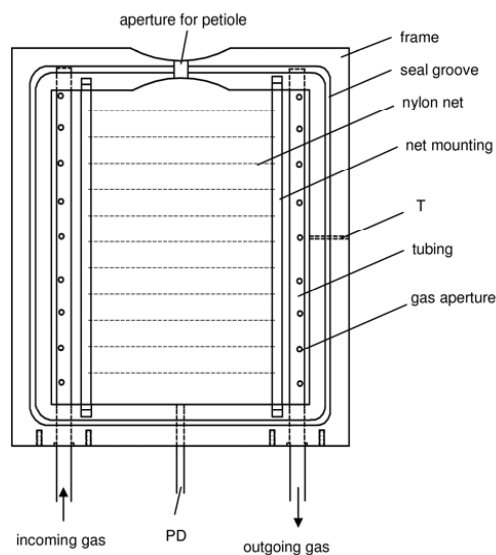


Figure 4. Schematic drawing of large whole-leaf chamber (XLC). The leaf chamber was made of stainless steel (frame) with transparents stuck on the bottom and the lid of the chamber. Leaf petiole was inserted in the aperture at one side of the chamber. Two nylon nets, one at the lower and one at the upper side of the leaf used to fix the leaf inside the chamber. Thermocouples were inserted at T to measure the temperature of the leaf and the air inside the chamber. The incoming and outgoing gas was led by tubing with apertures. The pressure difference to atmosphere was measured with a differential pressure transducer (PD; cf. Fig. 2; page 16).

2.3.3 Automation of the gas exchange system

The graphical programming language LabVIEW (National Instruments, Austin, Texas, USA) was used in combination with signal conditioning devices (SCXI: Signal Conditioning eXtension for Instrumentation, National Instruments, München Germany) to operate

the gas exchange system manually or automatically. This comprises the control of system components (valves, pumps etc.), generating of analog set points (for CO₂ concentration, gas flow, pressure inside the leaf chamber etc.). Analog and digital data could be acquired, calculated online and visualized on screen (for details see Jahnke & Proff 2001; Proff 2003).

2.3.4 Calculations and control measurements

The calibration of the system was described by Jahnke (2001). The net CO₂ exchange rate (*NCER*; $\mu\text{mol CO}_2 \text{ m}^{-2} \text{ s}^{-1}$) was calculated according to Jahnke et al. (2002).

The dewpoint temperature of the gas streams entering the reference or analyser cell of the IRGA were adjusted to the same value to avoid any problems of water vapour effect on $\Delta[\text{CO}_2]$ measurement; transpiration was measured by humidity sensors (H, cf. Fig. 2; page 16; for details see Jahnke 2001). When transpiration was measured by the IRGA, the water vapour effect on $\Delta[\text{CO}_2]$ was calculated in order to correct the measurement. The appropriate calculation of the water vapour effect on $\Delta[\text{CO}_2]$ was tested by keeping the $[\text{CO}_2]$ constant and varying the water vapour pressure.

Before starting experiments, controls were performed with the same protocol as in the experiment to fully define the properties of the gas exchange system (memory effects, leaks etc.; cf. Jahnke 2001). The obtained results were used to correct the experimental data.

2.4 Measurement of lateral diffusion inside leaves

2.4.1 Experimental protocol

The experiments were performed with plants grown in a growth chamber at the University Duisburg-Essen. To determine gas conductance of the mesophyll in lateral directions in leaf blades, experiments were performed in the dark where only respiration contributed to the exchange of CO₂. Before measurement, plants were kept in darkness for approximately 36 h as *NCERs* were stable after that period. *NCERs* were measured under different CO₂ concentrations with the following experimental protocol (see Fig. 8 a, page 36): (1) the

experiments started at low $c_{a,o}$ and $c_{a,i}$ ($350 \mu\text{L L}^{-1}$); (2) $c_{a,i}$ was increased to $2000 \mu\text{L L}^{-1}$ while $c_{a,o}$ was kept unchanged; (3) $c_{a,o}$ was also increased to $2000 \mu\text{L L}^{-1}$; (4) $c_{a,o}$ was kept high while $c_{a,i}$ was lowered to $350 \mu\text{L L}^{-1}$; (5) and finally, the starting conditions ($350 \mu\text{L L}^{-1}$ on both sides) were re-established. The temperature inside the leaf chamber was $23.5 \pm 0.5^\circ\text{C}$ and the water vapour pressure of the incoming air was 1.8 kPa; the resulting vapour pressure deficit for the leaf was 1.1 kPa.

2.4.2 Calculation of lateral gas conductance and conductivity

To calculate lateral gas conductance ($g_{leaf,l}$) according to Flick's first law of diffusion (Parkhurst 1994), the required parameters were obtained experimentally. The area of intercellular air space potentially open for lateral diffusion, $AR_{ias,l}$ (m^2), was calculated as:

$$AR_{ias,l} = L_{gasket} \bullet h_{leaf} \bullet porosity \quad \text{Eqn. 1}$$

where L_{gasket} (m) was the length (circumference) of the centre line of the leaf chamber gasket (LC_i) covering the leaf; h_{leaf} (m) was the thickness (height) of the leaf blade; *porosity* was the fraction of the volume of intercellular air space and the corresponding leaf volume. Calculation of $AR_{ias,l}$ by using L_{gasket} as defined in equation (1) is a simplification of the real situation. For example, for the circular leaf chamber (LLC) the concentric-cylinder geometry of the gaskets should be considered according to Crank (1975). Taking this into account for calculation of conductance (see below) the resulting correction factor was 1.0035, which means conductance was underestimated here by 0.35% when calculation was based on equation (1). This uncertainty was so much below the variability of different measurements that it was not regarded here; for details see appendix. To obtain leaf porosity, 8-10 leaf discs per plant were punched out ($r = 1.0 \text{ cm}$), intercellular air space volumes were determined (cf. Jahnke et al. 2002) and volumes of the leaf discs were calculated as $h_{leaf} \bullet r^2 \bullet porosity$. To determine leaf and tissue thickness, cross sections of the leaves were made by hand and measured by a microscope with a micrometer scale. Thicknesses of leaves, palisade and spongy tissues as well as leaf porosities are presented in table 2 (page 35).

Diffusive fluxes of CO₂ in lateral directions of the leaf blades ($J_{CO_2,l}$; $\mu\text{mol CO}_2 \text{ m}^{-2} \text{ s}^{-1}$) were calculated according to:

$$J_{CO_2,l} = (NCER_{ref} - NCER_{\Delta}) \bullet \frac{A_{leaf}}{A_{gas,l}} \quad \text{Eqn. 2}$$

where $NCER_{ref}$ was the measured net CO₂ exchange rate when [CO₂] was identical on both sides of the chamber gasket (i.e. $c_{a,i} = c_{a,o}$) and $NCER_{\Delta}$ was obtained when there was a difference in external [CO₂] between the two sides of the leaf chamber gaskets (i.e. $c_{a,i} > c_{a,o}$ or $c_{a,i} < c_{a,o}$); A_{leaf} was the projected leaf area clamped by the leaf chamber. Finally, lateral gas conductance ($g_{leaf,l}$; $\text{mmol CO}_2 \text{ m}^{-2} \text{ s}^{-1}$) was calculated as:

$$g_{leaf,l} = \frac{J_{CO_2,l}}{\Delta c_a} \quad \text{Eqn. 3}$$

with $\Delta c_a = c_{a,i} - c_{a,o}$ (cf. Fig. 3; page 17).

The calculation of gas conductance is analogous to Ohm's law of electricity ($I = V/R$) where I is the current, V voltage and R^{-1} electrical conductance (cf. Parkhurst 1994). However, for comparison of properties of different systems conductance as such is not very helpful. In electricity, the conductivity σ of a conductor was introduced and is defined as $\sigma = I * A^{-1} * R^{-1}$ where I is the length and A the cross-section area of the conductor (Gettys 1989). Gas conductance (g ; $\text{mmol CO}_2 \text{ m}^{-2} \text{ s}^{-1}$) already refers to the diffusion area A (cf. equations 2 and 3) and was taken, in analogy to electricity, to calculate gas conductivity of leaves (g^* ; $\text{mmol CO}_2 \text{ m}^{-1} \text{ s}^{-1}$). In the experiments presented here, the path length over which gas diffusion was measured was defined by the width of the chamber gaskets (w_{gasket} ; see Fig. 36; page 82), and lateral gas conductivity ($g^*_{leaf,l}$) of the intercellular airspace was calculated according to the equation:

$$g^*_{leaf,l} = g_{leaf,l} \bullet w_{gasket} \quad \text{Eqn. 4}$$

Conductance can also be expressed as $g = D/\Delta x$ where D describes the diffusivity (diffusion coefficient) and Δx the diffusion distance (Nobel 1991). Multiplication of gas conduc-

tance by diffusion distance (Eqn. 4; page 21) results in diffusivity which is identical with conductivity. In air, gas diffusivity is well characterised and, as long as the size of the pores does not hamper gas movement, maximum conductivity of an ideal open-porous medium is simply defined by porosity multiplied by the maximum diffusivity in free air (for CO₂: $1.51 \cdot 10^{-5} \text{ m}^2 \text{ s}^{-1}$ or $674 \mu\text{mol m}^{-1} \text{ s}^{-1}$ at 101.3 kPa and 20 °C, presented in figure 10 (page 40) by the dashed line; cf. Nobel 1991).

Theoretically, conductivity should not be dependent on the path length of diffusion over which conductance is measured. This was tested by calculating conductivities for the experiments in which the widths of chamber gaskets were changed gradually between 6, 14 and 22 mm. Published data on gas conductance of leaves almost exclusively deal with gas transport in the vertical direction of a leaf blade. To compare gas conductivities in lateral directions (as investigated here) with those in vertical direction, published values of vertical gas conductance were taken to calculate vertical conductivities according to equation 4 (page 21) with the leaf thickness of the particular species taken from the literature (Tab. 4; page 39).

2.4.3 Data analysis

The statistical analysis was performed by t-test, paired t-test and ANOVA using Sigma Plot (SPSS Inc. Version 7.101). Calculations of *NCERs* and apparent effects of CO₂ (*AE_{CO2}*) on *NCERs* due to lateral diffusion of CO₂ were performed according to Jahnke et al. (2002) where *AE_{CO2}* was named *ACE*.

2.5 Dark respiration measurement

The plants used in these experiments are shown in table 1 (page 13). The experiments were performed with the small double gasket leaf chamber (LC, cf. Fig. 3; page 17). Before measurement, plants were kept in darkness for approximately 36 h as *NCERs* were stable after that period. *NCERs* were measured under different CO₂ concentrations with an experimental protocol modified to what was described before (cf. Fig. 8 a; page 36). The experiments started at low *c_{a,o}* and *c_{a,i}* ($350 \mu\text{L L}^{-1}$); *c_{a,o}* was then increased to $2000 \mu\text{L L}^{-1}$ while *c_{a,i}* was kept unchanged; in the next step, *c_{a,o}* was also increased to $2000 \mu\text{L L}^{-1}$; and

finally, the starting conditions ($350 \mu\text{L L}^{-1}$ on both sides) were re-established. The experimental conditions were as described in chapter 2.4.2 and data analysis was performed according to chapter 2.4.3.

2.6 Gas exchange measurement in light

The experiments were performed with plants grown in the greenhouse at the Research Centre Jülich. The dependence of photosynthesis on photon flux density (PFD) was measured in order to estimate the PFD not limiting photosynthesis. Light curves were measured at PFDs of 600, 350, 180, 120, 80, 40, 900 and $1500 \mu\text{mol m}^{-2} \text{s}^{-1}$ and $[\text{CO}_2]$ of $600 \mu\text{L L}^{-1}$ to minimize the limitations due to low $[\text{CO}_2]$. For all plants under PFD of $500 \mu\text{mol m}^{-2} \text{s}^{-1}$ at least 90% of the maximum assimilation rate was measured. Thus, the dependence of photosynthesis on CO_2 (A/c_i curves) was measured at $\text{PFD}=500 \mu\text{mol m}^{-2} \text{s}^{-1}$ as the initial slope of A/c_i curves is independent of irradiance above $400\text{--}500 \mu\text{mol m}^{-2} \text{s}^{-1}$ (Sage, Sharkey, & Seemann 1990). Light was provided by a light unit (FL-460; Walz GmbH, Effeltrich, Germany) and measured by a LI-185B sensor (LI-COR Inc.). The leaf temperature ranged between 24.4 and 25.2°C during the experiments. The water vapour pressure of the incoming air was 1.7 kPa and the resulting vapour pressure deficit between the leaf and the air was 1.2 kPa .

The experiments were performed with the double gasket leaf chamber (LC, cf. Fig. 3; page 17). All experiments started with $c_{a,i}=c_{a,o}=350 \mu\text{L L}^{-1}$. In the next step, $c_{a,i}$ was decreased to $250 \mu\text{L L}^{-1}$ while $c_{a,o}$ was $350 \mu\text{L L}^{-1}$. After steady state $NCER$ was measured, $c_{a,i}$ and $c_{a,o}$ was adjusted to $250 \mu\text{L L}^{-1}$. In the next step, $c_{a,i}$ was decreased to $180 \mu\text{L L}^{-1}$ while $c_{a,o}$ was increased to $350 \mu\text{L L}^{-1}$; after measuring steady state $NCER$, $c_{a,o}$ was decreased to the same level as $c_{a,i}$ with $180 \mu\text{L L}^{-1}$. This procedure was repeated with following $[\text{CO}_2]$: 350, 240, 180, 120, 60, 570, 720 and $1230 \mu\text{L L}^{-1}$ (see Fig. 5; page 24). Every time $c_{a,i}$ was changed the reference and analyser cell of the IRGA were provided with the same air (by switching MV4, Fig. 2; page 16) and matched to the actual $[\text{CO}_2]$ (cf. LI-COR 2005). For each $c_{a,i}$ two different $NCER$ s were obtained. $NCER$ was measured when $c_{a,i}=c_{a,o}$ ($NCER_{ref}$, white circles, Fig. 5 b; page 24) and when $c_{a,o}=350 \mu\text{L L}^{-1}$ ($NCER_{\Delta}$, black circles, Fig. 5 b; page 24). The mean $NCER_{ref}$ and $NCER_{\Delta}$ obtained under the corresponding $c_{a,i}$ and $c_{a,o}$

were then plotted versus the calculated intercellular $[\text{CO}_2]$ (c_i ; cf. Küppers et al. 1999) which resulted in A/c_i curves (cf. Fig. 11; page 43).

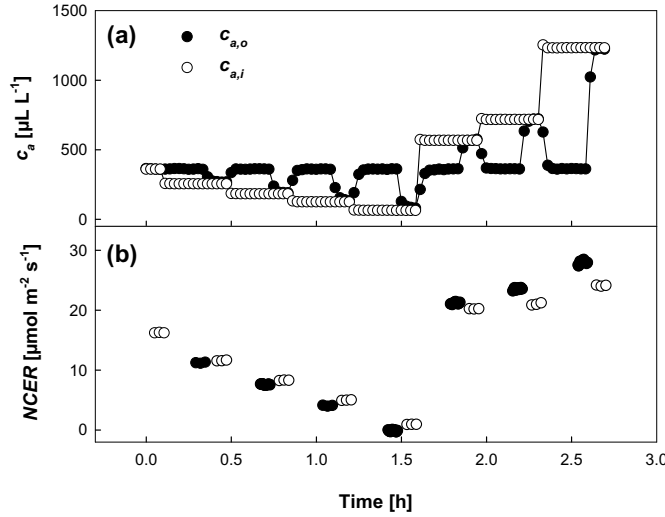


Figure 5. The experimental protocol used to measure the impact of lateral diffusion on the dependence of photosynthesis on $[\text{CO}_2]$, (A/c_i). (a) $[\text{CO}_2]$ in the inner ($c_{a,i}$, white circles) and in the outer ($c_{a,o}$, black circles) chamber; (b) the obtained net CO_2 exchange rates (NCERs) under the given $c_{a,i}$ and $c_{a,o}$ with NCER_{ref} (white circles) obtained when $c_{a,i}=c_{a,o}$ and NCER_{\downarrow} (black circles) measured when $c_{a,o}=350 \mu\text{L L}^{-1}$. The double gas-ket leaf chamber used in the experiments is presented in figure 3 (page 17).

2.6.1 Analysis of CO_2 response curves

Non-linear regression techniques, based on the equations of Farquhar, von Caemmerer, & Berry (1980), later modified by Sharkey (1985) and Harley & Sharkey (1991), were used to estimate the maximum rate of RubisCO mediated carboxylation (V_{max}) and the maximum rate of carboxylation limited by electron transport (J_{max}) for each A/c_i curve. The rate of respiration in the presence of light (R_D) was calculated as NCER measured at the CO_2 compensation point in absence of respiration (I^*) according to von Caemmerer (2000). The parameters incorporated in the biochemical model (K_c , K_o as the Michaelis-Menten constants for carboxylation and oxygenation of RubisCO, respectively and I^*) were taken from von Caemmerer (2000). Additionally, the CO_2 compensation point (I^*) was calculated as the intercept with the x-axis. To estimate V_{max} and R_D , NCERs measured at $c_{a,i}$ of 240, 180, 120, 60 $\mu\text{L L}^{-1}$ were used where it is assumed that assimilation is limited by the

amount, activity, and kinetic properties of RubisCO (Harley et al. 1992; Wullschleger 1993). The remaining portion of the A/c_i curves (at $c_{a,i} = 570, 720$ and $1230 \mu\text{L L}^{-1}$) was used to solve for J_{max} . The software SigmaPlot (SPSS Inc.) was used for the analysis.

2.6.2 Shading of the leaf part outside the leaf chamber

Well-watered plants grown in a growth cabinet at the University Duisburg-Essen were used in these experiments. Gas exchange was measured with the double gasket leaf chamber (LC, Fig. 3; page 17). The gasket (G_o) of the outer leaf chamber (LC_o) was removed so that the chamber was as a single gasket couvette for these experiments. The leaf chamber was placed in an experimental cabinet with controlled CO_2 concentration ($355 \pm 10 \mu\text{L L}^{-1}$), temperature ($23.5 \pm 0.5^\circ\text{C}$) and air humidity ($60 \pm 5\%$ r.h.; $VPD = 1.1 \text{ kPa}$). $NCEP$ was measured in the leaf chamber at low $[\text{CO}_2]$ ($60 \mu\text{L L}^{-1}$) to make potential effects of leaf internal lateral CO_2 transport more pronounced. The leaf part outside the leaf chamber was either exposed to the same light intensity as the clamped leaf part or shaded by a template made from black paper. Light was provided by a light unit (FL-460; Walz GmbH, Effeltrich, Germany) and measured by a LI-185B sensor (LI-COR Inc.). PFD was approximately $500 \mu\text{mol m}^{-2} \text{s}^{-1}$ whereas under the template it varied between $1\text{--}3 \mu\text{mol m}^{-2} \text{s}^{-1}$ due to diffuse radiation.

2.7 Gas exchange measurements under overpressure

The experiments were performed with plants grown in a growth cabinet at the University Duisburg-Essen. The large single gasket leaf chamber (LLC) was located in a growth chamber with constant conditions of $23.5 \pm 0.5^\circ\text{C}$. The water vapour pressure of the incoming air was 1.8 kPa ($VPD 1.1 \text{ kPa}$). The CO_2 concentration in the growth chamber could be changed variably between 350 and $2000 \mu\text{L L}^{-1}$. The pressure difference between the leaf chamber and the atmosphere ($\Delta P = \text{air pressure inside the chamber} - \text{atmospheric pressure}$) was activated by controlling the power of the suction pump GP2 (cf. Fig. 2; page 16). ΔP was continuously changed from an initial to a terminal value in a defined period of time ($\Delta P \text{ ramp}$). In most cases, the $\Delta P \text{ ramp}$ started at 0 kPa and ended at 3 kPa after $20\text{--}30$ minutes. The experiments were performed in darkness or under PFD of $700 \mu\text{mol photons m}^{-2} \text{s}^{-1}$.

The influence of ΔP on the measurement was tested in control experiments (Fig. 6; page 26). ΔP was switched between 0-3 kPa (Fig. 6 a; page 26) which had no influence on the gas flow in the gas exchange system (Fig. 6 b; page 26). The sensors (H) measuring water vapour pressure (WVP) of the incoming and outgoing gas were in the direct vicinity of the leaf chamber (cf. Fig. 2; page 16). The change in ΔP caused an increase of WVP of the incoming air (Fig. 6 c; page 26) influencing also the outgoing air in the same way which as a result had no influence on the water vapour pressure difference ΔWVP between the incoming and outgoing air (Fig. 6 d; page 26). No influence of ΔP on $[CO_2]$ measurement was observed because the IRGA was under constant atmospheric pressure (cf. Fig. 2; page 16).

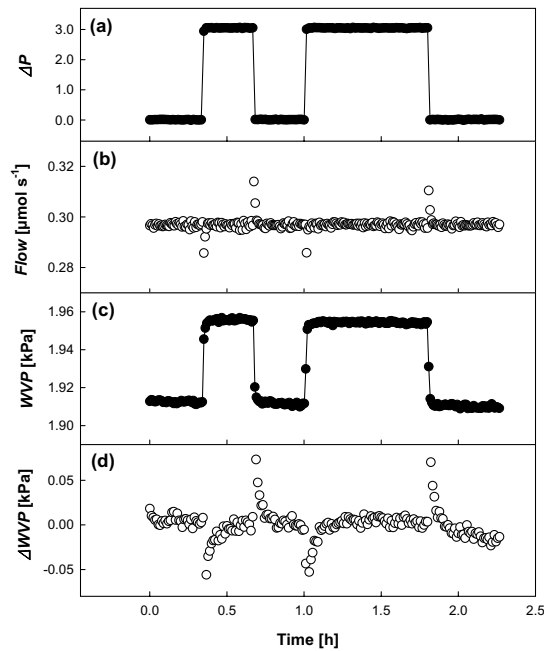


Figure 6. Control experiment to test the influence of overpressure inside the leaf chamber (ΔP) on gas exchange measurement. In (a) ΔP as the difference between the pressure inside the chamber and atmospheric pressure is shown. Under the respective ΔP , (b) gas flow ($flow$) into the leaf chamber (measured by the mass flow meter, MFM, Fig. 2; page 16), (c) water vapour pressure (WVP) of the incoming air and (d) the difference in water vapour pressure of the incoming and outgoing air (ΔWVP).

2.7.1 Influence of air pressure on gas diffusion – theoretical considerations

The volume percentage of gases in the air remains almost constant with changes in air pressure but the partial pressure or concentration of the gases (mass per volume) increases with rising pressure. According to Flick's first law of diffusion (Parkhurst 1994), diffusion depends mainly on the diffusion coefficient (D) and the gas gradient (Δc). D is reciprocally proportional to the atmospheric pressure, P_{air} ($D \sim 1/P_{air}$ and $D \sim \Delta c$) which determines the resistance (r) or the conductance (g) of gases because $D \sim 1/r$ (Brinkjans 1992). Thus, overpressure increases on the one hand the partial pressure of gases, which increases Δc , but on the other hand, it reduces the gas conductance. The resulting diffusion flux is independent on the air pressure under isothermic conditions (Gale 1972a). When the influence of overpressure on plant assimilation is regarded, the diffusion flux itself is not affected. However, overpressure causes an increase of CO_2 partial pressure of the air surrounding the leaf and inside the leaf. When $[CO_2]$ inside the leaf increases enhanced assimilation can be expected.

In general, overpressure influences the transpiration rate of plants according to the diffusion fluxes described above; overpressure causes an increase of WVP in the air and reduces the conductance. However, assuming relative humidity of 100% in leaves (Larcher 1995) WVP inside leaves is independent on the air pressure. When the stomatal conductance remains constant, an increase in air pressure causes a reduction of the WVP gradient between the leaf intercellular air space and the surrounding air which results in reduced transpiration rate (cf. Gale 1972b). This influence of overpressure on transpiration (E_{calc}) can be calculated according to the following equation:

$$E_{calc} = g_{leaf} \cdot \frac{VPD_{LA}}{P_{LC}} \quad \text{Eqn. 5}$$

Water vapour pressure deficit between the leaf and the surrounding air (VPD_{LA}) was calculated as $VPD_{LA} = VP_{leaf} - VP_{air}$ with water vapour pressure inside (VP_{leaf}) and outside (VP_{air}) the leaf. VP_{leaf} was calculated with regard to the leaf temperature according to the equation of Goff and Gratch (1946) (cf. von Willert, Matysek, & Herppich 1995). VP_{air} inside the

leaf chamber was calculated as the mean of VP_{air} between the air entering into and outgoing from the leaf chamber. Finally, the air pressure in the leaf chamber (P_{LC}) was calculated as $P_{LC} = P_{air} + \Delta P$ with P_{air} as the atmospheric pressure outside the chamber.

2.8 Photosynthesis of partly shaded leaves

Measurement of photosynthetic efficiency using chlorophyll fluorescence techniques of leaves partly shaded was performed at the University Duisburg-Essen with plants grown in a growth chamber (for growth conditions see chapter 2.2). A combination of simultaneous measurement of chlorophyll fluorescence and gas exchange was executed at the Research Centre Jülich with plants grown in the green house (for growth conditions see also chapter 2.2).

2.8.1 Measurement of chlorophyll fluorescence

Chlorophyll fluorescence was measured with a pulse modulated fluorometer with spatial resolution (Imaging-PAM Chlorophyll Fluorometer; Walz GmbH). A leaf area of about 20 x 14 mm was measured which is smaller than the maximum sample area of the instrument (Walz 2003). Homogeneity of actinic light provided by the light unit of the system was tested as follows. The camera of the Imaging-PAM was replaced by a commercial camcorder (DLR-TRV8E PAL; Sony Deutschland GmbH, Köln, Germany) and the actinic light was recorded on white filter paper at different light intensities. The obtained images were transferred from the camcorder to a computer via firewire cable and a frame grabber (DVBK-2000E; Sony). The resulting images (739 x 568 pixel) were gamma-corrected (gamma = 2.0) by the computer program Scion Image (Scion Corporation; www.scioncorp.de). It was found that pixel luminousness was highest in the middle of the illuminated area but did not vary by more than 5% from the average value of all pixels within the illuminated area at all tested light intensities. The kinetics of maximal chlorophyll fluorescence F_m was tested with a Teaching-PAM (Walz GmbH) and it was assured that F_m reached a plateau within the time of the saturation pulse of the Imaging-PAM (800 ms) for all plants investigated.

After plants were kept in the dark for about 1 h, leaves were clamped in the fluorometer and minimum (F_o) and maximum (F_m) fluorescence were recorded. When actinic light was

switched on, maximum fluorescence in the light (F_m') and steady state fluorescence prior to the flash (F_t) were measured (cf. Walz 2003) while saturated light flashes were applied. This allowed calculation of the effective quantum yield of photosystem II (Φ_{PSII}) and the linear electron transport rate $ETR = \Phi_{PSII} \cdot PFD_a \cdot 0.5$ (cf. Genty, Briantais, & Baker 1989) with PFD_a as the absorbed light fraction (0.84); 0.5 accounts for the partitioning of the energy between *PSI* and *PSII*. Non-photochemical quenching was calculated according to Maxwell & Johnson (2000) with $NPQ = (F_m - F_m')/F_m'$.

2.8.1.1 Experimental conditions

Homobaric plants of *V. faba*, *N. tabacum* and heterobaric plants of *Ph. vulgaris*, *G. max* were used 6 to 8 weeks after sowing. Experiments with well watered plants were performed under laboratory conditions with approximately 25°C and 50% r.h. Experiments in which drought stress was applied were performed in an experimental cabinet at air temperatures of $28 \pm 0.5^\circ\text{C}$; air humidity was then $50 \pm 5\%$ r.h. equivalent to *VPD* of 1.9 kPa. Plants exposed to drought stress were not irrigated for about 48 h before an experiment started. At that time, first symptoms of wilting became already visible on some leaves of *V. faba* and *N. tabacum* plants, while leaves of *G. max* and *Ph. vulgaris* showed no visible symptoms.

2.8.1.2 Experimental protocol

In a first set of experiments, leaves were partially shaded by templates made from black adhesive tapes that were fixed on both, the upper and lower surface of the leaves in order to close stomata artificially. This treatment was performed to simulate leaf chamber sealing. Chlorophyll fluorescence was then measured within the illuminated area of about 1 x 1 cm (cf. Fig. 19; page 57). In a second set of experiments, shading was performed by putting templates of black paper on the upper side of the leaves, a treatment by which stomatal conductance was not influenced (cf. Fig. 20 and Fig. 22; page 59 and 62). In both sets of experiments, leaves were first adapted to dark, then clamped in the imaging fluorometer and F_o and F_m was measured. Thereafter, actinic light was switched on providing a PFD of $290 \mu\text{mol m}^{-2} \text{s}^{-1}$ to the illuminated leaf area. Saturated light flashes were applied every 20th or 30th second. Below the templates of adhesive tape and black paper PFD was about 0

and $1\text{--}3\ \mu\text{mol m}^{-2}\text{ s}^{-1}$, respectively. Chlorophyll fluorescence was measured on the illuminated part of the leaves while the shadow was either moved over the leaf according to the protocol given in figure 20 (page 59) or fixed at one position (Fig. 22, page 62).

2.8.2 Combined measurements of chlorophyll fluorescence and gas exchange

The experiments were performed with mature leaves of *V. faba* and *G. max*. The plants were well irrigated and exposed to different drought stress between 1 to 6 days without irrigation.

The gas exchange system described previously (Chapter 2.3.1, Fig. 2; page 16) was used to perform the experiments combining measurements of chlorophyll fluorescence and gas exchange. The leaf chamber illustrated in figure 4 (page 18) allowed to enclose the whole leaf and to place the Imaging-PAM (Chapter 2.7.1) over the leaf chamber (cf. Fig. 7; page 31). The leaf temperature in the leaf chamber ranged between $23\text{--}23.5^\circ\text{C}$ in darkness, whereas when the actinic light was switched on, it ranged between $24\text{--}25^\circ\text{C}$ depending on the transpiration rate. The molar flow through the gas exchange system was $0.85\ \mu\text{mol s}^{-1}$ and a bypass pump (cf. GP3, Fig. 2; page 16) provided a volume flux through the chamber of approximately $60\ \text{cm}^3\text{ s}^{-1}$ in order to reduce the boundary layer resistance.

2.8.2.1 The experimental protocol

In order to measure photosynthesis under fluctuating light, the whole leaf was enclosed in the leaf chamber and gas exchange and chlorophyll fluorescence was measured. A piece of non-translucent paper with a circular opening of $d=23\text{ mm}$ (i.e. $4.15\ \text{cm}^2$) was put on the leaf so that only the leaf part underneath the opening was illuminated. On the paper was a mounting with a second piece of non-translucent paper which had an opening of $d=10\text{ mm}$, (i.e. $0.79\ \text{cm}^2$). The mounting allowed to move one piece of paper over the other one. Thus, the illuminated leaf area was defined either by the large or small opening (cf. Fig. 7 a, b; page 31). The illumination was performed with the LED ring of the Imaging-PAM which was mounted over the leaf chamber.

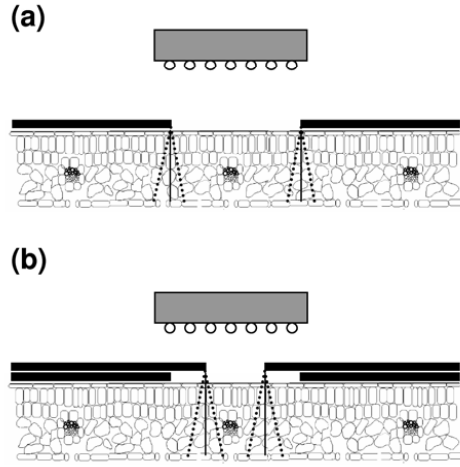


Figure 7. Schematic drawing of a leaf partly shaded by black paper. In (a) a large spot area is illuminated whereas in (b) a small spot area remained is lighted. The light source is indicated by the horizontal bar with a set of LEDs which represents the LED ring of the Imaging PAM. The dotted line indicates the diffuse light caused by the shade while the solid line points to ideal shading.

The experiments started with measurement of dark respiration of the whole leaf enclosed in the leaf chamber. Then the leaf area defined by the large opening of the non-translucent paper (large spot) was illuminated with actinic light ($150 \mu\text{mol m}^{-2} \text{s}^{-1}$). Gas exchange of the whole leaf and chlorophyll fluorescence parameters (Φ_{PSII} , NPQ and ETR cf. Chapter 2.7.1) of the large spot were measured for 8 minutes. In the subsequent step the paper with the small opening was moved over the large spot and whole leaf gas exchange and chlorophyll fluorescence of the illuminated small spot was measured for 8 minutes. Saturated light flashes were applied every 30th second in all treatments.

2.8.2.2 Data analysis

The net CO_2 uptake of the whole leaf under illumination with the small ($A_{leaf,s}$) or large ($A_{leaf,l}$) lightfleck was calculated as the difference between the net CO_2 exchange rate in darkness ($NCER_{dark}$) and under illumination ($NCER_{light}$) with $A_{leaf} = NCER_{dark} - NCER_{light}$.

The gross assimilation rates of the small (A_S) and large (A_L) illuminated lightfleck was calculated according to equation 6:

$$A_S = \frac{A_{leaf,s} \cdot LA_{leaf}}{LA_S} \quad \text{or} \quad A_L = \frac{A_{leaf,l} \cdot LA_{leaf}}{LA_L} \quad \text{Eqn. 6}$$

with LA_{leaf} as the area of the whole leaf and, LA_S and LA_L as the small and large illuminated leaf area, respectively.

Water use efficiency (WUE) was calculated under illumination with the large (WUE_L) and small spot (WUE_S) according to equation 7:

$$WUE_S = \frac{A_{leaf\ s}}{E_{leaf\ s}} \quad or \quad WUE_L = \frac{A_{leaf\ l}}{E_{leaf\ l}} \quad \text{Eqn. 7}$$

where $E_{leaf\ s}$ and $E_{leaf\ l}$ represent leaf transpiration when the small and large spot was illuminated, respectively.

Electron requirement for assimilated CO_2 (e/A) was calculated according to equation 8:

$$e / A_S = \frac{ETR_S}{A_S} \quad or \quad e / A_L = \frac{ETR_L}{A_L} \quad \text{Eqn. 8}$$

with ETR_S and ETR_L as the mean electron transport rate of the small and large spot, respectively.

The percentage of electrons used to reduce O_2 (PR , %) was calculated as the difference between the e/A regression curves obtained under photorespiratory ($e/A_{21\%}$) and non-photorespiratory ($e/A_{1\%}$) conditions according to the equation 9:

$$PR = 100 \bullet \frac{e / A_{21\%} - e / A_{1\%}}{A_{21\%}} \quad \text{Eqn. 9}$$

The quantum yield of CO_2 efficiency (Φ_{CO_2}) was measured under non-photorespiratory conditions and calculated according to equation 10:

$$\Phi_{CO_2\ s} = \frac{A_S}{PAR} \quad or \quad \Phi_{CO_2\ l} = \frac{A_L}{PAR} \quad \text{Eqn. 10}$$

Regression analysis was performed using the software TableCurve (SPSS Inc. Version 4) by using least squares analysis, the fit with the lowest sum of square residuals was used to compose the regression curve.

2.8.2.3 Estimation of measurement errors

Shading a leaf part with non-translucent paper led to slight light inhomogeneities in the illuminated area along the light-shade borderline (LSB). These inhomogeneities were due to diffuse light along the LSB. The diffusion of light appeared on the edge of the paper used for shading but also inside the leaf (Fig. 7; page 31). When the small spot was illuminated light diffusion was higher because the shading paper with the small spot was put on the paper with the large spot which doubled the distance between the edge of the paper and the leaf (Fig. 7 b; page 31). Additionally, bundle sheath extensions may have transferred light deep into the leaf resulting in enhanced photosynthetic capacity (Nikolopoulos et al. 2002).

The equations used to calculate quantum yield, ϕ_{PSII} , and non-photochemical quenching, NPQ , give information about the measurement error. ϕ_{PSII} is not, or only slightly, influenced by inhomogeneous light along the LSB. When regarding the equation with $\phi_{PSII} = (F_m' - F_o')/F_m'$ (cf. Maxwell et al. 2000), the terms F_m' and F_o' are influenced by diffuse light in the same way, relatively. This leads to minor changes of ϕ_{PSII} due to small light inhomogeneities. On the other hand, NPQ is calculated according to the equation: $NPQ = (F_m - F_m')/F_m'$ (cf. Maxwell et al. 2000) which contains the term F_m recorded at the beginning of an experiment and taken as a constant. Since F_m' is influenced by diffuse light NPQ may increase along LSB. In heterobaric leaves with strict mesophyll compartmentation NPQ should be constant independently of the size of the lightfleck. Thus, changes in NPQ of the small illuminated light spot relative to the large illuminated spot for leaves with heterobaric anatomy can be used as an estimate of the error caused by light inhomogeneities.

Chapter 3 Results

3.1 Diffusion inside leaves

3.1.1 Biometric parameters of the investigated leaves

The leaves of *G. max* and *P. vulgaris* display heterobaric anatomy (Jahnke 2001; Terashima 1992), whereas *V. faba* (Terashima 1992) and *N. tabacum* (Jahnke et al. 2002) are homobaric. All four plant species are characterised by amphistomatous leaves (Napp-Zinn 1984). A direct comparison of the obtained data with published ones was facilitated since most of the species taken from the literature (Tab. 4; page 39) were also amphistomatous; *Ficus carica* and *Tilia cordata* were the only two species in table 4 (page 39) to have hypostomatous leaves (Napp-Zinn 1984). Different biometric leaf parameters were collected to calculate potential internal lateral diffusion areas of the plant species investigated. Leaf thickness, thickness of spongy and palisade parenchyma as well as leaf porosity differed between the heterobaric and homobaric leaves (Tab. 2; page 35): the homobaric leaves were thicker and had significantly higher porosities (53% in broad bean, 38% in tobacco) as compared to the heterobaric ones.

Table 2. Anatomic leaf parameters of the investigated plant species. Thickness of leaves and the respective palisade and spongy tissues, leaf porosity (%) represents intercellular air space volume as percentage of the corresponding leaf volume. Results are given as arithmetic means \pm standard error of the mean (*SEM*); n, number of replicates. Statistical analysis was performed by t-test, different letters indicate that differences were significant ($p \leq 0.05$).

Leaf anatomy / Plant species	n	Leaf [μm]	Palisade tissue [μm]	Spongy tissue [μm]	Leaf porosity [μm]
homobaric					
<i>Vicia faba</i>	88	479 ± 6^a	184 ± 4^a	255 ± 4^a	53 ± 2^a
<i>Nicotiana tabacum</i>	90	373 ± 5^b	163 ± 3^b	177 ± 3^b	38 ± 1^b
heterobaric					
<i>Phaseolus vulgaris</i>	88	229 ± 3^c	95 ± 2^c	99 ± 1^c	32 ± 1^c
<i>Glycine max</i>	90	188 ± 2^d	84 ± 1^d	81 ± 1^d	32 ± 1^c

3.1.2 Gas conductance and conductivity of the intercellular air space

To quantify lateral gas diffusion, apparent rates of respiration were measured in the dark by using a double-gasket leaf chamber (Fig. 3, page 17). By changing the CO₂ concentrations on both sides of the inner chamber gasket ($c_{a,i}$ and $c_{a,o}$; Fig. 8 a; page 36), potential changes in $NCER$ were evaluated. In heterobaric leaves of *G. max*, no statistically significant effects of the treatments were observed (Fig. 8 b; page 36) but, in homobaric *V. faba* leaves, substantial changes in apparent $NCER$ became obvious (Fig. 8 c; page 36). Lateral gas conductance of individual leaves ($g_{leaf,l}$) was calculated on the basis of changes in apparent $NCER$ (see Eqn. 2 and 3; page 21). Heterobaric leaves of bean and soybean showed negligible lateral gas conductance ($g_{leaf,l}$) whereas, for homobaric leaves of broad bean and tobacco, the values were substantially larger (Tab. 3; page 37).

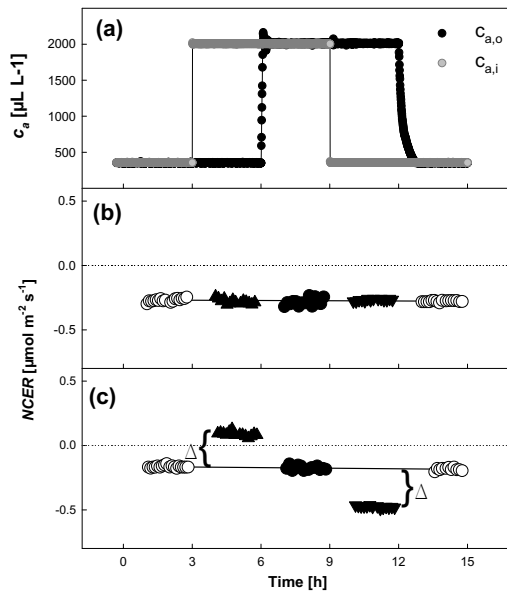


Figure 8. Apparent net CO₂ exchange rates ($NCER$) in the dark of *Glycine max* and *Vicia faba* leaves obtained under different CO₂ concentrations. (a) Atmospheric CO₂ concentration provided in the inner ($c_{a,i}$) and outer leaf chamber ($c_{a,o}$) of the double-gasket chamber (cf. Fig. 3; page 17). Under the respective atmospheric CO₂ concentrations, the apparent $NCER$ of (b) *G. max* and (c) *V. faba* leaves are shown. Differences ($\Delta = \Delta NCER$) between $NCER_{ref}$ obtained at $c_{a,o} = c_{a,i} = 350 \mu\text{L L}^{-1}$ and $\Delta NCER$ measured when there was a gradient between $c_{a,o}$ and $c_{a,i}$ were used to calculate lateral gas conductances of the leaves as described in the text. A regression line was drawn through the respiration rates at the beginning and the end of the experiment with $c_{a,o} = c_{a,i} = 350 \mu\text{L L}^{-1}$.

There was a positive relationship for homobaric leaves between biometric leaf parameters and calculated lateral gas conductance: highest conductances were obtained for broad bean

having thicker leaves and higher leaf porosity than tobacco (Tab. 2 and 3; page 35 and page 37).

Lateral gas conductance in the heterobaric leaves of *P. vulgaris* and *G. max* was found to be very small, while ranging between 8 and 28 mmol m⁻² s⁻¹ in homobaric leaves (Tab. 3; page 37). On the other hand, vertical conductances were between 17 and 333 mmol m⁻² s⁻¹ as taken from the literature (Tab. 4; page 39). When conductivities as a measure of specific leaf properties were calculated, lateral conductivities ($g_{leaf,l}^*$) of the homobaric leaves ranged between 67 and 209 $\mu\text{mol m}^{-1} \text{s}^{-1}$ (Tab. 3; page 37) while vertical conductivities ($g_{leaf,v}^*$) were between 3 and 78 $\mu\text{mol m}^{-1} \text{s}^{-1}$ as recalculated from published data (Tab. 4; page 39).

Table 3. Lateral gas conductance ($g_{leaf,l}$) and conductivity ($g_{leaf,l}^*$) inside leaves. The leaf chamber type refers to either the large (LLC; 7 cm in diameter) or the small sized leaf chamber (LC_i; 2 x 3 cm) with gasket widths of 8 and 6 mm, respectively. By taking the respective gasket widths into account, conductivities were calculated according to equation 4 (page 21). AE_{DR} , apparent CO₂ effect on respiration due to lateral gas diffusion when the gradient in CO₂ concentration (Δc_a) was 1650 $\mu\text{L L}^{-1}$ (with $c_{a,o} = 2000$ and $c_{a,i} = 350$ $\mu\text{L CO}_2 \text{L}^{-1}$); mean, arithmetic mean; n , number of replicates; SEM , standard error of the mean. Statistical analysis was performed by ANOVA; *, significant differences between the treatments ($p \leq 0.05$); n.s., non significant. ¹When conductances or conductivities were very low (i.e. around zero), calculation sometimes resulted in negative values which was within the limits of accuracy of the measurements.

Leaf anatomy/ Plant species	Leaf chamber	n	$g^{leaf,l}$ (mmol m ⁻² s ⁻¹)		$g^{* leaf,l}$ (μmol m ⁻¹ s ⁻¹)		AE_{DR} (%)		
			<i>mean</i>	<i>SEM</i>	<i>mean</i>	<i>SEM</i>	<i>mean</i>	<i>SEM</i>	<i>P</i>
<u>homobaric</u>									
<i>Vicia faba</i>	LLC	13	26.1	2.6	209.2	21.0	174.2	21.0	*
	LC _i	6	27.8	6.5	166.6	39.0	783.2	118.0	*
<i>Nicotiana tabacum</i>	LLC	14	7.8	0.8	67.8	6.0	59.3	6.1	*
	LC _i	6	13.4	6.2	80.1	6.9	306.2	36.6	*
<u>heterobaric</u>									
<i>Phaseolus vulgaris</i>	LLC	13	-0.7 ¹	0.7	-5.8 ¹	4.6	-0.8	1.1	n.s.
	LC _i	6	0.3	0.2	2.1	1.4	1.7	1.4	n.s.
<i>Glycine max</i>	LLC	9	0.3	0.7	0.6	5.7	-1.8	1.0	n.s.
	LC _i	6	0.4	0.4	0.4	2.2	-0.8	2.0	n.s.

The effect of diffusion path length on lateral gas conductance was investigated in more detail by increasing the width of the chamber gasket between 6, 14 and 22 mm. This

caused obvious changes in gas conductance between 28, 11 and 5.6 $\text{mmol m}^{-2} \text{s}^{-1}$ (Fig. 9 a; page 38) whereas gas conductivity was not substantially affected showing values of 170, 150 and 130 $\mu\text{mol m}^{-1} \text{s}^{-1}$, respectively (Fig. 9 b; page 38).

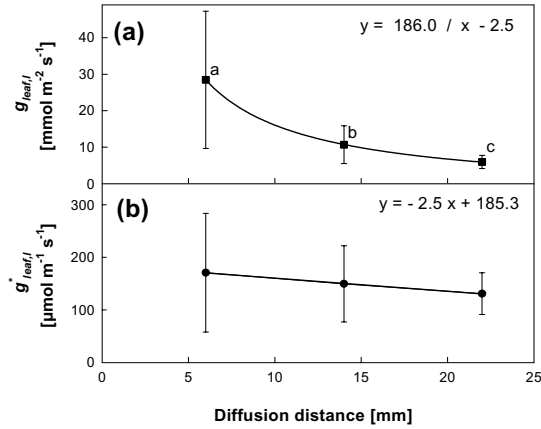


Figure 9. Lateral gas conductance (a) and conductivity (b) versus diffusion distance measured on leaves of *Vicia faba*. The solid lines present regression lines by using (a) the hyperbolic function $f(x) = a/x + b$ and (b) the linear function $f(x) = a \cdot x + b$. Arithmetic means \pm standard error of the mean ($n = 6$). Statistical analysis was performed by ANOVA, different letters, significant (in all cases $p \leq 0.05$) difference between the treatments.

The values of lateral conductivity ($g^*_{leaf,l}$) experimentally obtained from the investigated plant species were clearly smaller (Fig. 10; open symbols; page 40) than maximum conductivities in free air (dashed line). Diffusion pathways in intercellular air spaces of leaves are obstructed by the arrangement of cells inside the mesophyll, and tortuosity (τ) has thus to be considered (Parkhurst 1994). Terashima et al. (1996) proposed a tortuosity factor of 1.5 for spongy tissues which was used here to calculate exemplary conductivities corrected for tortuosity (Fig. 10; closed symbols; page 40). Gas conductivity of *V. faba* and *N. tabacum* leaves then reached 80% and 42% of the calculated maximum conductivity whereas, when tortuosity was not taken into account (open symbols), the respective values were 52% and 28%.

Table 4. Vertical gas conductances ($g_{leaf,v}$) of leaves. The data were collected from the literature and the corresponding vertical gas conductivities ($g_{leaf,v}^*$) were calculated here by using leaf thickness (vertical diffusion path length) for the particular species found in the literature.

Plant species	$g_{leaf,v}$ (mmol m ⁻² s ⁻¹)	Method used	Leaf thickness (μm)	$g_{leaf,v}^*$ (μmol m ⁻¹ s ⁻¹)
<i>Ficus carica</i> L.	174	CO ₂ exchange, fluorescence ¹	262 ⁶	46
<i>Gossypium herbaceum</i> L.	222	vertical diffusion of N ₂ O ²	130 ⁶	29
<i>Helianthus annuus</i> L.	249	CO ₂ exchange, fluorescence ¹	280 ⁶	70
<i>Tilia cordata</i> Mill.	141	CO ₂ exchange, fluorescence ¹	108 ⁶	15
<i>Vigna unguiculata</i> (L.) Walp.	176	CO ₂ exchange, fluorescence ¹	178 ⁶	31
<i>Xanthium strumarium</i> L.	164	vertical diffusion of He ³	235 ⁶	39
	154	CO ₂ exchange, fluorescence ¹		36
	333	vertical diffusion of CO ₂ ⁴		78
<i>Zea mays</i> L.	17	vertical diffusion of N ₂ O ⁵	165 ⁶	3

¹(Laisk & Loreto 1996); ²(Jarvis & Slatyer 1970); ³(Farquhar & Raschke 1978); ⁴(Mott & O'Leary 1984); ⁵(Long et al. 1989); ⁶(Napp-Zinn 1984)

Lateral gas conductance or conductivity obtained for leaves of a given plant species was almost independent of the size and type of the leaf chamber but the apparent relative effect of lateral CO₂ diffusion on measured $NCER$ differed largely. When measured with the large-sized leaf chamber, a gradient in CO₂ concentration (Δc_a) of 1650 μL L⁻¹ across the chamber gasket caused apparent CO₂ effects on $NCER_a$ of *V. faba* and *N. tabacum* leaves (174% and 59%, respectively; Tab. 3; page 37). Whereas, when using the small-sized chamber the effects were substantially larger (783% and 306%, respectively). For the heterobaric leaves, the effects of Δc_a on $NCER_a$ were not statistically significant.

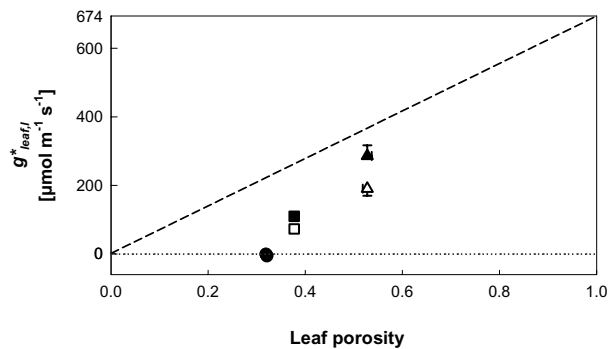


Figure 10. Lateral gas conductivity as a function of leaf porosity. Maximum gas conductivity in air at 101.3 kPa and 20 °C was calculated and drawn as dashed line. Experimental data are presented for leaves of *Glycine max* and *Phaseolus vulgaris* (circles), *Nicotiana tabacum* (squares) and *Vicia faba* (triangles). For each plant

species, leaf conductivities were calculated according to equations 1 – 4 (page 20-21) and presented by open symbols. The closed symbols show conductivities corrected for an assumed tortuosity factor of 1.5. Arithmetic means \pm standard error of the mean; $n = 88 - 90$ for leaf porosity and $n = 15 - 20$ for conductivity; cf. table 2 and 3 (page 35 and page 37).

3.1.3 Summary of diffusion inside leaves

Gas conductance of the intercellular air space of homobaric leaves in lateral (paradermal) direction was smaller than in vertical direction, i.e. across the leaf blade. However, gas conductance depends on the diffusion distance. Therefore gas conductivity was calculated, which renders the specific internal gas properties of leaves. Gas conductivity was in heterobaric leaves small but not zero. In homobaric leaves, it was larger in lateral than in vertical direction. Thus, potential lateral gas fluxes may be considerable, which may substantially influence gas exchange measurements when there is a gas gradient between the leaf chamber and the air outside the chamber.

3.2 Influence of lateral diffusion on gas exchange measurement

3.2.1 Measurement of dark respiration

The grade of homobary can be judged from gas exchange measurements by creating a gradient between the inner and outer leaf chamber (LC; cf. Fig. 3; page 17). The experiments were performed in darkness because no 'disturbing' processes like photosynthesis and photorespiration influence the potential lateral gas fluxes. The resulting lateral fluxes influence the apparent $NCER$ as presented in figure 8 (page 36). The experimental protocol,

however, was shortened, the step $c_{a,i}=2000 \mu\text{L L}^{-1}$ and $c_{a,o}=350 \mu\text{L L}^{-1}$ was not performed (cf. Fig. 8; page 36). The plants were taken from sites described in table 1 (page 13). For two plant species *Cyclamen persicum* and *Pulmonaria officinalis*, the protocol was further shortened by dropping the step $c_{a,i}=2000 \mu\text{L L}^{-1}$ and $c_{a,o}=2000 \mu\text{L L}^{-1}$ (cf. Fig. 8; page 36).

The respiration rates obtained under $c_{a,i}=c_{a,o}=350 \mu\text{L L}^{-1}$ were regarded as reference ($NCER_{ref}$, cf. chapter 3.1.2). When no significant change between $NCER_{ref}$ and the apparent respiration under a gradient between the inner and outer leaf chamber ($c_{a,i}=350 \mu\text{L L}^{-1}$ and $c_{a,o}=2000 \mu\text{L L}^{-1}$; $\Delta NCER$) was observed, the plant species were defined as heterobaric (Tab. 5; page 41). When significant differences were observed, the plant species were defined as homobaric (Tab. 6; page 42). The homobaric plants were then classified into three subgroups with slightly (10 species), medium (7 species) and highly homobaric leaves (2 species) (Tab. 6; page 42). Additionally, *N. tabacum* and *V. faba* can be added to the high homobary class, too (Tab. 3; page 37).

Table 5. Plant species with heterobaric leaves where no significant change in apparent CO_2 effect (AE_{DR}) on respiration was measured. AE_{DR} was obtained when the gradient in CO_2 concentration (Δc_a) was $1650 \mu\text{L L}^{-1}$ (with $c_{a,o}=2000$ and $c_{a,i}=350 \mu\text{L CO}_2 \text{ L}^{-1}$); $DR_{c_{a,o}=c_{a,i}}$, percentage of $NCER$ measured under $c_{a,o}=c_{a,i}=2000 \mu\text{L CO}_2 \text{ L}^{-1}$ and $c_{a,o}=c_{a,i}=350 \mu\text{L CO}_2 \text{ L}^{-1}$; mean, arithmetic mean; n , number of replicates; SEM , standard error of the mean. Statistical analysis was performed by paired t-test with significant differences for $P<0.05$.

Plant species	n	AE_{DR}			$DR_{ca,i=ca,o}$		
		[%]	SEM	P	[%]	SEM	P
<u>heterobaric</u>							
<i>Euphorbia amygdaloides</i> L.	6	3.8	6.8	0.3721	-0.6	10.6	0.9393
<i>Hedera helix</i> L.	6	12.6	9.3	0.0678	-9.1	25.6	0.8444
<i>Ligustrum vulgare</i> L.	5	4.2	4.2	0.1677	3.7	11.8	0.5868
<i>Mentha spec.</i> L.	6	10.1	8.9	0.1219	13.1	16.6	0.1335
<i>Nerium oleander</i> L.	6	9.1	12.7	0.2092	-23.7	40.7	0.4567
<i>Phragmites australis</i> (Cav.) Trin. ex Steud.	6	3.5	3.3	0.0639	-1.0	3.5	0.9939
<i>Rumex crispus</i> L.	6	5.8	4.1	0.0826	-7.9	8.4	0.1011
<i>Smilax spec.</i> L.	6	-2.3	1.8	0.1256	-23.1	24.5	0.1007
<i>Taraxacum officinale</i> F.H.Wigg.	6	11.2	8.3	0.0522	-8.7	19.7	0.5203
<i>Zea mays</i> L.	6	4.9	4.1	0.0543	7.4	8.3	0.1532

Both homobaric and heterobaric species showed no significant effect on respiration obtained at high $[\text{CO}_2]$ in the inner and outer chamber ($c_{a,i}=c_{a,o}=2000 \mu\text{L L}^{-1}$) and low $[\text{CO}_2]$ ($c_{a,i}=c_{a,o}=350 \mu\text{L L}^{-1}$) (Tab. 3, 5 and 6; pages 37, 41, 42).

Table 6. Plant species with leaves defined as homobaric where a significant change in apparent CO_2 effect (AE_{DR}) on respiration was measured. AE_{DR} was obtained when the gradient in CO_2 concentration (Δc_a) was $1650 \mu\text{L L}^{-1}$ (with $c_{a,o}=2000$ and $c_{a,i}=350 \mu\text{L CO}_2 \text{ L}^{-1}$); $DR_{c_{a,o}=c_{a,i}}$ percentage of $NCER$ measured under $c_{a,o}=c_{a,i}=2000 \mu\text{L CO}_2 \text{ L}^{-1}$ and $c_{a,o}=c_{a,i}=350 \mu\text{L CO}_2 \text{ L}^{-1}$; mean, arithmetic mean; n , number of replicates; SEM , standard error of the mean. Statistical analysis was performed by paired t-test with significant differences for $P<0.05$.

Plant species	n	AE_{DR}			$DR_{ca,i=ca,o}$		
		[%]	SEM	P	[%]	SEM	P
<u>slightly homobaric</u>							
<i>Acanthus mollis</i> L.	6	6.2	3.4	0.0410	0.9	6.9	0.7387
<i>Arum maculatum</i> L.	6	33.2	10.9	0.0061	5.1	14.7	0.7754
<i>Beta vulgaris</i> L.	6	35.9	13.9	0.0015	-22.6	22.2	0.0782
<i>Calendula arvensis</i> L.	5	28.3	15.3	0.0078	11.7	14.0	0.3469
<i>Cichorium intybus</i> L.	6	20.5	5.5	0.0008	-3.2	18.0	0.7665
<i>Dianthus barbatus</i> L.	6	20.6	7.8	0.0012	-2.8	5.1	0.4715
<i>Fallopia aubertii</i> (Henry) Holub	5	10.1	3.2	0.0005	0.3	5.7	0.8406
<i>Ilex aquifolium</i> L.	6	7.3	2.7	0.0255	3.5	9.1	0.8346
<i>Picris hieracioides</i> L.	4	12.2	5.0	0.0206	-4.5	4.6	0.1826
<i>Plantago lanceolata</i> L.	6	21.5	8.4	0.0003	2.5	5.6	0.5365
<u>medium homobaric</u>							
<i>Capsicum frutescence</i> L.	6	77.4	25.4	0.0003	7.1	5.8	0.0741
<i>Chenopodium album</i> L.	6	82.3	11.9	0.0001	2.4	9.5	0.7994
<i>Cirsium arvense</i> (L.) Scop.	6	62.3	39.0	0.0114	-19.7	20.5	0.1136
<i>Citrus spec.</i> L.	6	69.3	17.5	0.0071	10.0	9.0	0.0972
<i>Pulmonaria officinalis</i> L.	6	72.8	20.4	0.0000	n.m.	n.m.	n.m.
<i>Skimmia japonica</i> Nakai	6	70.5	27.6	0.0000	6.1	7.6	0.3168
<i>Cyclamen persicum</i> L.	6	97.5	76.5	0.0197	n.m	n.m	n.m
<u>highly homobaric</u>							
<i>Lupinus spec.</i> Rydb.	6	284.4	89.1	0.0001	-13.2	15.3	0.1834
<i>Mimulus guttatus</i> DC.	6	221.2	45.7	0.0000	10.4	11.8	0.2059

3.2.2 Measurement of photosynthesis

The influence of lateral diffusion on photosynthetic gas exchange was investigated by measuring the dependence of photosynthesis on CO_2 (A/c_i curves) for plants grown in the greenhouse at the research Centre Jülich. The experiments were performed at $500 \mu\text{mol}$

photons $\text{m}^{-2} \text{s}^{-1}$. Preexperiments had shown that photosynthesis was saturated at this light intensity.

The A/c_i curve obtained at identical $c_{a,i}$ and $c_{a,o}$ was taken as reference (open circles; Fig. 11; page 43). The profiles were analysed when $[\text{CO}_2]$ was changed in the different chambers of the double gasket leaf chamber. When $c_{a,o}$ was constant at $350 \mu\text{L L}^{-1}$ (closed circles, Fig. 11; page 43), a different curve profile was observed for *V. faba* (Fig. 11 a; page 43) and *N. tabacum* (data not shown) as compared to the reference. No difference was observed between the two curves obtained for *G. max* (Fig. 11 b; page 43) and *Ph. vulgaris* (data not shown). The parameters derived from the A/c_i curves showed significant differences between the two curves when regarding homobaric and heterobaric leaves (Tab. 7 - 10; page 44 and following).

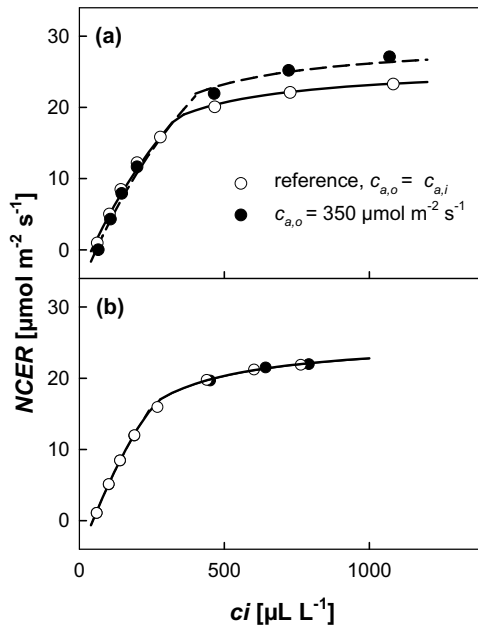


Figure 11. The dependence of photosynthesis on $[\text{CO}_2]$ (A/c_i) measured with a double gasket leaf chamber (cf. Fig. 3; page 17) for (a) homobaric leaves of *Vicia faba* and (b) heterobaric leaves of *Glycine max*. For each experiment two A/c_i curves were obtained when the $[\text{CO}_2]$ inside ($c_{a,i}$) and outside ($c_{a,o}$) the chamber was identical or when $c_{a,o}$ was kept constant at $350 \mu\text{L L}^{-1}$ and $c_{a,i}$ was varied according to the experimental protocol (cf. Fig. 5; page 24).

Both plant species with homobaric leaves, *V. faba* and *N. tabacum* showed significant increases of RubisCO mediated carboxylation (V_{cmax}) when there was a gradient between the inner and outer leaf chamber (4.3% and 2.4 %), respectively. *Ph. vulgaris* and *G. max*, as

heterobaric species, were not influenced by this gradient and showed not significant changes of V_{cmax} (Tab. 7; page 44)

Table 7. Maximum rate of RubisCO mediated carboxylation (V_{cmax} ; $\mu\text{mol m}^{-2} \text{s}^{-1}$) obtained under different $[\text{CO}_2]$ in the external leaf chamber. $V_{cmax,ref}$ was obtained under identical $[\text{CO}_2]$ in the inner ($c_{a,i}$) and outer ($c_{a,o}$) leaf chamber which is regarded as reference, $V_{cmax,\Delta}$ was measured under constant $c_{a,o}=350 \mu\text{L L}^{-1}$. The apparent effect on V_{cmax} ($AE_{V_{cmax}}$) denotes the change in V_{cmax} calculated as $100 \cdot (V_{cmax,\Delta} - V_{cmax,ref}) / V_{cmax,ref}$. Statistical analysis was performed with paired t-test with significant differences for $P < 0.05$. *SEM*, standard error of the mean; *n*, number of replicates.

Plant species	n	$V_{cmax,ref}$		$V_{cmax,\Delta}$		$AE_{V_{cmax}}$	
		mean	SEM	mean	SEM	[%]	P
<i>Vicia faba</i>	5	74.6	6.6	77.9	5.7	4.3	0.0032
<i>Nicotiana tabacum</i>	5	66.4	9.6	66.0	9.7	2.4	0.0015
<i>Phaseolus vulgaris</i>	5	67.7	7.2	67.1	7.7	-1.0	0.2900
<i>Glycine max</i>	5	66.3	13.9	66.3	13.4	-0.1	0.9146

The effect observed for V_{cmax} could also be seen for the maximal electron transport rate (J_{max}). However, the effect in homobaric plants was larger and showed a significant increase of J_{max} of 10.0 and 4.6 % for *V. faba* and *N. tabacum*, respectively. Heterobaric plants were not significantly affected (Tab. 8; page 44)

Table 8. Maximum rate of carboxylation limited by electron transport (J_{max} ; $\mu\text{mol m}^{-2} \text{s}^{-1}$) obtained under different $[\text{CO}_2]$ in the external leaf chamber. $J_{max,ref}$ was measured under identical $[\text{CO}_2]$ in the inner ($c_{a,i}$) and outer ($c_{a,o}$) leaf chamber which is regarded as reference, $J_{max,\Delta}$ was measured under constant $c_{a,o}=350 \mu\text{L L}^{-1}$. The apparent effect on J_{max} ($AE_{J_{max}}$) is the change of J_{max} calculated as $100 \cdot (J_{max,\Delta} - J_{max,ref}) / J_{max,ref}$. Statistical analysis was performed with paired t-test with significant differences for $P < 0.05$. *SEM*, standard error of the mean; *n*, number of replicates.

Plant species	n	$J_{max,ref}$		$J_{max,\Delta}$		$AE_{J_{max}}$	
		mean	SEM	mean	SEM	[%]	P
<i>Vicia faba</i>	5	109.3	7.6	120.2	8.0	10.0	0.0051
<i>Nicotiana tabacum</i>	5	96.5	17.4	101.0	17.7	4.6	0.0030
<i>Phaseolus vulgaris</i>	5	70.4	11.7	69.5	11.6	-1.5	0.1688
<i>Glycine max</i>	5	83.2	19.6	83.0	19.6	-0.3	0.4536

The CO_2 compensation point (I) as well as respiration in light (day respiration, R_D) was also influenced in homobaric plant species. I increased by 20 and 7.3% for *V. faba* and *N. tabacum*, respectively whereas I was not significantly influenced in heterobaric plants (Tab. 9; page 45). The apparent effect (AE_{RD}) on respiration in light was even larger, homobaric plants were affected by 114.9 and 36.2% for *V. faba* and *G. max*, respectively whereas heterobaric species were not significantly influenced (Tab. 10; page 45). This reveals a similarity to the dark respiration experiments where AE_{DR} was even more affected by lateral diffusion (Tab. 3; page 37).

Table 9. CO_2 compensation point (I) obtained under different $[\text{CO}_2]$ in the external leaf chamber. I_{ref} was measured under identical $[\text{CO}_2]$ in the inner ($c_{a,i}$) and outer ($c_{a,o}$) leaf chamber which is regarded as reference, I_{Δ} was measured under constant $c_{a,o}=350 \mu\text{L L}^{-1}$. The apparent effect on I (AE_I) is the change of I calculated as $100 \cdot (I_{\Delta} - I_{ref}) / I_{ref}$. Statistical analysis was performed with paired t-test with significant differences for $P < 0.05$. *SEM*, standard error of the mean; *n*, number of replicates.

Plant species	n	I_{ref}		G_D		AE_I	
		mean	SEM	mean	SEM	[%]	P
<i>Vicia faba</i>	5	47.2	2.2	56.7	4.3	20.0	0.0085
<i>Nicotiana tabacum</i>	5	50.1	4.2	53.8	4.2	7.3	0.0069
<i>Phaseolus vulgaris</i>	5	58.3	6.9	57.9	6.4	-0.6	0.3320
<i>Glycine max</i>	5	52.4	4.3	52.5	4.4	0.2	0.7536

Table 10. Respiration in light (day respiration, R_D) obtained under different $[\text{CO}_2]$ in the external leaf chamber. $R_{D,ref}$ was measured under identical $[\text{CO}_2]$ in the inner ($c_{a,i}$) and outer ($c_{a,o}$) leaf chamber which is regarded as reference, $R_{D,\Delta}$ was measured under constant $c_{a,o}=350 \mu\text{L L}^{-1}$. The apparent effect on R_D (AE_{RD}) is the change in R_D calculated as $100 \cdot (R_{D,\Delta} - R_{D,ref}) / R_{D,ref}$. Statistical analysis was performed with paired t-test with significant differences for $P < 0.05$. *SEM*, standard error of the mean; *n*, number of replicates.

Plant species	n	$R_{D,ref}$		$R_{D,\Delta}$		AE_{RD}	
		mean	SEM	mean	SEM	[%]	P
<i>Vicia faba</i>	5	-0.7	0.2	-1.6	0.4	114.9	0.0069
<i>Nicotiana tabacum</i>	5	-0.8	0.2	-1.1	0.2	36.2	0.0052
<i>Phaseolus vulgaris</i>	5	-1.5	0.6	-1.5	0.6	-3.3	0.2446
<i>Glycine max</i>	5	-1.0	0.2	-1.0	-0.5	-0.2	0.8454

In homobaric leaves, gradients in CO_2 between the leaf chamber and the surrounding air significantly influenced the measurement of CO_2 response of photosynthesis and the parameters derived from the A/c_i curves. In most gas exchange systems, measurement of A/c_i

curves is normally performed under ambient air outside the chamber, whereas inside the chamber $[\text{CO}_2]$ is varied. Thus, lateral gradients are unavoidable when a leaf part is enclosed in a clamp on leaf chamber.

3.2.3 Shading of the leaf part outside the leaf chamber

Partly shaded leaves show leaf internal gradients between shaded and illuminated leaf area. In shaded leaf part respiratory processes cause a CO_2 source and in illuminated areas photosynthetic CO_2 uptake generates a CO_2 sink, which entails lateral fluxes. A series of experiments was performed with leaves from which part was enclosed in the leaf chamber while the leaf area outside the chamber was shaded or illuminated at $c_{a,i}$ of $60 \mu\text{L L}^{-1}$ while $c_{a,o}$ was constant at $350 \mu\text{L L}^{-1}$. Leaf areas outside the leaf chamber were first shaded (closed circles; Fig. 12; page 46) and then illuminated (open circles; Fig. 12; page 46). When homobaric leaves of *V. faba* were investigated, a significant increase in $NCER$ was measured after removing the shade outside the cuvette (Fig. 12 a; page 46). For heterobaric leaves of *G. max*, shading or illuminating the leaf blade outside the leaf chamber had no effect on $NCER$ (Fig. 12 b; page 46).

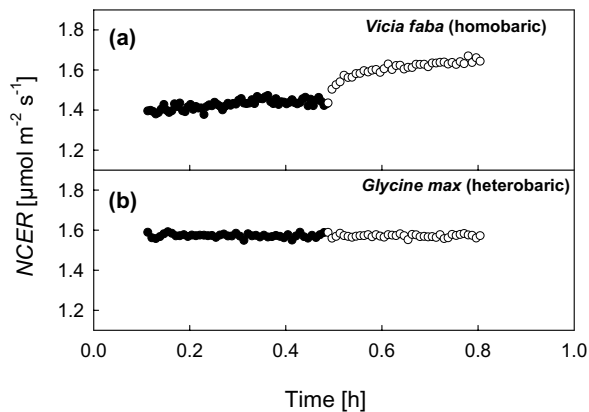


Figure 12. Net CO_2 exchange rates ($NCER$) of leaf areas enclosed in a clamp-on leaf chamber while leaf parts outside the chamber were exposed either to light or shade. Homobaric leaf of (a) *Vicia faba* and heterobaric one of (b) *Glycine max*. Closed circles represent $NCER$ when leaves were shaded outside the chamber while open circles show $NCER$ after the shade was removed. The photon flux density was $500 \mu\text{mol m}^{-2} \text{s}^{-1}$; $[\text{CO}_2]$ inside the chamber $60 \mu\text{L L}^{-1}$ and outside the chamber $350 \mu\text{L L}^{-1}$.

The assimilation rates obtained when the leaf area outside the chamber was shaded ($NCER_{shade}$) was 7.2 % and 6.7 % higher then the assimilation obtained under illumination of the leaf area inside and outside the chamber ($NCER_{ref,\Delta}$) for *V. faba* and *N. tabacum* (Tab. 11; page 47). In *Ph. vulgaris* and *G. max*, no significant influence of shading of the leaf area outside the chamber was observed (Tab. 11; page 47).

Table 11. Net CO₂ exchange rate ($NCER$) of a leaf part enclosed in a leaf cuvette while the leaf area outside was shaded ($NCER_{shade}$) or exposed to the same light intensity as the leaf area inside the chamber ($NCER_{ref,\Delta}$). The photon flux density (PFD) was 500 $\mu\text{mol m}^{-2} \text{s}^{-1}$ and [CO₂] inside $c_{a,i}=60 \mu\text{L L}^{-1}$ and outside $c_{a,o}=350 \mu\text{L L}^{-1}$. SEM , standard error of the mean; AE_{shade} , apparent effect of shade on $NCER$ calculated as $100 \cdot (NCER_{shade} - NCER_{ref,\Delta}) / NCER_{ref,\Delta}$; statistical analysis was performed with paired t-test with significant differences for $P < 0.05$; n , number of replicates.

Plant species	n	$NCER_{ref,\Delta}$		$NCER_{shade}$		AE_{shade}	
		$[\mu\text{mol m}^{-2} \text{s}^{-1}]$	SEM	$[\mu\text{mol m}^{-2} \text{s}^{-1}]$	SEM	[%]	P
<i>Vicia faba</i>	9	1.51	0.15	1.40	0.15	-7.20	0.0079
<i>Nicotiana tabacum</i>	4	1.16	0.36	1.08	0.36	-6.72	0.0022
<i>Phaseolus vulgaris</i>	4	1.12	0.27	1.12	0.27	0.08	0.3891
<i>Glycine max</i>	4	1.51	0.08	1.51	0.08	-0.01	0.7858

For the analysis of A/c_i curves (see paragraph 3.2.2), $NCER$ was also measured under different [CO₂] in the inner and outer leaf chamber (cf. Fig. 5; page 24 and Fig. 11; page 43). $NCER$ obtained under $c_{a,i}$ of 65 $\mu\text{L L}^{-1}$ is presented in table 12 (page 48). In contrast to the previous experiment, the illumination was homogeneous but $c_{a,o}$ was changed while $c_{a,i}$ remained constant. When $c_{a,i}=c_{a,o}=65 \mu\text{L L}^{-1}$ reference $NCER$ was measured ($NCER_{ref}$) and when $c_{a,o}$ was increased to 350 $\mu\text{L L}^{-1}$ ($NCER_{\Delta c}$). Creating a [CO₂] gradient between $c_{a,i}$ and $c_{a,o}$ influenced the apparent $NCER$ ($AE_{\Delta c}$) by 58.2 and 27.3% for *V. faba* and *N. tabacum* respectively (Tab. 12; page 48), whereas $NCER$ of *Ph. vulgaris* and *G. max* was not significantly influenced by this treatment (Tab. 12; page 48).

Table 12. Net CO₂ exchange rate ($NCER$) measured with a double gasket leaf chamber (LC, cf. Fig. 3; page 17) to obtain dependence of photosynthesis on CO₂ (cf. Fig. 11; page 43). $NCER$ obtained under [CO₂] inside and outside the leaf chamber $c_{a,i}=c_{a,o}=65 \mu\text{L L}^{-1}$ was regarded as reference ($NCER_{ref}$). When $c_{a,o}=65 \mu\text{L L}^{-1}$ the apparent assimilation rate was regarded as ($NCER_{\Delta c}$). Photon flux density (PFD) was $500 \mu\text{mol m}^{-2} \text{s}^{-1}$. SEM , standard error of the mean; $AE_{\Delta c}$, apparent effect of a CO₂ gradient on $NCER$ calculated as $100*(NCER_{\Delta c} - NCER_{ref})/NCER_{ref}$; statistical analysis was performed with paired t-test with significant differences for $P<0.05$; n , number of replicates.

Plant species	n	$NCER_{ref}$		$NCER_{\Delta c}$		$AE_{\Delta c}$	
		$[\mu\text{mol m}^{-2} \text{s}^{-1}]$	SEM	$[\mu\text{mol m}^{-2} \text{s}^{-1}]$	SEM	[%]	P
<i>Vicia faba</i>	5	0.99	0.07	0.41	0.32	-58.21	0.0081
<i>Nicotiana tabacum</i>	5	0.77	0.26	0.56	0.25	-27.27	0.0024
<i>Phaseolus vulgaris</i>	5	0.39	0.23	0.40	0.22	-1.31	0.5040
<i>Glycine max</i>	5	0.68	0.36	0.68	0.46	-1.74	0.2573

3.2.4 Summary of the impact of lateral diffusion on gas exchange measurements

The screening of differences in leaf anatomy on 33 plant species revealed that 21 species showed homobaric leaves (Tab. 3 and Tab. 6; page 37 and page 42) with different grades of homobary. There was an inter- and intraspecific variability in the properties of the intercellular air space which determined leaf internal gas fluxes in lateral direction of the leaf blades. The interspecific differences were mainly caused by differences in leaf thickness, porosity etc. A single leaf shows large veins which completely prevent gas movement in lateral directions while minor veins more or less prominently obstruct gas diffusion. Thus, the mere position of where the leaf chamber was clamped determined intraspecific differences.

Lateral diffusion significantly affected gas exchange measurements in light (A/c_i curves) and in darkness when there was a gradient between the leaf chamber and the air outside. The impact was substantial when small exchange rates were measured e.g. dark respiration, respiration in light, CO₂ compensation point in light etc. A gas gradient in lateral direction may also be enhanced by shading of a leaf part outside the chamber which causes an increase of intercellular CO₂ concentrations in the shaded leaf part due to respiration. The resulting increased lateral flux reduced apparent assimilation rate.

3.3 Gas exchange measurement under overpressure in the leaf chamber

The intercellular spaces of leaf mesophyll can provide an internal open-porous system in homobaric leaves allowing diffusive fluxes when there is a gas gradient. This raised the question whether the intercellular space system of homobaric leaves may also allow gas flow when pressure differences between the leaf chamber and the atmosphere are not zero and to what extent the pressure driven fluxes influence gas exchange measurements.

3.3.1 Measurement of dark respiration

A gradient in $[\text{CO}_2]$ changed the apparent $NCER$ for homobaric leaves of *V. faba* (Fig. 13 a and b; page 49) which was also observed in previous chapter (chapter 3.12; Fig. 8; page 36); however, no statistically significant difference was observed for 7 replicates when a slight overpressure of 2 kPa inside the leaf chamber (ΔP =leaf chamber pressure – atmospheric pressure) was established (Fig. 13 c; page 49).

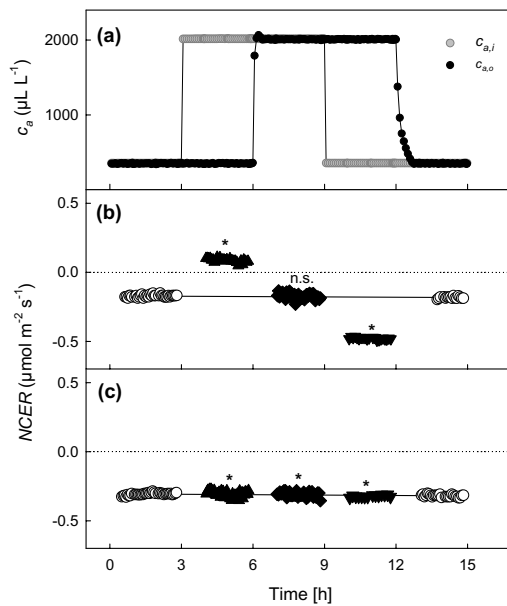


Figure 13. Apparent net CO_2 exchange rate ($NCER$) in the dark of *Vicia faba* leaves measured under different CO_2 concentrations and different pressure in the leaf chamber. (a) Atmospheric CO_2 concentration provided inside ($c_{a,i}$) and outside ($c_{a,o}$) the leaf chamber. Under respective atmospheric $[\text{CO}_2]$ the apparent $NCER$ measured (b) under atmospheric pressure and (c) overpressure with a pressure difference to the atmosphere of 2 kPa. * indicates statistically significant difference; n.s. no significant differences when compared with the reference $NCER$ obtained under $c_{a,i}=c_{a,o}=350 \mu\text{L L}^{-1}$; statistical analysis was performed with t-test with significant difference for $p<0.05$.

The influence of overpressure on *NCER* in darkness was investigated in more detail to study the interaction of diffusive and pressure driven fluxes and to clarify whether overpressure may influence dark respiration. *NCER* was measured while ΔP was continuously increased from 0 to 3 kPa. This procedure had no influence on *NCER* of heterobaric leaves of *G. max* independently of the CO_2 gradient between $c_{a,i}$ and $c_{a,o}$ and whether the whole leaf or a leaf part was enclosed in the leaf chamber (cf. Fig. 14 a; page 50). For homobaric leaves of *V. faba* no change of *NCER* was observed when the whole leaf was enclosed in the leaf chamber (open circles in Fig. 14 b and c; page 50). However, lateral gas fluxes affected the measurement when only a part of the same leaf was enclosed and there was a gradient between $c_{a,i}$ and $c_{a,o}$ (with $c_{a,i}=350 \mu\text{L L}^{-1}$ and $c_{a,o}=700 \mu\text{L L}^{-1}$, Fig. 14 b, and $c_{a,i}=700 \mu\text{L L}^{-1}$ and $c_{a,o}=350 \mu\text{L L}^{-1}$, Fig. 14 c, respectively; page 50). A substantial difference was observed between *NCERs* when ΔP was low, which disappeared when ΔP was only slightly increased (approximately 0.2 kPa; Fig. 14 b and c; page 50).

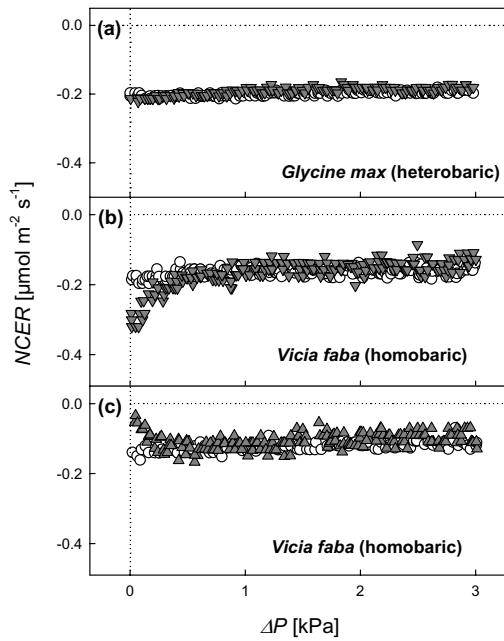


Figure 14. Net CO_2 exchange rate (*NCER*) plotted versus pressure difference between leaf chamber and atmosphere (ΔP). Either the whole leaf (open circles) or part (grey triangles) of the same leaf of (a) *Glycine max* and (b), (c) *Vicia faba* was enclosed in the leaf chamber while ΔP was increased from 0 to 3 kPa. In (a) and (b) $[\text{CO}_2]$ inside the leaf chamber ($c_{a,i}$) was $350 \mu\text{L L}^{-1}$ and outside ($c_{a,o}$) $700 \mu\text{L L}^{-1}$; in (c), reverse CO_2 concentrations with $c_{a,i}=700 \mu\text{L L}^{-1}$ and $c_{a,o}=350 \mu\text{L L}^{-1}$ were created.

Thus, dark respiration was not influenced by overpressure when a heterobaric leaves of *G. max* or whole leaves of *V. faba* (no lateral fluxes possible) were enclosed in the leaf chamber. When one leaf part was enclosed, a very small overpressure caused a pressure driven

flux which was larger than lateral gas diffusion because no impact of a gas gradient on *NCER* was observed. Further ΔP increase had no impact on *NCER*, which indicates that diffusion processes in darkness were not affected by overpressure.

3.3.2 Photosynthetic gas exchange under overpressure

Overpressure causes an increase in partial pressure of a single gas species in a given volume of air. Thus, an increase in air pressure by 3 kPa (i.e., approximately 3% when regarding normal atmospheric pressure as 100 kPa) inside the leaf chamber resulted in an enhanced CO_2 uptake (cf. Fig. 15; page 52). However, when the CO_2 partial pressure inside the leaf chamber was reduced by 3%, *NCER* was identical to the one measured under ambient atmospheric pressure (Fig. 15 c; page 52). This indicates that the impact of the increasing pressure was attributed to increased partial pressure of CO_2 . The increase of *NCER* in light with increasing ΔP was measured only when whole leaves of *V. faba* were enclosed in the leaf chamber. In this case, no lateral fluxes driven by the pressure gradient between the leaf chamber and atmosphere through the intercellular air space of the homobaric leaf were possible (Fig. 15; page 52). Whereas, when a leaf part was enclosed in the leaf chamber a pressure driven flux substantially influenced apparent CO_2 uptake (cf. Fig. 16; page 53).

The mean increase of *NCER* of *V. faba* leaves under overpressure of 3 kPa (whole leaf inside the chamber, $n=15$) was $0.14 \pm 0.1 \mu\text{mol m}^{-2} \text{s}^{-1} \text{kPa}^{-1}$, which was obtained under PFD of $700 \mu\text{mol m}^{-2} \text{s}^{-1}$ and $c_a=350 \mu\text{L L}^{-1}$. This value is similar to that calculated according to the model of Farquhar et al. (1980) with $0.13 \mu\text{mol m}^{-2} \text{s}^{-1} \text{kPa}^{-1}$. The calculation was performed using V_{cmax} (Tab. 7; page 44) and R_D (Tab. 10; page 45). Intercellular CO_2 (c_i) was assumed to be $240 \mu\text{L L}^{-1}$ (when atmospheric $[\text{CO}_2]$ is approximately $350 \mu\text{L L}^{-1}$) and ambient O_2 . The parameter K_c , K_o , I^* (cf. chapter 2.6) given in von Caemmerer (2000) were used for the calculation.

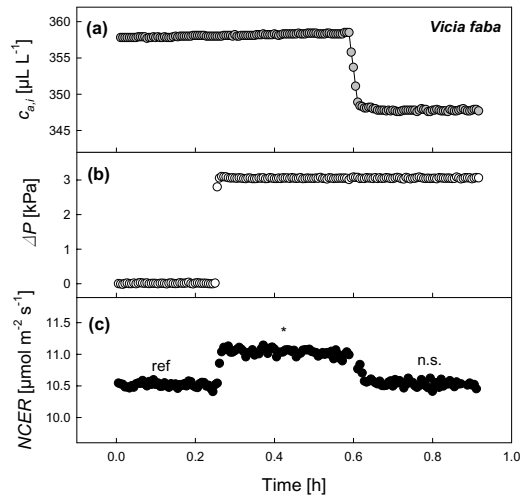


Figure 15. Net CO₂ exchange rate (NCER) of a whole leaf enclosed in a leaf chamber measured when air pressure and [CO₂] was changed in the leaf chamber. In (a) atmospheric CO₂ inside the leaf chamber (with a drop in $c_{a,i}$ from 358 to 347 $\mu\text{L L}^{-1}$); (b) pressure difference between the leaf chamber and atmosphere (ΔP); (c) NCER measured under the respective conditions in (a) and (b) and photon flux density (PFD) of 700 $\mu\text{mol m}^{-2} \text{s}^{-1}$. Statistical analysis was performed using t-test where the reference NCER (ref) was measured under $c_a=358 \mu\text{L L}^{-1}$ and

ΔP of 0 kPa and compared with NCER under the varying conditions presented in (a) and (b). *, statistically significant difference ($p<0.05$); n.s., non significant difference.

When only one part of the leaf was enclosed, heterobaric leaves of *G. max* showed a slight increase in NCER (Fig. 16 a; page 53) which corresponds to the increase observed in figure 15 (page 52). With *V. faba* leaves, a substantial decrease of the photosynthetic NCER of approximately 50 % at $\Delta P = 3 \text{ kPa}$ was observed (Fig. 16 b; page 53). This decrease was dependant on g_{leaf} . When the plant was exposed to drought stress, a decrease in g_{leaf} resulted in lower influence of ΔP on the apparent NCER, causing a lower slope with declining g_{leaf} (Fig. 16 c; page 53).

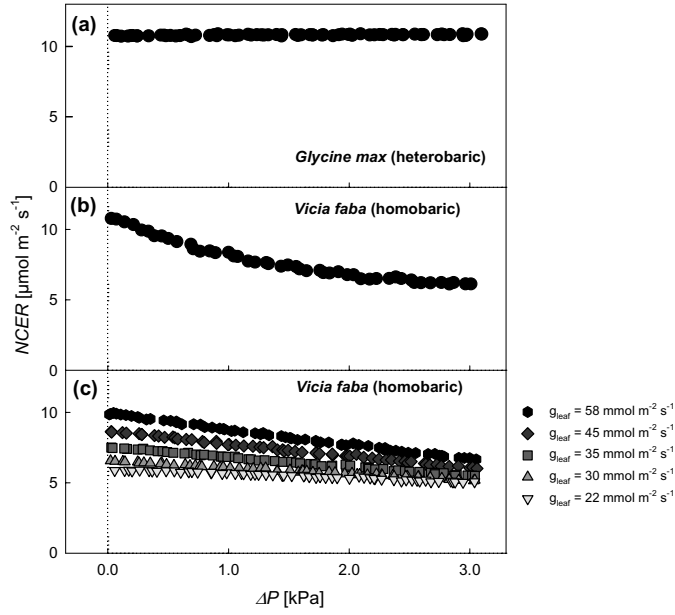


Figure 16. Net CO₂ exchange rate (*NCER*) plotted versus increasing pressure difference to atmosphere (ΔP). In (a) *NCER* of a heterobaric leaf of *G. max* and in (b) of a homobaric leaf of *V. faba* was measured. The experiments were performed under photon flux density of 700 $\mu\text{mol m}^{-2} \text{s}^{-1}$ and atmospheric [CO₂] inside and outside the leaf chamber of 350 $\mu\text{L L}^{-1}$ with well irrigated plants with high leaf conductance of $g_{\text{leaf}}=300 \mu\text{mol m}^{-2} \text{s}^{-1}$ and $g_{\text{leaf}}=160 \mu\text{mol m}^{-2} \text{s}^{-1}$ in (a) and (b), respectively. The plant in (c) was exposed to drought stress and showed decreasing stomatal conductance (g_{leaf}) during the experiment.

The drop in *NCER* with rising ΔP (Fig 16 c; page 53) was recalculated for all performed experiments with *V. faba* and the initial slopes were plotted versus g_{leaf} , which defined the dependence of *NCER* on ΔP ($NCER/\Delta P$; Fig. 17; page 54). The impact of ΔP on *NCER* under low g_{leaf} was small, but under high g_{leaf} *NCER* decreased substantially up to 7 $\mu\text{mol m}^{-2} \text{s}^{-1} \text{kPa}^{-1}$ (Fig. 17; page 54).

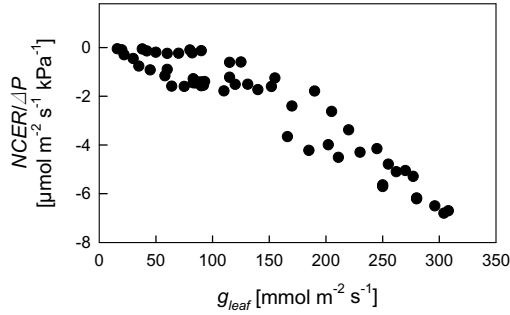


Figure 17. Dependence of net CO₂ exchange rate on pressure difference to atmosphere ($NCER/\Delta P$) versus leaf conductance g_{leaf} for leaves of *V. faba* when one part of the leaf was enclosed in the leaf chamber. The experiments were performed under photon flux density (PFD) of 700 $\mu\text{mol m}^{-2} \text{s}^{-1}$ and atmospheric CO₂ concentration of 350 $\mu\text{L L}^{-1}$ inside and outside the leaf chamber.

3.3.3 Transpiration and overpressure

Transpiration (E) decreased under overpressure when a heterobaric leaves of *G. max* was measured (data not shown) or when the whole homobaric leaf of *V. faba* was enclosed in the leaf chamber (Fig. 18 a; page 55) according to the calculated dependence of E on air pressure (Eqn. 5, page 27). Increasing air pressure increases the water vapour pressure in the air, but it has no influence on the water vapour pressure inside the leaf. Thus, overpressure reduces the vapour pressure deficit between the leaf and air resulting in decreased E . However, when a leaf part of *V. faba* was enclosed in the leaf chamber the pressure gradient between the leaf chamber and atmosphere caused a pressure driven flux within the leaf mesophyll and the measured E diverged substantially from the calculated E (Eqn. 5; page 27 and Fig. 18 b; page 55).

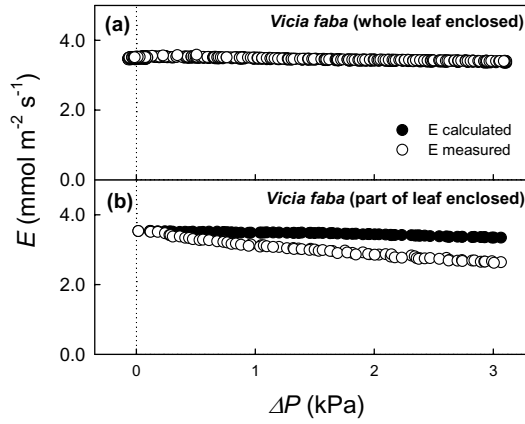


Figure 18. Influence of pressure difference to atmosphere (ΔP) on transpiration (E). In (a), a homobaric leaf of *V. faba* was measured when the whole leaf was enclosed in the leaf chamber and in (b), a part of the leaf part was enclosed in the leaf chamber. The transpiration was either measured (open circles) or calculated (closed circles) according to equation 5 (page 27).

3.3.4 Summary of the impact of overpressure on gas exchange measurement

When no lateral fluxes inside leaves were possible (i.e. heterobaric leaves or whole homobaric leaves enclosed in the leaf chamber) overpressure in the leaf chamber influenced gas exchange of leaves as theoretically deduced. Dark respiration was not influenced; photosynthetic CO_2 uptake increased because rising air pressure increased the CO_2 partial pressure; transpiration decreased due to reduced water pressure deficit between leaf and air. When one leaf part was enclosed, overpressure caused a pressure driven fluxes inside homobaric leaves. The impact of a gas gradient on dark respiration disappeared under low overpressure and further ΔP increase had no influence on dark respiration; photosynthetic CO_2 uptake showed almost linear decrease with increasing ΔP , which was large under high g_{leaf} and decreased at low g_{leaf} ; transpiration decreased under overpressure substantially more than the calculated decline with rising air pressure.

3.4 Chlorophyll fluorescence of partly shaded leaves

CO₂ gradients occur within a leaf when a leaf part is shaded and respiratory processes dominate (CO₂ source) whereas the adjacent leaf area is illuminated causing CO₂ uptake (CO₂ sink). Lateral gradients between CO₂ source and sink result in lateral fluxes, which were studied with chlorophyll fluorescence with spatial resolution with plants under different water status.

3.4.1 Well watered plants

In the first series of chlorophyll fluorescence studies, measurements were performed on well irrigated plants having no drought stress. Under these conditions no stomatal limitations on CO₂ supply from surrounding air can be expected. To simulate the gasket of a leaf chamber leaves were shaded by templates of adhesive tapes, which stuck tightly to the adaxial as well as the abaxial side of the leaves and sealed stomata.

After onset of illumination distinct heterogeneities in quantum yield (ϕ_{PSII} ; Fig. 19 a-d; page 57) were observed in the illuminated leaf area and temporal changes in the distribution of ϕ_{PSII} (Fig. 19 a-c; page 57). For regions in various distances from the shade on the imaged leaf part (ROIs 1-5; Fig. 19 c; page 57), ϕ_{PSII} values were averaged (Fig. 19 d; page 57). Quantum yield was higher close to the shade (ROI 3 and 5) than in the centre of the illuminated leaf segment (ROI 1). Spatial heterogeneities in ϕ_{PSII} were highest about 10 min after light was switched on, but were still present when ϕ_{PSII} values reached steady-state (Fig. 19 d; page 57). When *V. faba* leaves were covered with templates made of black paper, a treatment by which stomata in the shaded region were not sealed, no differences in ϕ_{PSII} between ROIs located at different distances to the shade were observed (data not shown).

When heterobaric leaves of *Ph. vulgaris* were shaded with adhesive tapes as described above, no effects on ϕ_{PSII} with respect to the distance from the shade were observed (Fig. 19 e-h; page 57). Quantum yield was more or less homogeneously distributed over the illuminated leaf area, and homogeneity was not altered between 10, 25 and 35 min after light was switched on (Fig. 19 e, f and g, respectively; page 57). The temporal profiles of

ϕ_{PSII} at different ROIs (Fig. 19 g; page 57) after onset of illumination (Fig. 19 h; page 57) also indicate that quantum yield was independent of the distance from the shade.

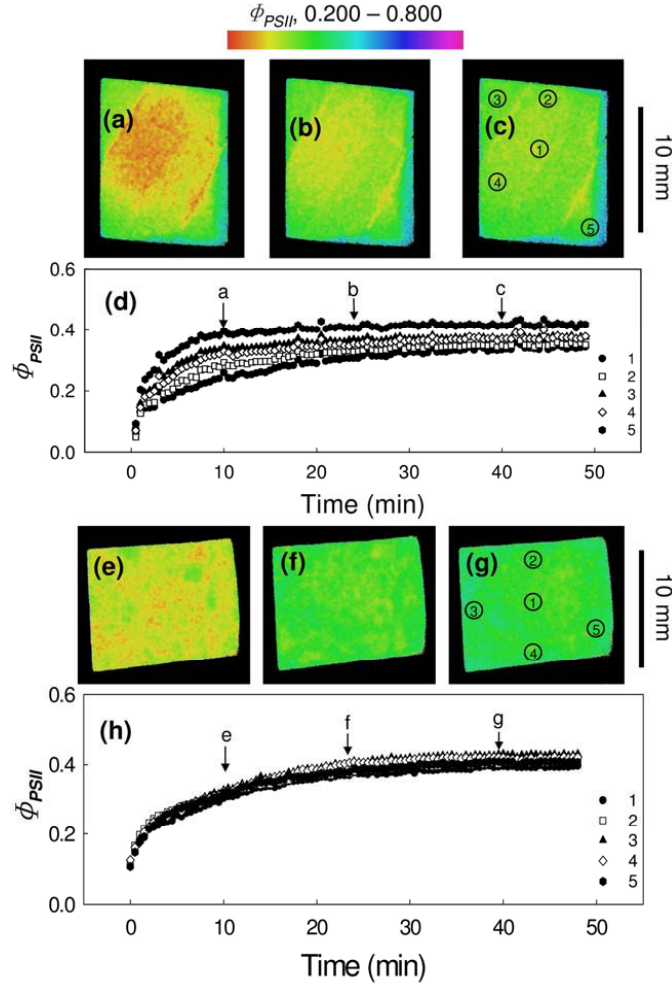
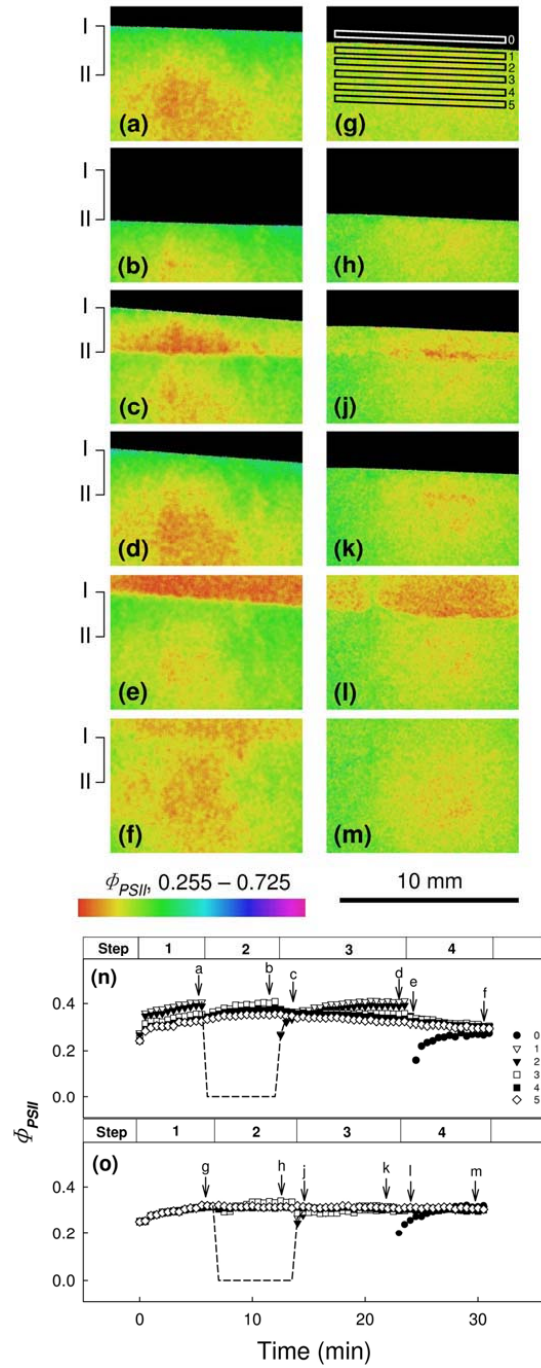


Figure 19. Quantum yield of photosystem II (ϕ_{PSII}) of rectangular leaf areas exposed to actinic light ($290 \mu\text{mol m}^{-2} \text{s}^{-1}$) and shaded outside by non-transparent adhesive tapes on both, the adaxial and abaxial side of the leaves, which simulated a gasket of a leaf chamber. Measurements on a homobaric leaf of *V. faba* (a-d) and a heterobaric leaf of *Ph. vulgaris* (e-h) are shown. The experiments were performed on well-watered plants. The numbered circles (1-5) in (c) and (g) indicate regions of interest (ROI) over which ϕ_{PSII} values were averaged and for which changes over time are plotted in (d) and (h), respectively. The experiments started at time 0 when the pre-darkened leaves were illuminated with actinic light. The times when the ϕ_{PSII} images (a - c, e - g) were captured are indicated by arrows in (d) and (h), respectively.

3.4.2 Plants under drought stress

In a second series of experiments, chlorophyll fluorescence studies were performed on *V. faba* plants under drought stress to study the impact of reduced stomatal conductance on lateral CO₂ fluxes when a part of a leaf is shaded with a template of black paper. The potential stomatal diffusion was not disturbed by this treatment. The position of the shade was varied (Fig. 20 a-f; shade position I and II; page 59). With varying distances to the light/shade border (LSB), ϕ_{PSII} values were averaged at ROIs 0-5 (Fig. 20 n, see Fig. 20 g for positions; page 59). At the start of the experiment LSB was at position I (Fig. 20 a; page 59), ROI 0 in the dark, and ROIs 1-5 in actinic light with a PFD of 290 $\mu\text{mol m}^{-2} \text{s}^{-1}$. ϕ_{PSII} developed a gradient with highest values adjacent to the shade (Fig. 20 n, step 1; page 59). After the LSB was moved to position II, ROIs 0-2 were shaded (Fig. 20 b; page 59); the gradient in ϕ_{PSII} between ROIs 3-5 vanished momentarily but recovered quickly (Fig. 20 n, step 2; page 59). When the LSB was placed back to position I, the former LSB at position II remained transitorily visible whereas at the new LSB a new gradient in ϕ_{PSII} evolved (Fig. 20 c; page 59); however, the gradient in ϕ_{PSII} between ROIs 1-5 reappeared within a few minutes (Fig. 20 d and n, step 3; page 59) to similar values as in step 1. After the shade was removed, the previously shaded area was still visible with almost uniform values in ϕ_{PSII} which were lower than the continuously illuminated leaf section (Fig. 20 e; page 59). Within a few minutes in actinic light, however, ϕ_{PSII} values were uniform over the whole illuminated leaf area (Fig. 20 f; page 59). Accordingly, the gradient in ϕ_{PSII} between ROIs 1-5 vanished (Fig. 20 n, step 4; page 59). At ROI 0, which was in the dark from the beginning of the experiment, ϕ_{PSII} values started at about zero but increased with time in the light and reached those of the other ROIs within approximately 6 minutes (Fig. 20 n, end of step 4; page 59).

A corresponding set of experiments was performed with heterobaric leaves of *G. max*. In this case, shading caused no, or only small, gradients in ϕ_{PSII} values with respect to the distance from the shade (Fig. 20 g, h and o; page 59). The only effect appeared when a previously shaded leaf part was again exposed to light which was the case when LSB was moved from position II back to position I (Fig. 20 j and o, step 3; page 59) or when shading was completely removed (Fig. 20 l and o, step 4; page 59).



Lateral CO₂ diffusion from shaded to illuminated leaf areas increased ϕ_{PSII} along the LSB only when stomatal conductance was low. Sticking adhesive tape on a leaf blade sealed stomata and CO₂ released under the tape had to diffuse laterally to the illuminated leaf part which increased ϕ_{PSII} . When stomatal conductance was high and a leaf part was shaded by a template of black paper (stomata were not sealed) CO₂ supply from surrounding air was large that no impact of lateral CO₂ diffusion was observed. Stomatal closure under drought stress limited CO₂ supply from the air and the impact of lateral CO₂ from shaded area was clearly visible along LSB. Movement of the shade over the leaf blade caused reappearance of heterogeneities in ϕ_{PSII} along LSB at each position of the shade while removal of the shade resulted in homogenous ϕ_{PSII} over the illuminated leaf area.

3.4.3 Quantification of the effect of lateral diffusion on photochemical and non-photochemical quenching

In order to analyse the effects of lateral diffusion on ϕ_{PSII} and non-photochemical quenching (NPQ), a series of experiments was performed similar to the protocol of step 1 shown in figure 20 n and o (page 59). Five ROIs (1-5) were defined were ROI 1 averaged fluorescence parameters measured at a distance of 1 mm from LSB, ROI 2 at a distance of 2 mm, and ROI 3-5 from 3-5 mm, respectively (similar to ROIs shown in Fig. 20 g; page 59). The mean of seven experiments describe the dependence of steady state ϕ_{PSII} and NPQ on diffusion distance (Fig. 21; page 61). For *V. faba* and *N. tabacum* similar characteristics of ϕ_{PSII} - dependence on the distance from the shade were observed. The highest value for ϕ_{PSII} was at ROI 1 and declined with increasing distance (Fig 21 a; page 61). NPQ dependence on the distance from the shade was also similar in both species. However, it showed reverse characteristics than ϕ_{PSII} with lowest value close to the shade and an increase with distance from LSB (Fig. 21; page 61). When ROI 5 was taken as reference assuming that it was not influenced by the shade, the relative increase of ϕ_{PSII} in ROI 1 was 13.0 % and 12.6 % for *V. faba* and *N. tabacum*, respectively. The relative change of NPQ , however, showed a decrease of 19.6 % for *V. faba* and 24.8% for *N. tabacum*. Therefore the effect on NPQ was twice as large as ϕ_{PSII} . Heterobaric leaves of *Ph. vulgaris* and *G. max* showed no statistically significant changes of the fluorescence parameters with distance from the shade (Fig. 21; page 61).

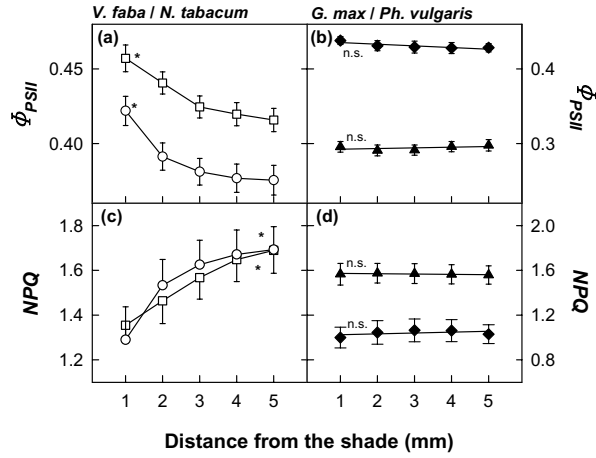


Figure 21. Change of quantum yield of PSII (Φ_{PSII}) and non-photochemical quenching (NPQ) over the illuminated leaf area with respect to the distance from the shade measured on plants under drought stress. In (a) mean Φ_{PSII} for the homobaric leaves of *Vicia faba* (open squares) and *Nicotiana tabacum* (open circles) and in (b) for the heterobaric leaves of *Glycine max* (closed triangles) and *Phaseolus vulgaris* (closed diamonds) are shown. The corresponding mean

NPQ are in (c) for plants with homobaric and (d) with heterobaric leaf anatomy, respectively. Arithmetic means ($n=7$) are plotted together with standard error of the mean. Statistical analysis was performed with ANOVA with significant difference for $p < 0.05$; * significant difference; n.s. not significant difference.

3.4.4 Re-watering of drought stressed plants

In order to study, if drought stress was actually responsible for the obvious difference between leaves of well-watered and water starved plants of *V. faba*, drought stressed plants were re-watered during the experiments. The (homobaric) leaves were partially shaded and different ROIs were identified with respect to distance from the shade (Fig. 22; page 62). In drought stress plants a gradient in quantum yield was established between ROIs 1-5 with highest Φ_{PSII} values near the shade (Fig. 22 a and Fig. 22 e between -12 and 0 min; page 62). However, when the plants were re-watered, quantum yield became homogeneously distributed over the illuminated leaf area with time (Fig. 22 b-d; page 62) and the gradient in Φ_{PSII} disappeared within 20 min (Fig. 22 e; page 62). Such effects were never found when heterobaric leaves of *G. max* plants were treated the same way: no gradients in Φ_{PSII} near the LSB were observed (cf. Fig. 19 e-h; page 57) and this was independent of the water status of the plant (data not shown).

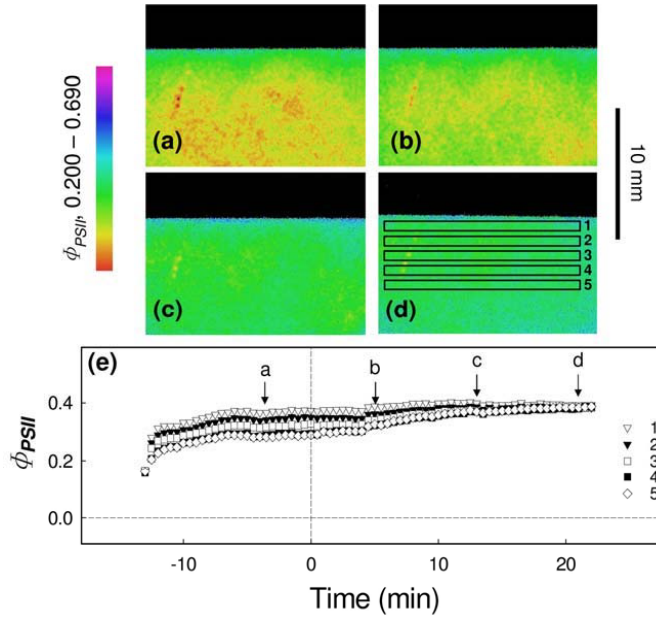


Figure 22. Quantum yield of photosystem II (Φ_{PSII}) of a homobaric leaf of *V. faba* when part of the leaf was shaded (black areas in a-d). In (a), Φ_{PSII} imaging was performed when the plant was under drought stress. The Φ_{PSII} images shown in (b), (c) and (d) were obtained at subsequent times after the plant was re-watered. In (d), five rectangular regions of interest (ROI) are shown for which the respective mean values of Φ_{PSII} were calculated; they are presented in (e) before and after the plants were re-watered at time 0. The arrows indicate the times the respective Φ_{PSII} images (a-d) were taken.

3.4.5 Summary of chlorophyll fluorescence of partly shaded leaves

Laterally diffusing CO_2 from shaded to illuminated leaf areas was visualised using chlorophyll fluorescence with spatial resolution. Re-fixation of respiratory CO_2 was visible when stomatal conductance was low either by simulating leaf chamber sealing where stomata were sealed with an adhesive tape or with plants under drought stress. Re-watering of the drought stressed plants caused stomatal opening and the impact of laterally diffusing CO_2 disappeared. Photochemical and non-photochemical quenching was influenced up to a distances of 3-4 mm from the shade in homobaric leaves, whereas in heterobaric leaves no influence of the shade was observed.

3.5 Photosynthesis of leaves illuminated with lightflecks

Combination of gas exchange and chlorophyll fluorescence measurement was applied to study the impact of lateral diffusion on photosynthetic performance of a leaf part illuminated with lightflecks differing in size. The mean photosynthetic performance of the whole illuminated spot areas was regarded assuming that the impact of lateral diffusion on the large illuminated area is relatively lower than on the small illuminated area. The ratio between the area and its circumference determines the relative CO₂ supply per illuminated spot area. The leaves of *V. faba* and *G. max* were illuminated first with a large spot and then with a small spot (Fig. 23; page 63). When the large spot area was illuminated, an area of 4.15 cm² was surrounded by a light/shade borderline (LSB_L) with the length of 7.2 cm. The large spot area was divided into a central spot area (corresponding to the small spot area when only the small spot was illuminated) and a peripheral spot area (Fig. 23 a; page 63). The peripheral spot area was either illuminated (when the large spot was illuminated) or it was shaded when the small spot area was illuminated. The small spot area (0.79 cm²) was then enfolded by a light/shade borderline defined as LSB_S (Fig. 23 b; page 63) with a circumference of 3.1 cm.

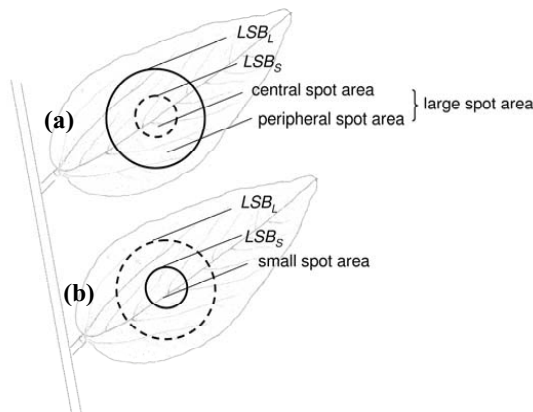


Figure 23. Definition of leaf areas illuminated with lightflecks of different size. In (a), a large spot area and in (b) a small spot area is illuminated. The solid lines indicate the light/shade borderline of the large spot (LSB_L) and small spot (LSB_S); the dashed line in (a) indicates the central spot area which corresponds to the small spot area in (b) when only the small spot was illuminated; in (b), the dashed line corresponds to the illuminated large spot area in (a); peripheral spot area is the area between LSB_L and LSB_S which was illuminated in (a) and shaded in (b).

3.5.1 Experiments with *Vicia faba*

Maximum quantum yield of dark adapted plants (F_v/F_m) was measured before every experiment started. The obtained mean value of 0.78 ± 0.02 indicates the absence of photoinhibition in the studied plants. Homobaric leaves of *V. faba* revealed higher quantum yield along the LSB as already demonstrated (Chapter 3.4). The effect was studied when the leaf was illuminated first with the large and then with the small lightfleck for 8 minutes under photorespiratory conditions with ambient air (CO_2 : $350 \mu\text{L L}^{-1}$; O_2 : 21%) (Fig. 24 a, b; page 65) and non-photorespiratory conditions (O_2 was lowered to 1%; data not shown) revealing similar profiles. The peripheral spot area showed substantially higher ϕ_{PSII} than the central spot area from the beginning of illumination (dark adapted for 40 min, Fig. 24 a; page 65). When the peripheral spot area was shaded, the small spot area remained illuminated (cf. Fig. 24 b; page 65) and ϕ_{PSII} increased substantially in this area (Fig. 24 c; page 65). The opposite was observed for NPQ which was lower along the LBS_L and LSB_S than the central spot area (Fig. 24 d, e; page 65). The averaged NPQ was lower in peripheral spot area than the central spot area when the large spot was illuminated (Fig. 24 f, 0-8 min; page 65). Shading of the peripheral spot area caused an immediate decrease of NPQ of the small spot area (Fig. 24 f; page 65). When the large spot was illuminated at time 0 min, $NCER$ increased within a few minutes. When only the small spot was lighted, $NCER$ decreased to a new steady state (Fig. 24 g; page 65). At the end of the experiments, the light was switched off and dark respiration was measured as in the beginning. The differences between $NCER$ in darkness and under illumination of the large or small spot were used to calculate gross assimilation rate of the large (A_L) and small (A_S) spots, respectively (Fig. 24 g; page 65 and Eqn. 6; page 31). The area of the large spot was 5.25 times larger than that of the small spot and one would expect that A_L should be 5.25 times larger than A_S . However, A_L was just twice as large as A_S (Fig. 24 g; page 65) which was measured only when leaf conductance of the whole leaf (g_{leaf}) enclosed in the leaf chamber was low (Fig. 24 h; page 65).

Recapitulating, lateral diffusion from shaded leaf area to illuminated spots increased ϕ_{PSII} and reduced NPQ along the LSB. The impact of lateral CO_2 flux was larger for the small spot, which is indicated by relatively high net CO_2 uptake of the small spot. The impact of re-fixation of respiratory CO_2 from shaded areas was larger for plants under drought stress.

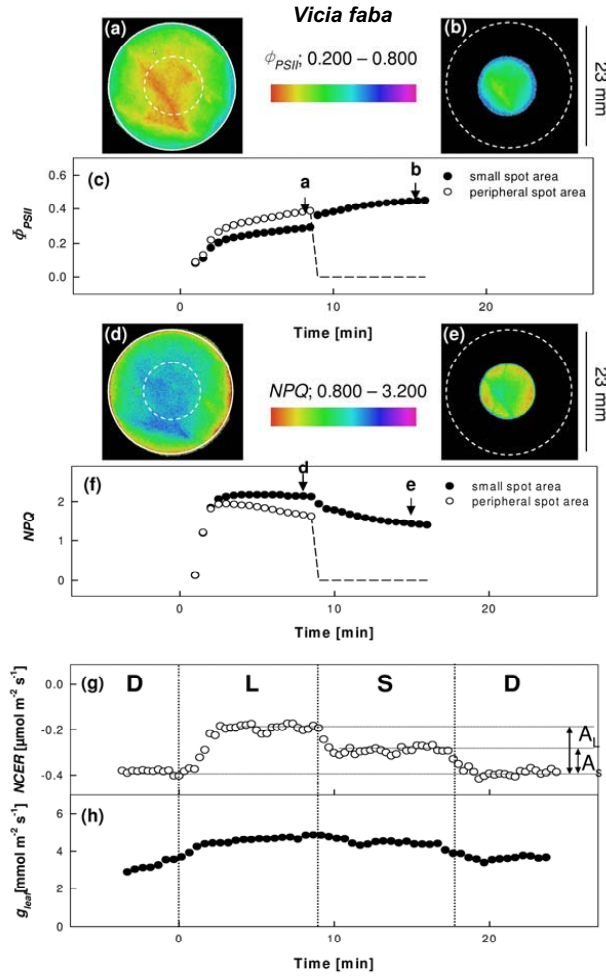


Figure 24. Combined measurement of chlorophyll fluorescence and gas exchange of a leaf of *V. faba* under photorespiratory conditions illuminated with actinic light ($150 \mu\text{mol m}^{-2} \text{s}^{-1}$). (a) Quantum yield images (ϕ_{PSII}) of the large spot area and (b) of the small spot area; (c) the averaged ϕ_{PSII} of the peripheral spot area and small spot area plotted versus time after start of illumination with arrows representing the time the images were taken, dashed line indicates that no data were measured in the shade; (d) non-photochemical quenching (NPQ) images of (d) the large spot area and of (e) the small spot area; (f) the averaged NPQ of the peripheral spot area and small spot area plotted versus time with arrows representing the time the images were taken, dashed line indicates that no data were measured in the shade; dashed lines in (a), (b), (d) and (e) correspond to those shown in figure 23 (page 63) defining illuminated areas. (g) Net CO₂ exchange rate (NCER) of the whole leaf; at time 0 light was switched on and NCER was measured when the large area (L) and small area (S) was illuminated; D represents darkness with approximately $1\text{--}3 \mu\text{mol photons m}^{-2} \text{s}^{-1}$. The difference between NCER in darkness and when the small or large spot was illuminated was used to calculate gross assimilation rate of the large spot (A_L) and small spot (A_S); (h) mean leaf conductance (g_{leaf}).

A_S and A_L obtained under photorespiratory (Fig. 25 a, page 66) and non-photorespiratory (Fig. 25 b; page 66) conditions showed similar profiles when plotted versus g_{leaf} . Under photorespiratory conditions the linear regression of the dependence of A_S and A_L on g_{leaf} showed similar slopes 0.12 and 0.14, respectively. The interception with the y-axis is larger for the small spot than for the large spot by 2.5 (Fig. 25 a; page 66). The assimilation rates obtained under non-photorespiratory conditions were higher than under photorespiratory condition which can be attributed to photorespiration. The regression slopes were similar for the small and large spot with 0.21 and the interception with the y-axis was 2.8 larger for the small than large spot (Fig. 25 b; page 66). The A_L/A_S ratio revealed maximal values of approximately 0.8 when g_{leaf} was high and it was substantially smaller at low g_{leaf} which was similar under photorespiratory and non- photorespiratory conditions (Fig. 25 c; page 66). Thus, A_S was larger than A_L under all measured g_{leaf} s, which indicated relatively higher re-fixation of CO_2 from adjacent shaded leaf areas, when the small spot was illuminated.

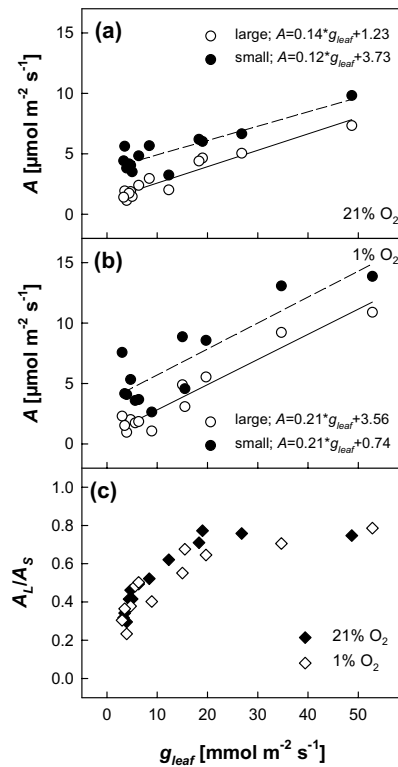


Figure 25. Assimilation rates of leaves of *V. faba* measured under a photon flux density (PFD) of $150 \mu\text{mol m}^{-2} \text{s}^{-1}$ when a small and large spot was illuminated. (a) Assimilation rates obtained under photorespiratory conditions (21% O_2); (b) assimilation rates obtained under non-photorespiratory conditions (1% O_2), the small spot (black circles, dashed regression line) and large spot (white circles, solid regression line); (c), the ratio between the assimilation rate of the small and large spot (A_L/A_S) plotted versus leaf conductance (g_{leaf}), under photorespiratory conditions (black diamonds, 21% O_2) and non-photorespiratory conditions (white diamonds, 1% O_2).

The ratio of water use efficiencies when the large and small spot was illuminated (WUE_L/WUE_S) reached values of 4 - 4.5 when g_{leaf} was high and declined substantially when g_{leaf} was low (Fig. 26 a; page 67). The WUE_L/WUE_S ratio (Fig. 26 a; page 67) showed similar profile to the A_S/A_L ratio (Fig. 25 c; page 66) which indicates that transpiration was slightly influenced by illumination of the large or small spot and the decrease of WUE_L/WUE_S was mainly influenced by changes in assimilation. Thus, higher re-fixation of respiratory CO_2 in the small spot resulted in increased water use efficiency of the leaf when the small spot was illuminated.

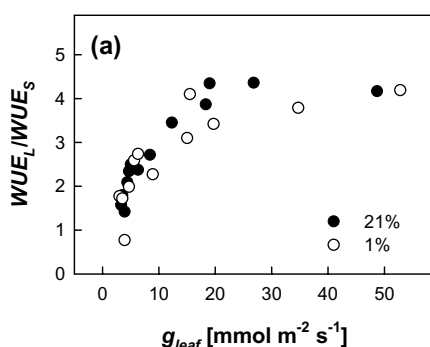


Figure 26. Ratio of water use efficiency of leaves of *V. faba* illuminated with the large and the small lightfleck (WUE_L/WUE_S) as a function of leaf conductance (g_{leaf}) measured under photorespiratory (closed circles, 21%) and non-photorespiratory conditions (white circles, 1%).

Combined measurements of gas exchange and chlorophyll fluorescence were used to calculate the electrons required to assimilate CO_2 (e/A ; Eqn. 8; page 32). When plotted versus g_{leaf} , e/A of the large spot was almost constant over a wide range of g_{leaf} under photorespiratory and non-photorespiratory conditions but increased when g_{leaf} became smaller at approximately $10 \text{ mmol m}^{-2} \text{ s}^{-1}$ (Fig. 27 a; page 68). However, e/A of the small spot was less influenced and showed only slight increase under low g_{leaf} (Fig. 27 b; page 68). The difference between e/A under photorespiratory and non-photorespiratory allowed an estimation of the fraction of electrons used for photorespiratory O_2 reduction (PR ; Eqn. 9; page 32). Under the experimental conditions (PFD: $150 \mu\text{mol m}^{-2} \text{ s}^{-1}$, $[CO_2]$: $350 \mu\text{L L}^{-1}$) when g_{leaf} was high, approximately 40% of the electrons were used to reduce O_2 and the fraction increased to approximately 60 % under low g_{leaf} when the large spot was illuminated (Fig. 27 a; page 68). When the small spot was illuminated, the increase in PR was lower than for the large spot rising from approximately 35% to 45 % under low g_{leaf} (Fig. 27 b; page 68). Lateral CO_2 supply from the shaded leaf areas reduced e/A ratio indicating reduced photorespiration. In the small spot photorespiration was substantially more reduced because of

the relatively larger lateral CO_2 re-fixation than in the large spot, which is determined by the area to circumference ratio.

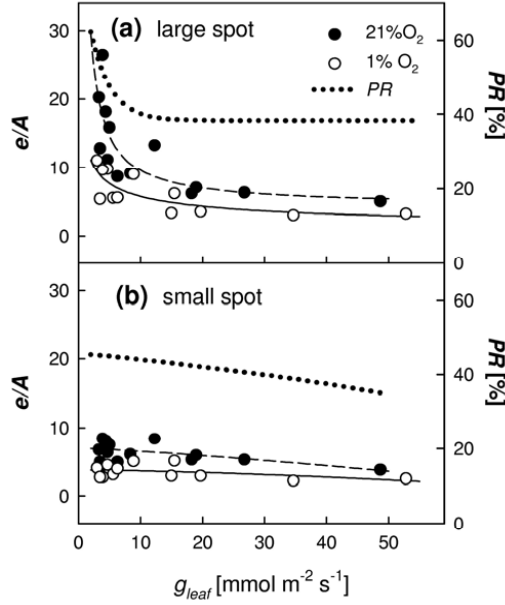


Figure 27. Electrons required for assimilated CO_2 (e/A) and the fraction of electrons used for photorespiration (PR) for leaves of *V. faba* under photon flux density (PFD) of $150 \mu\text{mol m}^{-2} \text{s}^{-1}$. In (a), large spot and in (b) small spot was illuminated. The experiments were performed under photorespiratory (21% O_2 , closed circles, dashed regression line) and non-photorespiratory conditions (1% O_2 , open circles, solid regression line). The fraction of electrons used for photorespiration in (a) and (b) is given as a difference between the regression curves for e/A obtained under 21% O_2 and 1% O_2 (dotted lines).

Quantum yield (ϕ_{PSII}) and quantum yield of CO_2 efficiency (ϕ_{CO_2}) relation was measured under 1% O_2 , thus photorespiration was eliminated and the regression lines should pass through the origin when no alternative electron sinks like the Mehler-peroxidase were available. Thus, the intercept with the y-axis indicates that the alternative electron sinks was low (0.07) when the large spot was illuminated (Fig. 28; page 69). For the small spot, however, the intercept with the y-axis was twice as large (0.14) but a large variation of the data was observed (Fig. 28; page 69). This variation may be caused by lateral CO_2 supply that varied because of the very position of the lightfleck. Veins may reduce lateral CO_2 supply more or less efficiently and influence ϕ_{PSII} (cf. Fig. 29 b; page 70) but also assimilation (cf. Fig. 25 b; page 66) resulting in large variation in ϕ_{PSII} vs. ϕ_{CO_2} relation, which was larger for the small than the large spot (Fig. 28; page 69).

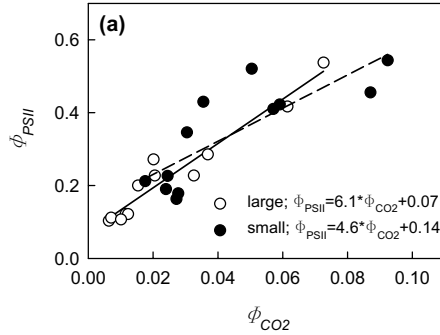


Figure 28. Quantum yield of PSII (ϕ_{PSII}) as a function of quantum efficiency of CO₂ assimilation (ϕ_{CO2}) measured under non-photorespiratory conditions on leaves of *V. faba*. Photon flux density (PFD) was 150 $\mu\text{mol m}^{-2} \text{s}^{-1}$ and CO₂ concentration 350 $\mu\text{L L}^{-1}$, when the large spot (open circles, solid regression line) and the small spot (black circles, dashed regression line) was illuminated.

During illumination, ϕ_{PSII} and NPQ showed obvious differences when regarding the small spot and central spot areas as presented in figure 29 a, c (page 70). Central spot area was not influenced by the shade due to the long distance to LSB_L (6.5 mm, cf. Fig. 24 a, d; page 65). When the small spot was illuminated, a substantial increase of ϕ_{PSII} along the LSB was observed (cf. Fig 24 b, e; page 65). Under photorespiratory conditions decreasing g_{leaf} caused a reduction of ϕ_{PSII} which was smaller when the small spot was illuminated because of lateral CO₂ supply (Fig. 29 a; page 70). The opposite was detected when regarding NPQ ; under low g_{leaf} , the increase of the central spot area was smaller than for the small spot. Under non-photorespiratory conditions, the difference in ϕ_{PSII} and NPQ between central spot area and the small spot was not obvious because of the large variation especially under low g_{leaf} (Fig. 29 b, d; page 70). As stated above, this variation may be caused by differences in lateral CO₂ supply due to the position of the lightspot where veins variably influence lateral CO₂ diffusion. The variable CO₂ supply affected ϕ_{PSII} and NPQ more under non-photorespiratory conditions because under 1% O₂ photosynthesis is more vulnerable to changes in CO₂. Whereas under 21% O₂ photorespiration may smooth the variable lateral CO₂ input.

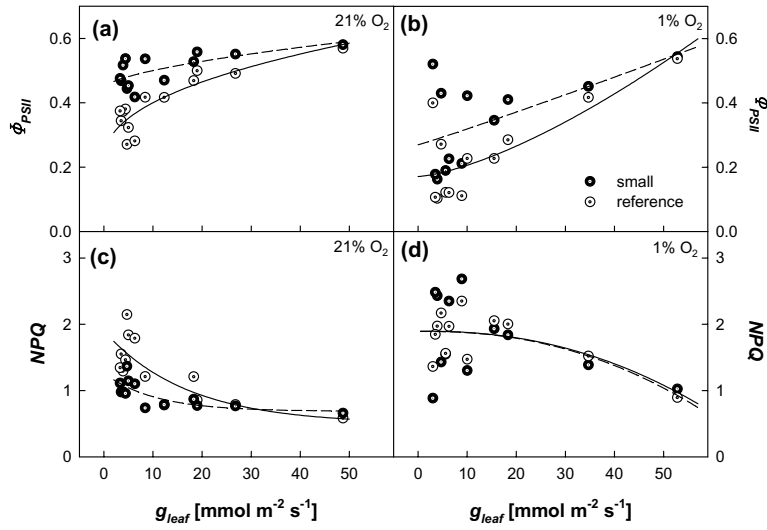


Figure 29. Quantum yield (ϕ_{PSII}) and non-photochemical quenching (NPQ) as a function of leaf conductance (g_{leaf}) of leaves of *V. faba* illuminated with actinic light of $150 \mu\text{mol photons m}^{-2} \text{s}^{-1}$. In (a) ϕ_{PSII} was measured under photorespiratory (21% O_2) and in (b) under non-photorespiratory (1% O_2) conditions. In (c) NPQ was measured under photorespiratory (21% O_2) and in (d) under non-photorespiratory (1% O_2) conditions. Small spot area (black circles, dashed regression line); central spot area (white circles, solid regression line); for definition of terms see figure 23 (page 63).

3.5.2 Experiments with *Glycine max*

Similar experiments as described for *V. faba* were performed with heterobaric leaves of *G. max*. F_v/F_m was 0.79 ± 0.02 for studied leaves indicating no photoinhibition of the leaves. Under photorespiratory conditions, no effect of the shade on ϕ_{PSII} along the LSB was observed (Fig. 30 a, b; page 72) as already described in chapter 3.4. The averaged ϕ_{PSII} of the peripheral spot area and the small spot area showed no influence of the shade on ϕ_{PSII} (Fig. 30 c; page 72). NPQ was also not influenced by the LSB (Fig. 30 d, e; page 72). The averaged NPQ showed similar values for peripheral spot area and the central spot area when the large spot was illuminated (Fig. 30 f; 0-8 min; page 72) but shading of the peripheral spot area caused an increase of NPQ of the small spot (Fig. 30 f; page 72). This increase was caused by diffusive light along the LSB (cf. Fig. 7, page 31) which were similar for *V. faba* and *G. max*. In homobaric leaves of *V. faba*, the light inhomogeneities were obscured because of lateral CO_2 diffusion. For heterobaric leaves of *G. max*, the diffusive light af-

affected NPQ , especially of the small spot (cf. chapter 2.8.2.3). Under photorespiratory conditions, change of NPQ of the small spot ranged between reduction by 7% and an increase by 17% as compared to large spot. Under non-photorespiratory conditions, NPQ increase ranged between 2% and 29%. Gas exchange of *G. max* leaves (Fig. 30 g, h; page 72) showed a similar pattern as for *V. faba* (Fig. 24 g, h; page 65). A_L was larger than A_S which approximately rendered the ratio of the small and large illuminated leaf areas (Fig. 30 g; page 72) even when the experiment was performed under drought stress indicated by low g_{leaf} (Fig. 30 h; page 72). Under non-photorespiratory conditions, similar results were obtained as under photorespiratory condition (data not shown).

The dependence of A_S and A_L on g_{leaf} was linear and revealed small differences between the large and small spot under photorespiratory (Fig. 31 a; page 73) and non-photorespiratory conditions (Fig. 31 b; page 73). However, the assimilation rates under non-photorespiratory conditions were larger than under photorespiratory conditions and decreasing g_{leaf} influenced the assimilation more as indicated by different slopes with 0.18 and 0.19 under photorespiratory and 0.25 and 0.28 under non-photorespiratory conditions for the large and small spot, respectively (Fig. 31 a, b; page 73). The A_L/A_S ratio was slightly influenced by g_{leaf} ranging between 0.8 and 1.0 due to diffuse light along LSB which was larger for the small than large spot (Fig. 31 c; page 73). No difference of A_L/A_S ratio under photorespiratory and non-photorespiratory conditions was observed (Fig. 31 c; page 73).

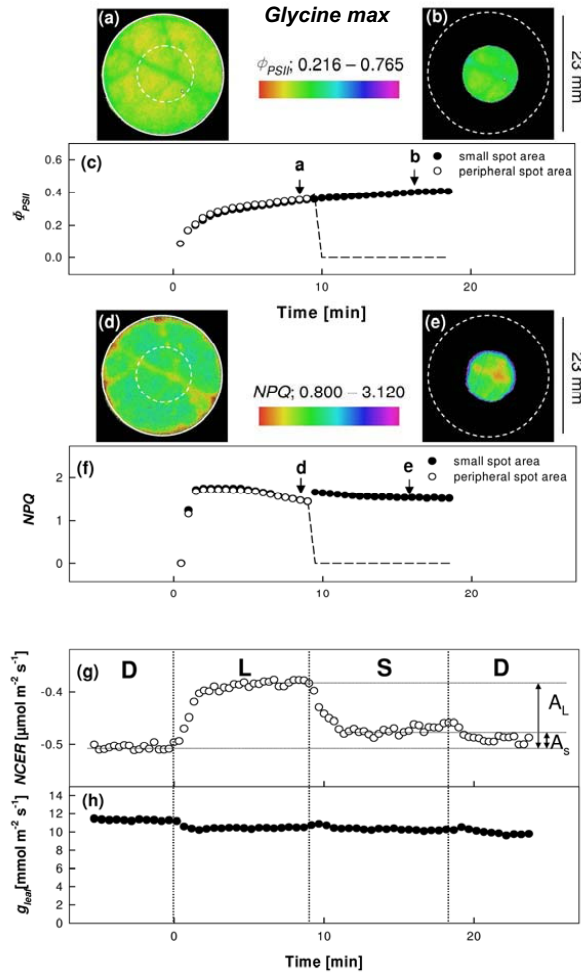


Figure 30. Combined measurement of chlorophyll fluorescence and gas exchange of a leaf of *G. max* under photorespiratory conditions illuminated with actinic light ($150 \mu\text{mol photons m}^{-2} \text{s}^{-1}$). (a) Quantum yield images (ϕ_{PSII}) of the large spot area and (b) of the small spot area; (c) the averaged ϕ_{PSII} of the peripheral spot area and small spot area plotted versus time after start of illumination with arrows representing the time the images were taken, dashed line indicates that no data were measured in the shade; (d) non-photochemical quenching (NPQ) images (d) of the large spot area and (e) of the small spot area; (f) the averaged NPQ of the peripheral spot area and small spot area plotted versus time with arrows representing the time the images were taken, dashed line indicates that no data were measured in the shade; dashed lines in (a), (b), (d) and (e) correspond to those shown in figure 23 (page 63) defining illuminated areas. (g) Net CO₂ exchange rate (NCER) of the whole leaf; at time 0 light was switched on and NCER was measured when the large area (L) and small area (S) was illuminated; D represents darkness with approximately $1\text{--}3 \mu\text{mol photons m}^{-2} \text{s}^{-1}$. The difference between NCER in darkness and when the small or large spot was illuminated was used to calculate gross assimilation rate of the large spot (A_L) and small spot (A_S); (h) mean leaf conductance (g_{leaf}).

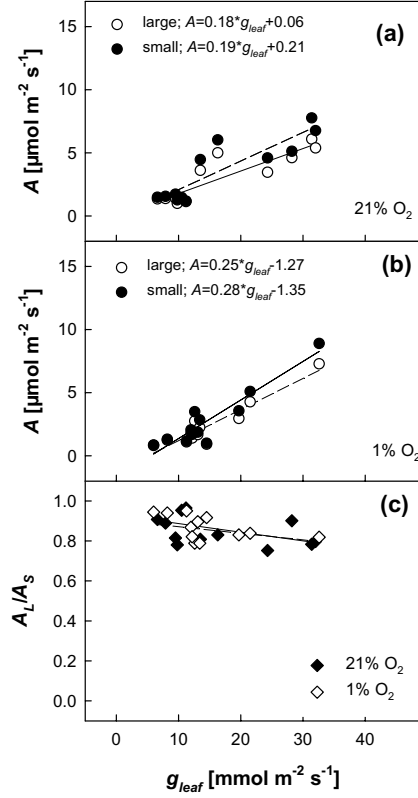


Figure 31. Assimilation rates of *G. max* leaves plotted versus leaf conductance (g_{leaf}) which was measured under photon flux density (PFD) of 150 $\mu\text{mol photons m}^{-2} \text{s}^{-1}$. (a) Assimilation rates obtained under photorespiratory conditions (21% O_2); (b) assimilation rates obtained under non-photorespiratory conditions (1% O_2), the small spot (black circles, dashed regression line) and large spot (white circles, solid regression line); (c), the ratio between the assimilation rate of the small and large spot (A_L/A_S) plotted versus leaf conductance (g_{leaf}), under photorespiratory conditions (black diamonds, 21% O_2) and non-photorespiratory conditions (white diamonds, 1% O_2).

The WUE_L/WUE_S ratio ranges between 4 and 5 under all measured g_{leaf} (Fig. 32 a; page 74). This indicates that assimilation and transpiration remained constant approximately rendering the ratio of the large and small lightfleck of 5.25.

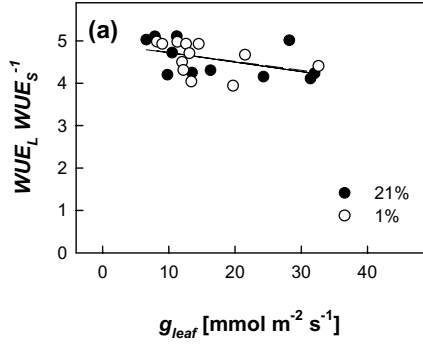


Figure 32. Ratio of water use efficiency of the leaves of *G. max* illuminated with the large and the small lightfleck (WUE_L/WUE_S) as a function of leaf conductance (g_{leaf}), measured under photorespiratory (21%, black circles, dashed regression line) and non-photorespiratory conditions (1%, white circles, solid regression line).

The e/A dependence on g_{leaf} was similar for the large and small spot with continuous non-linear increase with declining g_{leaf} (Fig. 33 a, b; page 74). The fraction of electrons used to reduce O_2 increased slightly from approximately 35% at high g_{leaf} to almost 45% at low g_{leaf} when the large and small spot was illuminated (Fig. 33 a, b; page 74).

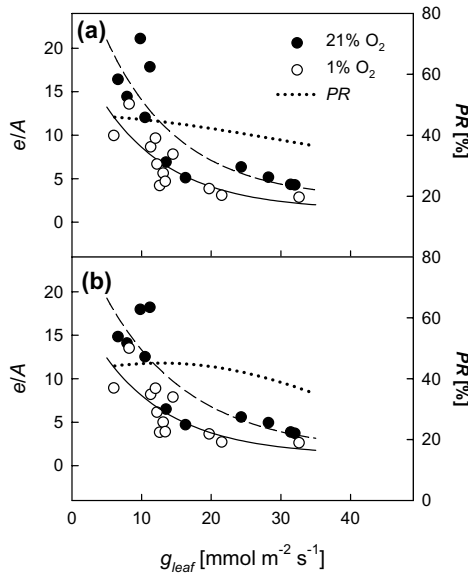


Figure 33. Electrons required for assimilated CO_2 (e/A) and the fraction of electrons used for photorespiration (PR) for leaves of *G. max* measured under photon flux density (PFD) of $150 \mu mol m^{-2} s^{-1}$. In (a) large spot, in (b) small spot was illuminated. The experiments were performed under photorespiratory (21% O_2 , closed circles, dashed regression line) and non-photorespiratory conditions (1% O_2 , open circles, solid regression line). The fraction of electrons used for photorespiration (dotted line) in (a) and (b) is given as the difference between the regression curves for e/A under 21% O_2 and 1% O_2 (cf. Eqn. 9; page 32).

The relation between quantum yield (ϕ_{PSII}) and quantum yield of CO_2 fixation (ϕ_{CO_2}) is linear for the large and small spot with similar slopes, 4.6 and 4.3 for the large and small

spot, respectively (Fig. 34 a; page 75). The Mehler-ascorbate reaction indicated by the intercept with the y-axis under non-photorespiratory conditions was also low and similar for both spots (0.10, Fig. 34 a; page 75).

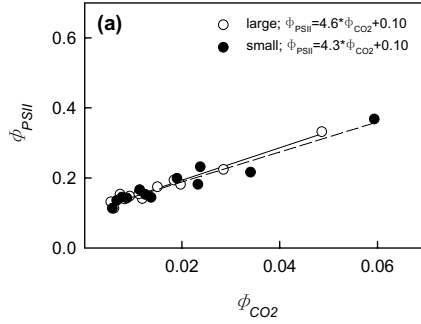


Figure 34. Quantum yield of PSII (ϕ_{PSII}) as a function of quantum efficiency of CO_2 assimilation (ϕ_{CO_2}) measured under non-photorespiratory conditions on leaves of *G. max*. Photon flux density (PFD) was $150 \mu\text{mol m}^{-2} \text{s}^{-1}$, CO_2 concentration $350 \mu\text{L L}^{-1}$ when the large spot (open circles, solid regression line) and the small spot was illuminated (black circles, dashed regression line).

In general, similar dependence of ϕ_{PSII} and NPQ on g_{leaf} was observed for both plant species, with a decrease in ϕ_{PSII} and increase of NPQ when g_{leaf} declined (cf. Fig. 29 and Fig. 35; page 70 and page 76). However, the chlorophyll fluorescence parameter ϕ_{PSII} and NPQ , revealed no differences between the peripheral spot area and the small spot of *G. max* under photorespiratory conditions (Fig. 35 a, c; page 76) or non-photorespiratory conditions (Fig. 35 b, d; page 76). This shows a clear difference to the measurements of *V. faba* where the small spot showed smaller decrease of ϕ_{PSII} and lower increases of NPQ with rising g_{leaf} compared to the central spot area (Fig. 29 a, c; page 70). For both plant species, *V. faba* and *G. max*, ϕ_{PSII} and NPQ was more influenced under non-photorespiratory conditions showing a decrease of ϕ_{PSII} and an increase of NPQ under rather high g_{leaf} (Fig. 29 b, d and Fig. 35 b, d; page 70 and page 76)

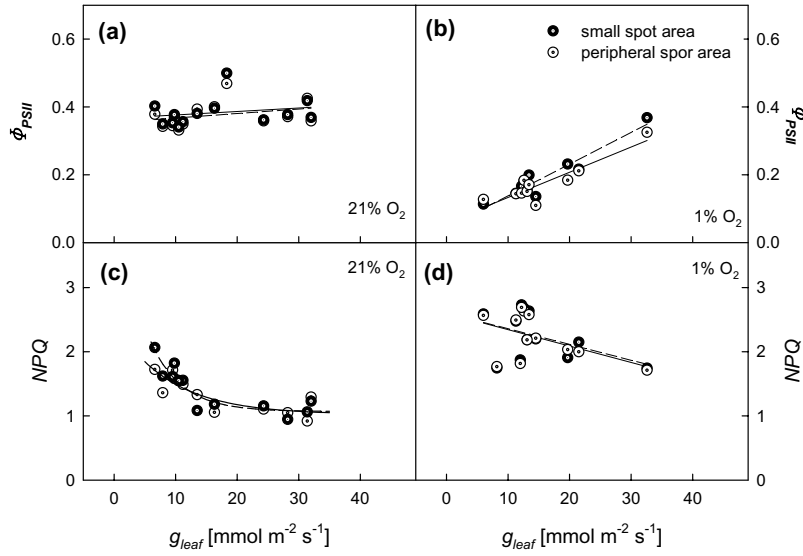


Figure 35. Quantum yield (ϕ_{PSII}) and non-photochemical quenching (NPQ) as a function of leaf conductance (g_{leaf}) of leaves of *G. max* illuminated with actinic light of $150 \mu\text{mol photons m}^{-2} \text{s}^{-1}$. In (a) ϕ_{PSII} was measured under photorespiratory (21% O_2) and in (b) under non-photorespiratory (1% O_2) conditions. In (c) NPQ was measured under photorespiratory (21% O_2) and in (d) under non-photorespiratory (1% O_2) conditions. Small spot area (black circles, dashed regression line); peripheral spot area (white circles, solid regression line); for definition of terms see Fig. 23 (page 63).

3.5.3 Summary of photosynthesis of leaves illuminated with lightflecks

Lateral diffusion in homobaric leaves of *V. faba* from shaded to illuminated leaf areas significantly influenced photosynthetic performance of the illuminated leaf area. The impact of lateral CO_2 flux was larger under low g_{leaf} and the small spot was more influenced than the large one. Thus, re-fixation of respiratory CO_2 released in shaded leaf areas increased the net CO_2 uptake, which also resulted in an increase of water use efficiency. Recycling of respiratory CO_2 from distant shaded areas reduced photorespiration and NPQ and increased ϕ_{PSII} . For heterobaric leaves of *G. max*, however, the illumination of a leaf part with a large or small spot showed no differences in photosynthetic performance of the illuminated area. Assimilation rates of the large spot were similar to that of the small spot independently of drought stress level. Therefore, no differences between water use efficiency were observed. Photorespiration and Mehler-ascorbate reaction was also similar for

the large and small spot as well as ϕ_{PSII} and NPQ , which showed similar response to drought stress with regard to the large and small illuminated leaf area.

Chapter 4 Discussion

4.1 Carbon fluxes in and out of leaves

Processes of carbon fluxes into and out of leaves in light are numerous. Photosynthetic CO₂ uptake, photorespiratory CO₂ evolution and mitochondrial respiration take place simultaneously (Haupt-Herting, Klug, & Fock 2001; Hoefnagel, Atkin, & Wiskich 1998; Loreto, Velikova, & Di Marco 2001; Pinelli & Loreto 2003; Pons & Welschen 2002). In contrast, carbon fluxes in darkness are only due to respiration. Consequently, quantification of CO₂ diffusion fluxes inside leaves turned to be much more accurate in darkness especially when measurement was performed under stable respiration rates after prolonged phase in the dark (Penning De Vries 1975). Even in the dark when respiration is measured under different [CO₂] several issues have to be considered (1) a potential direct effect of atmospheric CO₂ concentration on respiration as discussed in literature, and (2) measurement artefacts in gas exchange measurement.

Autotrophic respiration, on a global scale, produces 50-60 Gt C year⁻¹ released as CO₂ to the atmosphere. Global fossil-fuel emissions amount to approximately 6 Gt C year⁻¹, thus small errors in determining autotrophic respiration would substantially alter the apparent models of carbon cycle (Gifford 2003). Therefore, it is important to have methods that allow precise and reliable measurement of respiratory processes in light and darkness.

4.1.1 Influence of elevated CO₂ on respiration – direct effect

Several studies claimed that elevated CO₂ can reduce dark respiration between 15-18 % when doubling the atmospheric [CO₂] (cf. Drake et al. 1999; Gonzalez-Meler & Siedow 1999). However, it has been shown in recent studies that there is convincing evidence that elevated [CO₂] has no instantaneous effect on respiration (Amthor et al. 2001; Davey et al. 2004; Jahnke 2001; Jahnke et al. 2002). In agreement with that no influence of elevated [CO₂] on *NCER* in darkness was observed here with 27 different species (Tab. 5 and Tab. 6; page 41 and page 42).

4.1.2 Measurement artefacts

Respiration rates are small and therefore prone to measurement errors especially when small 'clamp-on' leaf chambers are used. Possible artefacts in measurement of dark respiration have been mentioned only rarely in literature (cf. Amthor 2000; Drake et al. 1999). Pons et al. (2002) found that leakiness between the leaf surface and the gasket can influence gas exchange measurement substantially. A systematic analysis of measurement artefacts due to technical problems was performed by Jahnke (2001). Several artefacts and their influence on gas exchange measurement were quantified. When these technical measurement artefacts were avoided, any effect on *NCER* in the dark due to changes in atmospheric CO₂ concentration can be interpreted as being caused by lateral transport of CO₂ inside leaves. The magnitude of the effect depends on the intrinsic properties of a leaf (homobaric or heterobaric), the very position of where the leaf chamber is clamped on a leaf blade (cf. Jahnke et al. 2002), and the size of the leaf chamber (see Tab. 3; page 37).

4.1.3 Gas conductance and conductivity in lateral and vertical direction

The anatomy of leaves is a major factor in defining internal gas fluxes. In bifacial leaves, the spongy parenchyma is generally thicker than the palisade parenchyma (cf. Tab. 2; page 35) and spongy tissue has larger porosity than palisade parenchyma (Terashima 1992). Lateral diffusion in leaves is thus likely to occur preferentially in the spongy parenchyma whereas vertical diffusion encompasses both spongy and palisade tissue. Since air-filled spaces are larger in spongy than in palisade mesophyll, one might expect gas conductance (*g*) to be larger in the lateral direction than in the vertical. However, pathway length is an intrinsic parameter when conductance of a system is evaluated (cf. Evans et al. 1996; see also Eqn. 4; page 21 and Fig. 9 a; page 38). Lateral conductances of leaves were measured here over distances of 6 - 8 mm whereas the vertical conductances taken from the literature might have been observed over much smaller distances (108 – 280 µm; see Tab. 4; page 39). Under these conditions, gas conductances obtained on homobaric leaves of *V. faba* and *N. tabacum* in lateral directions reached about 2 – 20 % of those published for vertical direction (cf. Tab. 3 and 4; pages 37, 39). The very low value of vertical conductance published for *Zea mays* leaves (17 mmol m⁻² s⁻¹) has not been considered in the calculation

since it seems to be an exception due to rather narrow air ducts in the mesophyll of this monocotyledonous species.

Gas conductance is hyperbolically dependent on the distance of gas diffusion according to Flick's first law (cf. Fig. 9 a; page 38). In order to facilitate a direct comparison of tissue specific properties, gas conductivity (g^*) was derived from measured gas conductance. In analogy to electrical conductivity describing the general property of a conductor independent of its size or form (Gettys, 1989), gas conductivity is independent of the path length of diffusion. However, when measured in homobaric *V. faba* leaves, gas conductivity showed a small decrease with increasing path length (Fig. 9 b; page 38). This can be explained by the fact that, in a given leaf, intercellular air space is not simply a homogeneous system but may vary throughout a leaf blade. Lateral conductivity as calculated by linear regression accounted to $185.3 \mu\text{mol m}^{-1} \text{s}^{-1}$ (Fig. 9 b; page 38) and was very close to the mean of all conductivity data ($195 \mu\text{mol m}^{-1} \text{s}^{-1}$) obtained from *V. faba* leaves (cf. Tab. 3; page 37). In general, the measured gas conductivities in lateral directions of homobaric leaves were notably higher than those in vertical direction re-calculated from the literature (Tab. 3 and 4; page 37 and page 39).

4.1.4 Gas fluxes in lateral direction

Lateral gas conductance and conductivity obtained in this work can be seen as an approximation of the true values for several reasons. First, the calculated lateral diffusion areas ($A_{ias,l}$; Eqn. 1; page 20) are maximum values since the effective areas would be smaller when larger veins were located directly under the chamber gaskets. Second, to accurately quantify lateral gas conductance ($g_{leaf,l}$) it would be best to use the effective differences in leaf internal CO_2 concentrations across the chamber gaskets (i.e. $\Delta c_i = c_{i,i} - c_{i,o}$ instead of Δc_a ; cf. Fig. 36; page 82 and Eqn. 3; page 21). However, since the measured respiration rates in the dark were very low (cf. Penning De Vries 1975) and differences between c_a and c_i can then be considered small (cf. Amthor 1997), calculation of $g_{leaf,l}$ was simplified by using measured c_a values according to equation 3 (page 21). Third, the effective lateral conductivity of the mesophyll was potentially underestimated because measurements included gas movement through the stomata on both sides of the gaskets (Fig. 36 b; dotted arrows; page 82); i.e., the path length must have been longer than simply the gasket widths

(w_{gasket}) used for calculation (Eqn. 4; page 21). Fourth, in addition to the previous point, the true path length of diffusion can be considered longer due to tortuosity of the mesophyll; assuming a tortuosity factor of 1.5 (Terashima et al. 1996), the conductivities in table 4 (page 39) would be 50% higher which, for demonstration, is drawn in Fig. 10 (closed symbols; page 40).

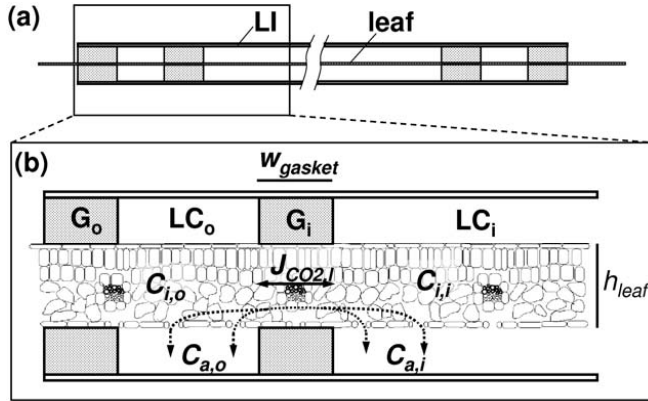


Figure 36. Schematic drawing of diffusion pathways inside a homobaric leaf when part of the leaf was enclosed in a clamp-on leaf chamber. (a) A cross-section through the double-gasket leaf chamber is drawn with a leaf thickness in due proportion to the gaskets which were 6 mm in widths. (b) Part of (a) is schematically enlarged together with potential diffusion pathways inside the leaf mesophyll; leaf dimensions are drawn out of scale when compared to those of the gaskets. The solid-lined arrows point to the minimum diffusion distance ($J_{CO2,l}$) which was used to calculate gas conductivities. The 'true' diffusion lengths are denoted by dotted-lined arrows and may have been even longer due to tortuosity of the mesophyll (see text). $c_{a,i}$, $c_{a,o}$, atmospheric CO₂ concentration in the inner and outer leaf chamber; $c_{i,i}$, $c_{i,o}$, leaf internal CO₂ concentration at the inner and outer leaf chamber; $J_{CO2,l}$, lateral diffusion CO₂ flux; LI, chamber lid; w_{gasket} , gasket width. For the other abbreviations, see legend of figure 3 (page 17).

4.2 Influence of lateral diffusion on gas exchange measurement

Gas transport in lateral rather than in vertical direction can be higher than usually considered with significant implications for experimentalists. Whenever there is a difference in CO₂ concentration between the leaf chamber and the air outside, leaf internal gas fluxes may affect measurements. This is a point especially when clamp-on leaf chambers are small. The chamber size defines the ratio between length (circumference) of the leaf chamber gasket and the enclosed leaf area; the larger the ratio the larger the potential effect on

measured *NCER* eventually causing erroneous results (cf. Tab. 3; page 37). For reliable gas exchange measurements, small leaf chambers are therefore not the appropriate tools, at least for homobaric leaves.

4.2.1 Screening for species with different leaf anatomy

Lateral gas diffusion inside leaves can substantially influence measurement of dark respiration which was shown by (Jahnke et al. 2002; Pieruschka et al. 2005). However, the impact varied largely between species. Lateral gas diffusion in heterobaric leaves was very low due to compartmentation of the mesophyll (Neger 1918). But several of the investigated species showed very large impact of a CO_2 gradient on *NCER*, which may imply that in some of the species defined as heterobaric, small lateral gas fluxes may occur (see Tab. 5; page 41). In some plant species, bundle sheath extensions accompany the veins throughout their length while in others bundle sheath extensions are completely absent (Fahn 1982). Moreover, different patterns of vascular bundles with or without bundle sheath extensions can be found with varying distances between the bundles encircled by the extensions (Esau 1969). Intercellular space systems of leaves may also be connected with each other even across the main veins (Williams 1948). The resulting interconnectivity of the gas spaces within leaves can vary substantially between species. The majority of the investigated plant species with homobaric leaves were grouped as slightly or medium homobaric. However, several species can be characterised as highly homobaric with large open intercellular air space (Tab. 3 and Tab. 6; page 37 and page 42). There was not only a difference between the species but also in the individual experiments with leaves of one species. This diversity within a single species was larger when the leaves were characterised as medium and highly homobaric (Tab. 3 and Tab. 6; page 37 and page 42). This can be explained by the fact that (effective) lateral diffusion areas within leaf blades defined by shape and size of intercellular air spaces may vary between individual leaves or experiments. Large veins completely prevent gas movement in lateral directions; minor veins may be more or less prominent and can obstruct gas diffusion to varying degrees. In leaves where veins of different orders are differently shaped as in *N. tabacum*, variability of the experimental results was particularly large because the mere position where the leaf chamber was clamped affected measurements of *NCERs* (Jahnke et al. 2002). In general, there must be a broad variability of interconnectivity inside intercellular gas spaces of leaves, which can be

modified by plant internal constraints (e.g. genetics or stage of development) as well as external ones (e.g. exposure to light or temperature).

4.2.2 Influence of lateral diffusion on gas exchange in light

Lateral gas fluxes inside leaves can influence gas exchange measurement whenever there is a CO_2 gradient. Such gradients arise when photosynthetic CO_2 response curves (A/c_i) are measured (Fig. 5 and Fig. 11; page 24 and page 43). Measuring A/c_i curves implies that $[\text{CO}_2]$ inside the chamber is varied between approximately 50 and 1000 $\mu\text{L L}^{-1}$ (cf. Long & Bernacchi 2003; see also Fig. 5; page 24) whereas ambient $[\text{CO}_2]$ is outside the chamber. The resulting lateral fluxes influence $NCER$ and, as a consequence, A/c_i curve analysis performed according to the biochemical model proposed by Farquhar et al. (1980) and subsequently modified von Caemmerer & Farquhar (1981) and Sharkey (1985). This mechanistic model is commonly used to interpret changes of CO_2 assimilation affected by various environmental conditions, e.g., plant nutrition (Pons & Westbeek 2004; Pooter & Evans 1998), temperature (Bernacchi et al. 2001; Sage 2002) but also to investigate the influence of rising atmospheric CO_2 on plants (Ainsworth & Long 2005; Long et al. 2004); it has also been incorporated as a submodel into various other models (Collatz et al. 1991; dePury & Farquhar 1997; Pearcy, Gross, & He 1997; Sellers et al. 1992).

One of the assumptions and uncertainties of the model described by Farquhar et al. (1980) is that small gradients in $[\text{CO}_2]$ may develop across the leaf (von Caemmerer 2000). These gradients, however, refer mainly to vertical heterogeneities in c_i across the leaf blade. However, lateral fluxes and lateral heterogeneities of c_i may even affect the apparent $NCER$ and the calculated c_i in homobaric leaves (Fig. 11; page 43). The parameters derived from the CO_2 response curves are also affected: maximum carboxylation velocity (V_{cmax}), maximum rate of electron transport rate (J_{max}), the CO_2 compensation point in the presence of respiration (I) and respiration in light (day respiration, R_D). Gradient in $[\text{CO}_2]$ from substomatal to carboxylation sites depend on mesophyll conductance which depends on temperature (Bernacchi et al. 2002) and is related to mesophyll surface of leaves (Evans et al. 1996). Mesophyll conductance (g_i) is composed of the conductance of the cell walls and membranes (g_{liq} , often described as liquid phase conductance) and conductance of the intercellular air space (g_{LAS}) (Evans et al. 1996). The magnitude of g_i will affect the estimates

of V_{max} and J_{max} made from CO_2 response curves (von Caemmerer 2000). Correct estimation of g_i is difficult to obtain (Epron et al. 1995; Lloyd et al. 1992; Loreto et al. 1992) and lateral diffusion inside leaves may even increase the uncertainty because lateral CO_2 fluxes influence intercellular $[\text{CO}_2]$ affecting g_{LAS} which is a component of g_i (Fig. 11; page 43 and Tab. 7 – 10; page 44 and following).

In the present work, V_{max} of *V. faba* was reduced by approximately 4% (Tab. 7; page 44) and J_{max} by 10% (Tab. 8; page 44) when there was a gradient between the atmospheric $[\text{CO}_2]$ outside the chamber ($c_{a,o}=350 \mu\text{L L}^{-1}$) and inside the chamber ($c_{a,i}$; ranging between 60 and $1200 \mu\text{L L}^{-1}$, cf. Fig. 5; page 24). This influence of lateral diffusion on V_{max} and J_{max} is in the order of magnitude to the response of photosynthesis to rising CO_2 (Ainsworth et al. 2005). However, many of the experiments about the influence of atmospheric CO_2 on plants were performed with heterobaric leaves of plants like *G. max* (Rogers et al. 2004) where an influence of leaf homobaricity can be excluded. However, in homobaric plants lateral gas fluxes can substantially alter the data obtained in A/c_i curves. Therefore, it is substantial to characterise leaves of plants used in different studies to avoid any artefacts due to lateral gas fluxes in homobaric leaves.

The compensation point in presence of respiration in the light depends on the slope of the CO_2 response curve and Γ is therefore likely to vary with factors such as leaf age, nutrition, temperature and irradiance (Brooks & Farquhar 1985) but also oxygen concentration and seasonal variations (Azcon-Bieto, Farquhar, & Caballero 1981). There is also a linear relation between R_D and Γ , which correlates with ontogenetic changes. However, precise estimation of Γ is very difficult because low NCERs are measured and in such a case (Fig. 5 and Fig. 11; page 24 and page 43), additional, lateral diffusion may result in substantial overestimation of the compensation points (Tab. 9; page 45).

Low CO_2 exchange rates are also measured when respiration processes both in darkness and light are studied. The leaf-level response of R_D is a vital component of a plant energy and carbon balance (Hoefnagel et al. 1998) being matter of controversial debate in numerous studies. Respiration in light was thought to be fully inhibited by light (Heber & Heldt 1981). Recent investigation showed that R_D was partly inhibited by light and was lower than dark respiration during the night (R_N) (Atkin, Evans, & Siebke 1998; Shapiro et al. 2004), whereas it was also concluded that reduction in R_D was unchanged and the apparent

reduction is caused by photosynthetic re-fixation of respiratory CO_2 (Loreto et al. 2001; Pinelli et al. 2003). There are two methods commonly used to estimate R_D , the Kok method (cf. Shapiro et al. 2004) and the Laisk method (cf. Brooks et al. 1985). Both methods refer to measurement of CO_2 exchange rates in light under low $[\text{CO}_2]$ inside the leaf chamber whereas outside the chamber normally prevails ambient $[\text{CO}_2]$. Thus, there is a gradient between $c_{a,o}$ and $c_{a,i}$ that may substantially influence the apparent $NCERs$ when 'clamp-on' leaf chambers are applied. Respiration rates both in light and darkness are prone to substantial errors that were observed when there was a gradient between $c_{a,o}$ and $c_{a,i}$ (Tab. 10; page 45). The magnitude of the effect was similar for R_D and R_N (Tab. 3, Tab 6, and Tab. 10; page 37, 42, and 45).

4.2.2.1 Lateral gradients within homobaric leaves caused by shading

Lateral gas fluxes are forced in homobaric leaves when artificial gradients in $[\text{CO}_2]$ inside and/or outside the leaf chamber are established, e.g., during measurement of CO_2 response curves. To obtain A/c_i curves (Fig. 11; page 43), $NCER$ was measured under $c_{a,i}=65 \mu\text{L L}^{-1}$ whereas outside the leaf chamber $c_{a,o}$ was switched between 65 and $350 \mu\text{L L}^{-1}$. Assuming a c_i/c_a quotient of 0.7 (Long et al. 2004), the gradient within a leaf, i.e., between $c_{i,i}$ and $c_{i,o}$ (cf. Fig. 36; page 82) was approximately $200 \mu\text{L L}^{-1}$ which substantially reduced the apparent $NCER$ (Tab. 12; page 48). When the gradient between $c_{i,i}$ and $c_{i,o}$ was maintained, shading of the leaf part outside the chamber additionally reduced the apparent $NCER$ (Tab. 11; page 47). In shaded leaf parts, respiratory processes prevail and intercellular $[\text{CO}_2]$ increases. This causes lateral gradients in $[\text{CO}_2]$ resulting in lateral CO_2 fluxes to the illuminated leaf areas inside the chamber. Such fluxes cause an increase of c_i in the illuminated leaf part that reduces the gradient between the leaf and the air inside the chamber; eventually this results in a decreased apparent $NCER$ (Fig. 12 a; page 46). In heterobaric leaves on the other hand, shading had no influence on the apparent $NCER$ (Fig. 12 b; page 46).

The use of 'clamp-on' leaf chambers provides shade to the measured leaves at least underneath the gaskets fixed on a leaf blade. Consequently, even if there is the same CO_2 partial pressure on both sides of the gasket, respiratory CO_2 released under gaskets has to escape laterally because the gaskets seal the stomata. This causes measurement artefacts that de-

pend on the size of a leaf chamber. The effect can only be avoided by enclosing a whole leaf into the chamber (cf. chapter 4.1.2).

4.3 Gas exchange measurement and overpressure

The influence of absolute air pressure on plant growth has been generally investigated with regard to growth under low atmospheric pressure at high altitudes in alpine ecosystems (Körner 1999). As total atmospheric pressure decreases with altitude, the partial pressures of CO_2 and O_2 are smaller, which reduces oxygenation relatively more than carboxylation efficiency of RubisCO (Körner et al. 1991; Terashima et al. 1995). Experiments with pressure chambers were also performed at NASA, Johnson Space Centre, in order to investigate the influence of hypobaric pressure and different air composition on plant growth in future life support systems such as lunar and marcian bases (Corey, Barta, & Henninger 1997; Corey, Barts, & Adams 1996; Daunicht & Brinkjans 1992; Daunicht & Brinkjans 1996). No literature was found which dealt with an influence of overpressure on terrestrial plants since plants rarely have to cope with overpressure. However, small overpressure inside leaf chambers has been commonly applied in gas exchange systems to avoid leakage in the leaf chamber, e.g., between the leaf surface and the gasket (cf. Küppers et al. 1999).

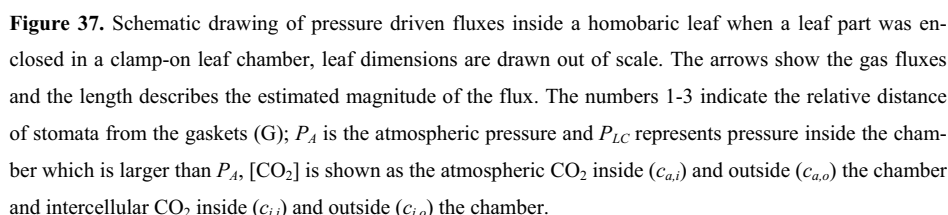
Diffusion of CO_2 from surrounding air into the intercellular air space is not influenced by air pressure (Gale 1972a; Terashima et al. 1995; see also chapter 2.3.1). It was observed that an overpressure of 3 kPa had no influence on dark respiration when lateral fluxes in homobaric leaves were avoided or when heterobaric leaves were measured (Fig. 14; page 50). No influence on dark respiration was also found when the air pressure was reduced to 70 kPa (Corey et al. 1997). Although diffusion processes in air are not affected by air pressure varying atmospheric pressure influences partial pressure of gases, which has an effect on gas exchange processes of leaves in light (Terashima et al. 1995). The concentration of a given gas species in the liquid phase is proportional to its partial pressure in the gas phase (Henry's law; Nobel 1991). When $[\text{CO}_2]$ is homogenous throughout the intercellular air space, an increase in air pressure increases the CO_2 partial pressure and thus the molar fraction in the liquid phase which results in increased CO_2 uptake (Terashima et al. 1995). This enhancement in CO_2 assimilation is in agreement with the photosynthesis model described by Farquhar et al. (1980). This was also experimentally found here since *NCER* in

light was dependent on the partial pressure of CO₂ but not on air pressure (Fig. 15; page 52).

4.3.1 CO₂ exchange under overpressure in homobaric leaves

A [CO₂] gradient caused lateral diffusion fluxes inside homobaric leaves, which significantly influenced apparent *NCER* in darkness (Fig. 13 a, b; page 49) but, an overpressure of 2 kPa in the leaf chamber completely eliminated the effect on *NCER* (Fig. 13 c; page 49). When part of a homobaric leaf is enclosed in a chamber, an applied overpressure creates a pressure gradient between the leaf chamber and the atmosphere causing a gas flow inside the leaf mesophyll. In darkness, an overpressure of 0.1 to 0.2 kPa was sufficient to produce a pressure driven flux that compensated lateral diffusion and *NCER* remained constant independently of further pressure increase (Fig. 14; page 50). When the light was switched on, increasing overpressure caused a small increase of *NCER* for heterobaric leaves of *G. max* (Fig. 16 a; page 53). Whereas a continuous decrease of assimilatory *NCER* was observed for homobaric leaves of *V. faba* (Fig. 16 b; page 53) which was dependent on stomatal conductance (Fig. 16 c and Fig. 17; page 53 and page 54).

Assuming constant stomatal conductance, a defined overpressure in the leaf chamber causes an air flux into the leaf interior through the stomata, which then follows the pressure gradient in lateral direction (cf. Fig. 37; page 89). The air flux through the stomata prevents diffusive gas exchange. The flux through stomata is larger in areas close to the gasket (1, Fig. 37; page 89) declining with distance from the gasket (arrows 2 or 3). That means, the pressure gradient reduces the effective leaf area enclosed in the leaf chamber where diffusion between $c_{i,i}$ and $c_{a,i}$ can take place. When the pressure gradient increases, then the fluxes in the regions 1-3 increase and additional stomata may be included in the pressure driven flux. It is obvious that stomatal closure reduces the pressure driven flux through the stomata and the effect of the gradient on apparent *NCER* then declines (cf. Fig. 17; page 54).



4.3.2 Impact of air pressure on transpiration

89

However, when a leaf part of a homobaric leaf was measured and ΔP was increased, a pressure gradient between the leaf chamber and the outer air was created which resulted in a lateral gas flux causing a decrease in transpiration, which was larger than calculated (Fig. 18 b; page 55). The reduced transpiration may be explained by a pressure driven gas flux through stomata into the leaf, which prevents any diffusion of water vapour near the gas-kets (cf. chapter 4.3.1, and Fig. 37; page 89). On the other hand, the air in the leaf chamber is not saturated with water and when this air entered the intercellular air space it absorbed water vapour, which reduced potential transpiration, especially in leaf part where pressure driven fluxes are low and potential transpiration may occur.

As discussed in the previous chapter, overpressure affected apparent *NCER* but also apparent transpiration rates. Transpiration is commonly used to calculate stomatal conductance which is needed to estimate the intercellular $[CO_2]$ and for measurement of CO_2 response curves (cf. von Caemmerer et al. 1981). Thus it is essential to control the air pressure inside the leaf chamber and to avoid any pressure gradients. Substantial measurement artefacts may appear otherwise, especially, when the leaf chamber is small and stomatal conductance is large.

4.4 Influence of leaf anatomy on gas exchange measurement - conclusion

The impact of leaf anatomy on gas exchange measurements occurred when only a part of a leaf was enclosed in the leaf chamber and a gradient between the leaf chamber and outer air existed. The gradient creates a diffusion or a pressure driven mass flux, respectively. There is a large variation in the interconnectivity of gas spaces within a leaf, which may alleviate or enhance gas fluxes providing different conductances. Finally, the ratio of the enclosed area to the circumference of this area also substantially affects the measurement error.

The resulting impact of these lateral fluxes on gas exchange measurement is presented in table 13 (page 92). For the estimation of the measurement artefacts, gradients were taken into consideration which may commonly occur in experiments, e.g., doubling of atmospheric CO_2 in experiments regarding the influence of rising atmospheric CO_2 on plants

(Ainsworth et al. 2005; Long et al. 2004; Norby et al. 2001). In general, diffusion affects CO_2 exchange rates in a very large way, when the exchange rates are low, e.g. when respiration in light or dark respiration is measured. In this study, dark respiration was measured when there was a CO_2 gradient of $1650 \mu\text{L L}^{-1}$ ($2000 - 350 \mu\text{L L}^{-1}$ between the chamber and external air) which is not common in many experiments. However, the impact of a reduced gradient ranging between $350\text{--}400 \mu\text{L L}^{-1}$ can be easily estimated because lateral flux inside leaves is proportional to the gradient. Thus, a decrease of the diffusion gradient by factor 4-5 would still substantially influence apparent respiration (cf. Tab. 3 and Tab. 6; page 37 and page 42).

CO_2 response curves are less influenced by diffusion artefacts because the obtained assimilation rates are larger than respiration rates and the relative impact of lateral diffusion declines. However, some parameters (respiration in light R_D , CO_2 compensation point) derived from the A/c_i curves are vulnerable to measurement artefacts. Additionally, measurement of CO_2 response curves under drought stress may be more prone to errors because of low CO_2 exchange rates.

Gas exchange measurement can also be influenced by different light intensity inside and outside the leaf chamber (cf. Fig. 12; page 46). Shading occurred also in the leaf area under the leaf chamber sealing and the respiratory CO_2 evolved in this area cannot escape through stomata because they are closed by the sealing artificially. Thus, there is a continuous lateral CO_2 flux from this area into the leaf chamber.

Measurement artefacts may also appear when there is overpressure in the leaf chamber, which is often used to avoid diffusion influence through leaks in the leaf chamber (cf. Küppers et al. 1999). However, one hardly finds any hints about the magnitude of the overpressure. The overpressure may vary due to different cross-sections of tubes with incoming and outgoing air. In heterobaric leaves changes in air pressure influenced the transpiration and assimilation rate were according to theoretical considerations. For homobaric leaves, however, changes in air pressure in the leaf chamber causes a pressure driven flux along the gradient. These fluxes may substantially affect both transpiration and assimilation measurement, especially when stomatal conductance is high.

Table 13. Estimated impact of the anatomy of heterobaric and homobaric leaves on gas exchange measurement caused by lateral diffusion and pressure driven fluxes.

	homobaric	heterobaric
Impact of lateral diffusion on gas exchange measurement		
dark respiration	very large	no
transpiration	no	no
CO ₂ response curves:		
V_{cmax}	low	no
J_{max}	medium	no
I^*	large	no
R_D	very large	no
Impact of overpressure on gas exchange measurement		
$NCER$ in darkness	no	no
$NCER$ in light	very large – low, depending on g_{leaf}	increase with rising CO ₂ partial pressure
transpiration	medium	low

4.5 Visualisation of lateral CO₂ diffusion

Gradients between CO₂ concentrations inside and outside a leaf chamber may substantially influence photosynthesis when different light intensities are provided to leaf areas inside or outside the cuvette. When a homobaric leaf of *V. faba* was shaded outside the cuvette, apparent $NCER$ was smaller than under illumination (Fig. 12 a; page 46). This response can be explained by higher intercellular CO₂ concentrations (c_i) outside the leaf chamber due to respiration causing a net lateral CO₂ flux directed to the illuminated leaf part clamped inside the chamber (cf. chapter 4.2.2.1). This reasoning was supported by chlorophyll fluorescence experiments performed with well-watered plants. When a leaf was partially shaded by a piece of black paper, no heterogeneity or gradient in chlorophyll fluorescence was observed in the illuminated leaf part. When stomata underneath the shading were not blocked, vertical CO₂ exchange through the stomata prevailed and obviously no lateral CO₂ gradient could evolve. However, when stomata in the shaded area were sealed by gas-tight adhesive tapes on the upper and lower surface of homobaric *V. faba* leaves (which simulates a leaf chamber gasket), an increase in quantum yield within the illuminated leaf area adjacent to the shade was observed (Fig. 19 a-d; page 57). This result can be interpreted by an increase in c_i within the shaded leaf area causing lateral CO₂ transport and, as a consequence, higher photosynthetic rates in the light along the light/shade borderline.

Gas exchange measurements, on the other hand, indicated lower apparent assimilation rates inside the leaf chamber when leaves were shaded outside (Fig. 12 a; page 46). The results obtained by gas exchange measurement and chlorophyll fluorescence imaging thus appear to be conflicting. However, lateral CO₂ fluxes across a LSB causing an increase in c_i in the illuminated areas explain these contradictory findings. On the one hand, additional CO₂ is available for photosynthesis, which is supported by the chlorophyll fluorescence data (Fig. 19 – 22; page 57 and following). On the other hand, an increase in c_i lowers the CO₂ gradient (and thus CO₂ diffusion) between ambient air and the leaf inside the leaf chamber resulting in a decrease in measured *NCER* (Fig. 12 a; page 46). This, however, would be an experimental artefact: gas exchange measurements only detect changes in external [CO₂] and cannot reflect true *NCER* when there is an internal lateral supply of CO₂ into a clamped leaf region.

4.5.1 Stomatal conductance and lateral flux of CO₂ inside leaves

Adjustment of stomatal conductance is the main mechanism by which plants control gas exchange and leaf temperature (Farquhar et al. 1982). Stomatal conductance decreases under mild or moderate drought stress that reduces c_i and affects photosynthesis (Lawlor 2002). Under pronounced drought stress, increased quantum yield along a light/shade border was observed in homobaric leaves (Fig. 19 – 23; page 57 and following) which is explained by an increase in c_i due to lateral CO₂ flux from shaded to illuminated leaf areas. Thus, respiratory CO₂ released in distant leaf parts can be re-fixed which increases photochemical efficiency and reduces *NPQ* (Fig. 21 and Fig. 24; page 61 and page 65). *NPQ* is thought to be essential in protecting leaves from light induced damage by processes in which light induced formation of the zeaxanthin is involved (Demmig-Adams et al. 1992; Horton et al. 1996). The decrease of *NPQ* in leaf areas close to the shade was even larger than the increase in ϕ_{PSII} (Fig. 21, page 61). Protection from overexcitation by lateral influx of CO₂ is potentially more beneficial than an increase in ϕ_{PSII} when leaves are under drought stress. The amount of re-fixed respiratory CO₂ depends on g_{leaf} which determines the supply of CO₂ from the air into the leaf. Thus, low g_{leaf} of plants under drought stress entails large lateral CO₂ supply whereas re-watering of the plants causing re-opening of stomata reduced the lateral CO₂ supply (Fig. 22; page 62). Consequently, the ratio between

the lateral and stomatal conductance determines the amount of re-fixation of respiratory CO₂ from distant leaf areas.

4.6 Lightflecks

Lateral gas diffusion can be visualised with chlorophyll fluorescence imaging techniques, which indicates that lateral diffusion inside homobaric leaves may have an ecophysiological impact on plants (cf. chapter 4.5). In order to elucidate this question a whole, attached leaf was enclosed in the leaf chamber and a leaf part was illuminated with lightflecks with different size in order to mimic natural conditions. Gas exchange and chlorophyll fluorescence was measured simultaneously. This method, however, comprises few disadvantages. Only the mean transpiration rate and consequently mean g_{leaf} of the whole leaf, the shaded and illuminated leaf area can be estimated. Without exact g_{leaf} , no intercellular CO₂ can be calculated.

The experiment was started with dark adapted leaves and after light was switched on photosynthetic induction started. The induction phases comprise a fast induction phase associated with RubP regeneration, which limits the rates of increase in assimilation during the first 1-2 minutes of illumination (Pearcy et al. 1994). Light activation of RubisCO is largely completed within 7-10 minutes but stomatal opening may cause a continuing, but generally small further increase in assimilation rate for up to 1 hour (Pearcy et al. 1994; Pearcy & Krall 1996; Valladares et al. 1997). For most plants, 90% of final steady state assimilation can be reached within 4 - 10 minutes (Pearcy et al. 1996; Valladares et al. 1997). In the present work, the fast induction state was complete within a few minutes and was followed by small rise of assimilation and quantum yield (Φ_{PSII}) (Fig. 24 c, g and Fig. 30 c, g; page 65 and page 72). Thus, photosynthetic induction reached rather high levels. As observed in figure 20 (page 59), the leaf area at top of the figure (ROI 0) was shaded during a long time. After illumination, Φ_{PSII} in ROI 0 reached within approximately 6 minutes similar values as the continuously illuminated leaf part, which indicates that high photosynthetic induction state was obtained within this time period. It was observed that the rise in stomatal conductance always lags behind the CO₂ assimilation (Valladares et al. 1997). The delayed response of stomata to illumination was mitigated by lateral supply of respiratory CO₂ from shaded areas. The small spot showed under all measured g_{leaf} higher

assimilation rates (Fig. 25; page 66) but also ϕ_{PSII} was higher in the small than in the large spot (Fig 24 and Fig 29; page 65 and page 70). Mesophyll compartmentation in heterobaric leaf of *G. max* prevented lateral CO₂ supply and assimilation rate, quantum yield was thus similar for the large and small spot (Fig. 30, Fig. 31 and Fig. 35; page 72 and following).

Heat dissipation as indicated by *NPQ* values reached very quickly steady state conditions (Fig. 24 f and Fig. 30 f; page 65 and page 72). Rapid engagement of thermal dissipation during lightflecks indicates that plants are able to engage photoprotective mechanisms quickly in response to sunflecks. De-epoxidation of pigments related to heat dissipation can occur rapidly enough on exposure to high light to provide protection during a sunfleck. The levels in de-epoxidised pigments (antheraxanthin and zeaxanthin) remain high and photoprotection against excess light will be regulated mainly via the magnitude of transthylacoid ΔpH (Horton et al. 1996), providing a mechanism which is very sensitive to changes in PFD (Watling et al. 1997). On returning to low light, high levels of antheraxanthin and zeaxanthin can be maintained up to 60 min (Watling et al. 1997). It was even reported that heat dissipation was maintained by selection because it provides a tolerance to rapidly fluctuating excitation pressure rather than protection against high light conditions (Külheim, Agren, & Jansson 2002).

4.6.1 Photosynthesis under drought stress

Photosynthesis is progressively diminished under drought and the basis for this reduction is under debate. Several processes were proposed to substantially affect photosynthesis under drought stress: (1) diffusion limitations due to stomatal closure and reduced CO₂ availability in the chloroplasts (Bota, Medrano, & Flexas 2004; Medrano et al. 2002); (2) decreased RubisCO activity (Parry et al. 2002; Tezara et al. 2002); (3) impaired capacity for RubP regeneration (Bota et al. 2004; Escalona, Flexas, & Medrano 1999; Kitao et al. 2003; Pankovic et al. 1999) which may decline because of decreased ATP synthesis through ATPase impairment (Tezara et al. 1999). Carboxylation efficiency, however, remains unaffected until drought stress is severe (Kitao et al. 2003; Parry et al. 2002; Wingler et al. 1999).

It has been found recently that stomatal conductance represents a more integrative basis for overall effects of drought than leaf water potential or relative water content and that photosynthetic responses can be understood as direct adjustment of photosynthetic metabolism to CO₂ availability (Bota et al. 2004; Flexas et al. 2002; Medrano et al. 2002). Several photosynthetic parameters were found to be significantly correlated to g_{leaf} with low variation among different species: net and gross assimilation, ϕ_{PSII} , F_v/F_m , R_D , R_N , NPQ and others. Moderate decrease of g_{leaf} under drought stress (from 400 – 150 $\mu\text{mol m}^{-2} \text{s}^{-1}$) was paralleled by a decline in assimilation mainly due to stomatal limitations and the electron requirement for CO₂ assimilation (e/A) increased indicating increased rates of photorespiration. Further decline in g_{leaf} (from 150 - 50 $\mu\text{mol m}^{-2} \text{s}^{-1}$) comprises stomatal and non-stomatal limitation with decrease of ETR and carboxylation efficiency. Severe g_{leaf} decline ($< 50 \mu\text{mol m}^{-2} \text{s}^{-1}$) led to non-stomatal limitations to photosynthesis, under this conditions F_v/F_m may decrease (Flexas, Escalona, & Medrano 1998; Flexas et al. 2002; Medrano et al. 2002).

In the present work, the plants or illuminated leaf parts were exposed to relatively low light (150 $\mu\text{mol m}^{-2} \text{s}^{-1}$) and c_a of 350 $\mu\text{L L}^{-1}$. Under low light, quenching of absorbed energy is thought to be mainly photochemical (Weis & Berry 1987). However, low c_i occurring under stomatal closure can cause light stress even under low light intensity (Long, Humphries, & Falkowski 1994; Ort et al. 2002). The g_{leaf} obtained in this work represents the mean conductance of the leaf rather than of the illuminated leaf area, which can differ substantially. Therefore, direct comparison of gas exchange and chlorophyll fluorescence data obtained here with literature data with regard to stomatal conductance is not viable. However, the photosynthetic response to drought stress observed in this study corresponded to the general observations reported in literature. Under drought stress, stomata close in proportion of the degree of stress progressively limiting CO₂ availability in chloroplasts (cf. Lal, Ku, & Edwards 1996; Medrano et al. 2002). A progressive linear decline of assimilation rates with decreasing g_{leaf} was observed in both species *V. faba* and *G. max* (Fig. 25 a, b and Fig. 31 a, b; page 66 and page 73). No changes in F_v/F_m were observed in any of the plants during the experiments, indicating that reduced rates of photosynthesis quantum yield (Fig. 29 and Fig. 35; page 70 and page 76) did not result in photoinhibition under the drought stress conditions imposed in the experiment. ETR depends on [CO₂] and the rate of CO₂ assimilation and probably g_{leaf} are driven by ETR (Weis et al. 1987). Decrease in ETR (see ϕ_{PSII} Fig. 29 a, b and Fig. 35 a, b; page 70 and

page 76) with declining g_{leaf} was smaller than the decline in gross assimilation (Fig. 25 a, b and Fig. 31 a-d; page 66 and page 73) which resulted in increase in e/A (Fig. 27 and Fig. 33; page 68 and page 74). The increase in e/A (often described as ETR/A^* ; A^* gross assimilation rate; Bota et al. 2004; Cornic et al. 2002; Flexas et al. 1998; Kitao et al. 2003; Medrano et al. 2002) has been recognized as an indicator for stomatal limitations paralleled by an increase of alternative pathway of electron flow as photorespiration, Mehler-peroxidase reaction. In *V. faba* and *G. max* (Fig. 27 and Fig. 33; page 68 and page 74) the increase of alternative electron flow pathways can be mainly attributed to photorespiration. Valentini et al. (1995) observed that 40 % of electrons were used for photorespiration increasing under midday depression up to 50-60 %. The contribution of Mehler-peroxidase reaction was estimated from the relation Φ_{PSII} vs. Φ_{CO_2} (quantum yield of CO_2 assimilation) under non-photorespiratory conditions (Fig. 28 and Fig 34; page 69 and page 75). In both plant species, *V. faba* and *G. max*, Mehler-ascorbate pathway was low for both plants indicated by the intercept of the y-axis of the relation between Φ_{PSII} vs. Φ_{CO_2} (Cornic et al. 2002); (Fig. 28 and Fig 34; page 69 and page 75). Mehler-peroxidase appears to be an effective alternate dissipation pathway against photodamage under prolong drought (Kitao et al. 2003). Whereas, rapid withholding of water did not lead to enhanced Mehler-peroxidase reaction (Cornic et al. 2002). For *V. faba*, however, the Φ_{PSII} vs. Φ_{CO_2} relation showed large variation especially for the small spot (Fig. 28; page 69). This may be explained by variable lateral CO_2 flux due to different leaf internal conductance. Veins may reduce lateral CO_2 supply more or less efficiently due to their size and position within the mesophyll tissue. The resulting variable influences Φ_{PSII} (Fig. 29; page 70) but also assimilation (cf. Fig. 25; page 66) which also influences the dependence of Φ_{PSII} on Φ_{CO_2} . Under non-photorespiratory conditions the effect is larger because photosynthetic processes depend more on changes in CO_2 than under photorespiration conditions where photorespiration may buffer the variable lateral CO_2 supply. Different positions of the light/shade borderline on the leaf define the lateral diffusion flux because of the location of veins with different extension influencing the gas conductance.

When stomatal conductance decreases considerably at an advanced stage of drought stress, down regulation of PSII activity was observed resulting in reduced electron transport rates and an increase in thermal energy dissipation (Flexas et al. 2002; Medrano et al. 2002; Omasa & Takayama 2003; Souza et al. 2004). This effect may be mediated by cycling electron transport (Cornic et al. 2002; Golding & Johnson 2003). Non-photochemical en-

ergy dissipation reduces the quantum yield to maintain a balance with electron requirement for carbon metabolism (Weis et al. 1987). NPQ increase under progressive drought stress was also observed in this work (Fig. 29 and Fig. 35; page 70 and page 76). Under non-photorespiratory conditions, a substantially higher NPQ was observed than under photorespiratory conditions which emphasises the role of photorespiration in consuming excess light energy in order to protect the photosynthetic apparatus from photoinhibitory damage (Cornic et al. 2002; Medrano et al. 2002; Ort 2001; Ort et al. 2002; Osmond et al. 1997).

4.6.2 Reduction of drought stress symptoms by lateral CO_2 diffusion

Low CO_2 availability due to stomatal closure is mainly responsible for reduced photosynthetic efficiency under drought stress (Bota et al. 2004; Flexas et al. 2002; Medrano et al. 2002). Lateral CO_2 diffusion, however, from shaded to illuminated leaf parts can increase the intercellular CO_2 concentration and reduce the impact of low c_i on photosynthesis under drought. It was shown that along the LSB quantum yield as well as heat dissipation was influenced by lateral diffusion (Fig. 19 – 22; page 57 and following) up to a distance of 3–4 mm from the shade under the provided conditions with PFD of $290 \mu\text{mol photons m}^{-2} \text{ s}^{-1}$ (Fig. 21; page 61). The illumination of a leaf with a large and small lightfleck caused a substantial increase of ϕ_{PSII} and a decrease of NPQ along LSB in homobaric leaves of *V. faba* (Fig. 24 a-f; page 65). Thus, the lateral CO_2 flux along the LSB influenced the mean photosynthetic efficiency of the illuminated leaf areas, which depends on the ratio between the illuminated area to the circumference of this area. The area of an illuminated spot determines the vertical CO_2 diffusion from the air into the leaf and the circumference of the spot accounts for the lateral diffusion area within the leaf blade. Because an circular area is proportional to the square of the radius and the circumference to the radius, a reduction of the spot size entails a larger increase of the lateral flux (dependent on the circumference) than the vertical flux (dependent on the area).

Additional re-fixation of laterally diffusing respiratory CO_2 from shaded areas caused an increase of water use efficiency with decreasing g_{leaf} in *V. faba* (Fig. 26; page 67). The quotient of water use efficiency of the large to small illuminated lightfleck (WUE_L/WUE_S) approximately renders the ratios of the areas of the large to small lightfleck of 5.25 under high g_{leaf} (Fig. 26; page 67). The calculation of WUE_L and WUE_S comprises the transpira-

tion of the whole leaf and the CO_2 uptake related to the whole leaf area. Thus, when the leaf was illuminated with the large lightfleck, the potential photosynthetic active area was 5.25 times larger than in case of illumination with the small fleck. This indicates that changes in WUE when the large and small spot were illuminated were mainly influenced by changes in CO_2 uptake whereas transpiration and g_{leaf} were less influenced by the shading. For this reason, WUE_L/WUE_S mirrors A_L/A_S (cf. Fig. 25 and Fig 26; page 66 and page 67).

Re-fixation of respiratory CO_2 supplied from distant leaf parts can be a useful tool to increase photosynthetic efficiency and attenuate effects of drought stress by reducing potential damage of photosynthetic apparatus arising from overexcitation. The extra CO_2 in the small spot resulted in a small decrease of ϕ_{PSII} with stomatal closure when compared to the large spot (Fig. 29; page 70). Thus, the absorbed light was used more efficiently in terms of carbon gain indicated by the e/A ratio, which was substantially lower for the small than for the large spot indicating reduced heat dissipation, by alternative electron pathways (Fig. 27; page 68). Thus, carbon gain was increased due to lateral CO_2 diffusion from shaded to illuminated leaf part, which increased the CO_2 availability for photosynthetic processes. Moreover, reduced alternative electron sinks (photorespiration) and light stress contributed to carbon gain additionally.

The illumination of the large spot and subsequent shading of the peripheral spot area was also performed to study whether post-illuminatory CO_2 evolution might have an impact on assimilation in the adjacent illuminated area. Shading of an illuminated leaf part causes in addition to mitochondrial respiration an increase in CO_2 which can be attributed to decarboxylation processes described as post-illumination burst (PIB). PIB is associated with photorespiration where photorespiratory glycolate and glycine are oxidised within 15-40 seconds after darkening (Bulley & Tregunna 1971; Doehlert, Ku, & Edwards 1979). On the other hand, light enhanced dark respiration (LEDR) arises after shading through an increased delivery of non-photorespiratory substrates (for example malate and/or pyruvate) that were formed during photosynthesis. LEDR can last some minutes after darkening (Azcon-Bieto & Osmond 1983; Xue et al. 1996). These two processes would increase intercellular CO_2 after shading and thus enhance lateral CO_2 diffusion and photosynthetic efficiency in illuminated leaf parts along the LSB. However, after shading no impact of a CO_2 burst on ϕ_{PSII} was detected. Even complete shading of the illuminated leaf area re-

vealed no increase in CO₂ release (cf. Fig. 24 g and Fig. 30 g; page 65 and page 72). Post illumination CO₂ fixation (cf. Pons et al. 1992) but also the volume of the leaf chamber (cf. Fig. 4; page 57), which diminishes the detection of dynamic changes in gas exchange rates, might have masked the CO₂ burst.

4.7 Impact of lateral diffusion on photosynthesis - conclusion

The influence of leaf anatomy on photosynthetic efficiency of partly shaded leaves is concluded in table 14 (page 100). Lateral diffusion of respiratory CO₂ from shaded to illuminated leaf parts increased intercellular CO₂ concentration in the illuminated leaf part along the light/shade borderline. This CO₂ rise resulted in higher quantum yield and reduced heat dissipation up to 3 - 4 mm from the shade when plants were under drought stress and stomatal conductance was low. The lateral CO₂ flux increased net CO₂ uptake of a leaf, which is relatively larger when a small leaf area is illuminated. Enhanced CO₂ uptake resulted in an increased water use efficiency since the impact of partial shading influenced transpiration rates slightly. Thus, carbon gain was increased because of increased CO₂ availability due to lateral CO₂ supply from shaded areas but also because of reduced heat dissipation and alternative electron sinks like photorespiration which was indicated by decrease in e/A ratio. The benefit of increased c_i is larger when the plant is under drought stress, g_{leaf} is low and the illuminated leaf area is small.

Table 14. Impact of leaf anatomy on photosynthetic performance of partially illuminated leaves.

	homobaric	heterobaric
Chlorophyll fluorescence along the light/shade borderline		
Φ_{PSII}	increase up to 3-4 mm	no
NPQ	increase up to 3-4 mm	no
Photosynthetic performance of leaf parts illuminated with lightflecks		
A	increase	no
WUE	increase	no
Φ_{PSII}	increase	no
e/A	decrease	no
NPQ	decrease	no

4.8 Ecology of plants with homobaric leaves

The results presented in this work allow a rough ecological classification of plants with homobaric leaves, which, however, has to be speculative at this stage of research and requires further studies. The screening results revealed that 21 plant of 33 investigated species had homobaric leaves (Tab. 3 and Tab. 6; page 37 and page 42). However, the plants were chosen arbitrarily from different locations so that a systematic characterisation is not possible. The applied method of gas exchange measurement with a laboratory system is not suitable to characterise an ecosystem with respect to leaf homobary. According to Ellenberg et al (1992) and Oberdorfer (1994) the plants species defined as homobaric showed no common preferences towards environmental growth conditions like light environment, temperature, soil moisture, soil pH and nutrient availability. Moreover, the plant species with homobaric leaves are from very different systematic groups (data not shown). Thus, no clues about the ecological niche can be concluded from the screening.

Lateral CO₂ diffusion and recycling of respiratory CO₂ increased carbon gain, water use efficiency and reduces light stress. Thus, plants with homobaric leaves may be less susceptible to drought. Plants which can withstand drought stress are more effective in conserving tissue hydration than drought susceptible plants (cf. Grzesiak, Grzesiak, & Hura 1999). They reduce water loss by effective stomatal closure but then have to cope with a diminished supply of CO₂. Under such conditions, homobaric leaf anatomy may be an adaptation for assimilation of respiratory CO₂ from remote leaf areas and re-fixation of respiratory CO₂ released from shaded leaf parts increases *WUE*. On the other hand, as can be deduced from the results presented here for heterobaric leaves, internal barriers to gas diffusion may hinder plants to potentially profit from remotely evolved CO₂. Plants with higher *WUE* generally grow in relatively dry habitats (Larcher 1995) and one may speculate whether homobaric leaf anatomy may prevail in plant species native to such areas. Under drought, leaves tend to be smaller and thicker because of lower evaporative demand (Pena-Rojas et al. 2005) with low frequency of bundle sheath extensions (Esau 1977). Thicker leaves tend to have lower tissue density and therefore higher intercellular air space (Mediavilla, Escudero, & Heilmeyer 2001; Pena-Rojas et al. 2005) and increasing internal air volume had a positive effect on *WUE* (Mediavilla et al. 2001). (Wylie 1952) presented a survey on 348 plant species with respect to the occurrence of bundle sheath extensions which are the main

barriers for lateral gas movement. Approximately 40% of the species he investigated had homobaric leaves and most of the species were from subtropical regions whereas plants with heterobaric leaves were mostly from northern (temperate) areas. In warmer habitats, plants often face low relative humidity as one of the key factors mediating changes in stomatal sensitivity to CO₂ (Talbot, Rahveh, & Zeiger 2003) and high vapour pressure deficit causing a decrease in stomatal conductance (Monteith 1995). Thus, low stomatal conductance may favour internal CO₂ re-fixation which may allow plants with homobaric leaves growth in regions with limited water availability. Whether plants providing homobaric leaf anatomies may benefit from utilizing CO₂ from remote parts under natural environments has yet to be evaluated.

References

- Ackerly D.D. (2003) Community assembly, niche conservatism, and adaptive evolution in changing environments. *International Journal of Plant Sciences* **164**, S165-S184.
- Ainsworth E.A. & Long S.P. (2005) What have we learned from 15 years of free-air CO₂ enrichment (FACE)? A meta-analytic review of the responses of photosynthesis, canopy properties and plant production to rising CO₂. *New Phytologist* **165**, 351-372.
- Allen M.T. & Pearcy R.W. (2000) Stomatal versus biochemical limitations to dynamic photosynthetic performance in four tropical rainforest shrub species. *Oecologia* **122**, 479-486.
- Amthor J.S. (1997) Plant respiratory responses to elevated carbon dioxide partial pressure. In: *Advances in Carbon Dioxide Effects Research* (eds L.H.Allen et al.), American Society of Agronomy, Crop Science of America, Soil Science of America, Madison, Wisconsin.
- Amthor J.S. (2000) Direct effect of elevated CO₂ on nocturnal *in situ* leaf respiration in nine temperate deciduous tree species is small. *Tree Physiology* **20**, 139-144.
- Amthor J.S., Koch G.W., Willms J.R. & Layzell D.B. (2001) Leaf O₂ uptake in the dark is independent of coincident CO₂ partial pressure. *Journal of Experimental Botany* **52**, 2235-2238.
- Atkin O.K., Evans J.R. & Siebke K. (1998) Relationship between the inhibition of the leaf respiration by light and enhancement of leaf dark respiration following light treatment. *Australian Journal of Plant Physiology* **25**, 437-443.
- Azcón-Bieto J., Farquhar G.D. & Caballero A. (1981) Effects of temperature, oxygen concentration, leaf age and seasonal variations on the CO₂ compensation point of *Lolium perenne* L. Comparison with a mathematical model including non-photorespiratory CO₂ production in the light. *Planta* **152**, 497-504.
- Azcón-Bieto J. & Osmond C.B. (1983) Relationship between photosynthesis and respiration. The effect of carbohydrate status on the rate of CO₂ production by respiring in darkened and illuminated wheat leaves. *Plant Physiology* **71**, 574-581.
- Beerling D.J. & Woodward F.I. (1995) Stomatal responses of variegated leaves to CO₂ enrichment. *Annals of Botany* **75**, 507-511.
- Bernacchi C.J., Portis A.R., Nakano H., von Caemmerer S. & Long S.P. (2002) Temperature response of mesophyll conductance. Implications for the determination of Rubisco enzyme kinetics and for limitations to photosynthesis in vivo. *Plant Physiology* **130**, 1992-1998.
- Bernacchi C.J., Singsaas E.L., Pimentel C., Portis A.R. & Long S.P. (2001) Improved temperature response functions for models of Rubisco-limited photosynthesis. *Plant, Cell and Environment* **24**, 253-259.
- Bolhár-Nordenkamp H.R. & Draxler G. (1993) Functional leaf anatomy. In: *Photosynthesis and Production in a Changing Environment* (eds D.O.Hall et al.), Chapman and Hall, London.
- Bota J., Medrano H. & Flexas J. (2004) Is photosynthesis limited by decreased Rubisco activity and RuBP content under progressive water stress? *New Phytologist* **162**, 671-681.
- Brinkjans H.J. (1992) Wirkungen des Luftdrucks auf Gaswechsel und Wachstum von Tomatenpflanzen (*Lycopersicon esculentum* Mill.), Thesis, Berlin.
- Brooks A. & Farquhar G.D. (1985) Effect of temperature on the CO₂/O₂ specificity of ribulose-1,5-bisphosphate carboxylase/oxygenase and the rate of respiration in the light. *Planta* **165**, 397-406.

- Bulley N.R. & Tregunna E.B. (1971) Photorespiration and the postillumination CO₂ burst. *Canadian Journal of Botany* **49**, 1277-1284.
- Collatz G.J., Ball J.T., Griver C. & Berry J.A. (1991) Physiological and environmental regulation of stomatal conductance, photosynthesis and transpiration - A model that includes a laminar boundary layer. *Agricultural and Forest Meteorology* **54**, 107-136.
- Corey K.A., Barta D.J. & Henninger D.L. (1997) Photosynthesis and respiration of a wheat stand at reduced atmospheric pressure and reduced oxygen. *Advanced Space Research* **20**, 1869-1877.
- Corey K.A., Barts M.B. & Adams S.L. (1996) Carbon dioxide exchange of lettuce plants under hydrobaric conditions. *Advanced Space Research* **18**, 265-272.
- Cornic G. & Fresneau C. (2002) Photosynthetic carbon reduction and carbon oxidation cycles are the main electron sinks for photosystem II activity during a mild drought. *Annals of Botany* **89**, 887-894.
- Cornic G. & Massacci A. (1996) Leaf photosynthesis under drought stress. In: *Photosynthesis and the Environment* (ed N.R.Baker), Kluwer Academic Publishers, Dordrecht.
- Cowan I.R. (1977) Stomatal behaviour and environment. *Advances in Botanical Research* **4**, 117-228.
- Crank J. (1975) *The mathematics of diffusion*, Clarendon Press, Oxford.
- Daunicht H.J. & Brinkjans H.J. (1992) Gas exchange and growth of plants under reduced air pressure. *Advanced Space Research* **12**, 107-114.
- Daunicht H.J. & Brinkjans H.J. (1996) Plant responses to reduced air pressure: advanced techniques and results. *Advanced Space Research* **18**, 273-281.
- Davey P.A., Hunt S., Hymus G.J., DeLucia E.H., Drake B.G., Karnosky D.F. & Long S.P. (2004) Respiratory oxygen uptake is not decreased by an instantaneous elevation of [CO₂], but is increased with long-term growth in the field at elevated [CO₂]. *Plant Physiology* **134**, 520-527.
- Demmig-Adams B. & Adams III W.W. (1992) Photoprotection and other responses of plants to high light stress. *Annual Review of Plant Physiology and Plant Molecular Biology* **43**, 599-626.
- dePury D.G.G. & Farquhar G.D. (1997) Simple scaling of photosynthesis from leaves to canopies without the errors of big-leaf models. *Plant, Cell and Environment* **20**, 537-557.
- Doehlert D.C., Ku M.S.B. & Edwards G.E. (1979) Dependence of the post-illumination burst of CO₂ on temperature, light, CO₂ and O₂ concentration in wheat (*Triticum aestivum*). *Physiologia Plantarum* **46**, 299-306.
- Drake B.G., Azcón-Bieto J., Berry J.A., Bunce J.A., Dijkstra P., Farrar J., Gifford R.M., Gonzalez-Meler M.A., Koch G.W., Lambers H., Siedow J.N. & Wulfschleger S.D. (1999) Does elevated atmospheric CO₂ concentration inhibit mitochondrial respiration in green plants? *Plant, Cell and Environment* **22**, 649-657.
- Epron D., Godard D., Cornic G. & Genty B. (1995) Limitation of net CO₂ assimilation rate by internal resistance to CO₂ transfer in the leaves of 2 tree species (*Fagus sylvatica* L. and *Castanea sativa* Mill). *Plant, Cell and Environment* **18**, 43-51.
- Esau K. (1969) *Pflanzenanatomie*. Gustav Fischer Verlag, Stuttgart, Germany.
- Esau K. (1977) *Anatomy of seed plants*. John Wiley & Sons, New York.
- Escalona J.M., Flexas J. & Medrano H. (1999) Stomatal and non-stomatal limitations of photosynthesis under water stress in field-grown grapevines. *Australian Journal of Plant Physiology* **26**, 421-433.

References

- Evans J.R. & von Caemmerer S. (1996) Carbon dioxide diffusion inside leaves. *Plant Physiology* **110**, 339-346.
- Fahn A. (1982) *Plant Anatomy*. Pergamon Press, Oxford, England.
- Farquhar G.D. & Sharkey T.D. (1982) Stomatal conductance and photosynthesis. *Annual Review of Plant Physiology* **33**, 317-345.
- Farquhar G.D., von Caemmerer S. & Berry J.A. (1980) A biochemical model of photosynthetic CO₂ assimilation in leaves of C₃ species. *Planta* **149**, 78-90.
- Farquhar G.D. & Raschke K. (1978) On the resistance to transpiration of the sites of evaporation within the leaf. *Plant Physiology* **61**, 1000-1005.
- Fay P.A. & Knapp A.K. (1993) Photosynthetic and stomatal responses of *Avena sativa* (Poaceae) to a variable light environment. *American Journal of Botany* **80**, 1369-1373.
- Flexas J., Escalona J.M. & Medrano H. (1998) Down-regulation of photosynthesis by drought under field conditions in grapevine leaves. *Australian Journal of Plant Physiology* **25**, 893-900.
- Flexas J. & Medrano H. (2002) Drought-inhibition of photosynthesis in C₃ plants: stomatal and non-stomatal limitations revisited. *Annals of Botany* **89**, 183-189.
- Gale J. (1972a) Availability of carbon dioxide for photosynthesis at high altitudes: theoretical considerations. *Ecology* **53**, 494-497.
- Gale J. (1972b) Elevation and transpiration: some theoretical considerations with special reference to Mediterranean-type climate. *Journal of Applied Ecology* **9**, 691-702.
- Genty B., Briantais J.M. & Baker N.R. (1989) The relationship between the quantum yield of photosynthetic electron transport and quenching of chlorophyll fluorescence. *Biochimica et Biophysica Acta* **990**, 87-92.
- Gettys, W.E. (1989) *Physics, Classical and Modern*. McGraw-Hill Companies, New York.
- Gifford R.M. (2003) Plants respiration in productivity models: conceptualisation, representation and issue for global terrestrial carbon-cycle research. *Functional Plant Biology* **30**, 171-186.
- Golding A.J. & Johnson G.N. (2003) Down-regulation of linear and activation of cyclic electron transport during drought. *Planta* **218**, 107-114.
- Gonzalez-Meler M.A. & Siedow J.N. (1999) Direct inhibition of mitochondrial respiratory enzymes by elevated CO₂: does it matter at the tissue or whole-plant level? *Tree Physiology* **19**, 253-259.
- Grzesiak S., Grzesiak M. & Hura T. (1999) Effects of soil drought during the vegetative phase of seedling growth on the uptake of ¹⁴CO₂ and the accumulation and translocation of ¹⁴C in cultivars of field bean (*Vicia faba* L. var. minor) and field pea (*Pisum sativum* L.) of different drought tolerance. *Journal of Agronomy and Crop Science* **183**, 183-192.
- Harley P.C., Loreto F., Di Marco G. & Sharkey T.D. (1992) Theoretical considerations when estimating the mesophyll conductance to CO₂ flux by analysis of the response of photosynthesis to CO₂. *Plant Physiology* **98**, 1429-1436.
- Harley P.C. & Sharkey T.D. (1991) An improved model of C₃ photosynthesis at high CO₂: reserved O₂ sensitivity explained by lack of glycerate re-entry into the chloroplast. *Photosynthesis Research* **27**, 169-178.
- Haupt-Herting S., Klug K. & Fock H.P. (2001) A new approach to measure gross CO₂ fluxes in leaves. Gross CO₂ assimilation, photorespiration, and mitochondrial respiration in the light in tomato under drought stress. *Plant Physiology* **126**, 388-396.

- Heber U. & Heldt H.W. (1981) The chloroplast envelope: structure, function, and role in leaf metabolism. *Annual Review of Plant Physiology* **32**, 139-168.
- Hoefnagel H.N., Atkin O.K. & Wiskich J.T. (1998) Interdependence between chloroplasts and mitochondria in the light and the dark. *Biochimica et Biophysica Acta* **1366**, 235-255.
- Horton P., Ruban A.V. & Walters R.G. (1996) Regulation of light harvesting in green plants. *Annual Review of Plant Physiology and Plant Molecular Biology* **47**, 655-684.
- Jahnke S. (2001) Atmospheric CO₂ concentration does not directly affect leaf respiration in bean or poplar. *Plant, Cell and Environment* **24**, 1139-1151.
- Jahnke S. & Krewitt M. (2002) Atmospheric CO₂ concentration may directly affect leaf respiration measurement in tobacco, but not respiration itself. *Plant, Cell and Environment* **25**, 641-651.
- Jahnke S. & Proff B. (2001) Gas exchange measurements on plants using LabVIEW. In: Virtuelle Instrumente in der Praxis: Begleitband Zum Kongress VIP 2001 (eds R.Jamal & H.Jaschinski), pp. 52-57. Hüthling-Verlag, Heidelberg, Germany.
- Jarvis P.G. & Slatyer R.O. (1970) The role of mesophyll cell wall in leaf transpiration. *Planta* **90**, 303-322.
- Jifon J.L. & Syvertsen J.P. (2003) Moderate shade can increase net gas exchange and reduce photoinhibition in citrus leaves. *Tree Physiology* **23**, 119-127.
- Johnson J.D., Tognetti R., Michelozzi M., Pinzauti S., Minotta G. & Borghetti M. (1997) Ecophysiological responses of *Fagus sylvatica* seedlings to changing light conditions. II. The interaction of light environment and soil fertility on seedling physiology. *Physiologia Plantarum* **101**, 124-134.
- Kitao M., Lei T.T., Koike T., Tobita H. & Maruyama Y. (2003) Higher electron transport rate observed at low intercellular CO₂ concentration in long-term drought-acclimated leaves of Japanese mountain birch (*Betula ermanii*). *Physiologia Plantarum* **118**, 406-413.
- Körner C. (1999) Alpine plant life: functional plant ecology of high mountain ecosystems. Springer Verlag, Berlin, Germany.
- Körner C., Farquhar G.D. & Wong C. (1991) Carbon isotope discrimination by plants follows latitudinal and altitudinal trends. *Oecologia* **88**, 30-40.
- Külheim C., Agren J. & Jansson S. (2002) Rapid regulation of light harvesting and plant fitness in the field. *Science* **297**, 91-93.
- Küppers M. & Häder D.-P. (1999) Methodik der Photosyntheseforschung - Messung und Interpretation des CO₂ Gasaustausches von intakten Blättern. In: Photosynthese (ed D.-P.Häder), Thieme Verlag, Stuttgart.
- Küppers M., Heiland I., Schneider H. & Neugebauer P.J. (1999) Light-flecks cause non-uniform stomatal opening - studies with special emphasis on *Fagus sylvatica* L. *Trees* **14**, 130-140.
- Küppers M., Timm H.C., Orth F., Stöber R., Schneider H., Paliwal K., Karunaichamy K.S.T. & Ortiz, R. (1996) Effect of light environment and successional status of lightfleck use by understory trees of temperate and tropical forests. *Tree Physiology* **16**, 69-80.
- Laisk A. & Loreto F. (1996) Determining photosynthetic parameters from leaf CO₂ exchange and chlorophyll fluorescence. *Plant Physiology* **110**, 903-912.
- Lal A., Ku M.S.B. & Edwards G.E. (1996) Analysis of inhibition of photosynthesis due to water stress in the C₃ species *Hordeum vulgare* and *Vicia faba*: Electron transport, CO₂ fixation and carboxylation capacity. *Photosynthesis Research* **49**, 57-69.
- Larcher W. (1995) Physiological Plant Ecology. Springer Verlag, Berlin, Germany.

References

- Lawlor D.W. (2002) Limitation to photosynthesis in water-stressed leaves: stomata vs. metabolism and the role of ATP. *Annals of Botany* **89**, 871-885.
- Leakey A.D.B. Press M.C., Scholes J.D. & Watling J.R. (2002) Relative enhancement of photosynthesis and growth at elevated CO₂ is greater under sunflecks than uniform irradiance in a tropical rain forest tree seedling. *Plant, Cell and Environment* **25**, 1701-1714.
- LI-COR (2005) LI-7000 CO₂/H₂O Analyser Instruction Manual. Lincoln, Nebraska, USA
ftp://ftp.licor.com/perm/env/LI-6400/Manual/Using_the_LI-6400-v5.3.pdf.
- Lloyd J., Syvertsen J.P., Kriedmann P.E. & Farquhar G.D. (1992) Low conductance for CO₂ diffusion from stomata to the sites of carboxylation in leaves of woody species. *Plant, Cell and Environment* **15**, 873-899.
- Long S.P., Ainsworth E.A., Rogers A. & Ort D.R. (2004) Rising atmospheric carbon dioxide: Plants FACE the future. *Annual Review of Plant Biology* **55**, 591-628.
- Long S. P. & Bernacchi, C. J. (2003) Gas exchange measurements, what can they tell us about the underlying limitations to photosynthesis? Procedures and sources of error. *Journal of Experimental Botany* **54**, 2393-2491.
- Long S.P., Humphries S.W. & Falkowski P.G. (1994) Photoinhibition of photosynthesis in nature. *Annual Review of Plant Physiology and Plant Molecular Biology* **45**, 633-662.
- Long S.P., Farage P.K., Bolhár-Nordenkamp H.R. & Rohrhofer U. (1989) Separating the contribution of the upper and the lower mesophyll to photosynthesis in *Zea mays* L. leaves. *Planta* **177**, 207-216.
- Loreto F., Delfine S. & Di Marco G. (1999) Estimation of photorespiratory carbon dioxide recycling during photosynthesis. *Australian Journal of Plant Physiology* **26**, 733-736.
- Loreto F., Harley P.C., Di Marco G. & Sharkey T.D. (1992) Estimation of mesophyll conductance to CO₂ flux by three different methods. *Plant Physiology* **98**, 1437-1443.
- Loreto F., Velikova V. & Di Marco G. (2001) Respiration in the light measured by ¹²CO₂ emission in ¹³CO₂ atmosphere in maize leaves. *Australian Journal of Plant Physiology* **28**, 1103-1108.
- Maxwell K. & Johnson G.N. (2000) Chlorophyll fluorescence - a practical guide. *Journal of Experimental Botany* **51**, 659-668.
- Mediavilla S., Escudero A. & Heilmeyer H. (2001) Internal leaf anatomy and photosynthetic resource-use efficiency: interspecific and intraspecific comparisons. *Tree Physiology* **21**, 251-259.
- Medrano H., Escalona J.M., Bota J., Gulias J. & Flexas J. (2002) Regulation of photosynthesis of C₃ plants in response to progressive drought: Stomatal conductance as a reference parameter. *Annals of Botany* **89**, 895-905.
- Meidner H. & Mansfield, T.A. (1968) Physiology of stomata. McGraw-Hill Book Company, New York, USA.
- Monteith J.L. (1995) A reinterpretation of stomatal responses to humidity. *Plant, Cell and Environment* **18**, 357-364.
- Mott K.A. & Parkhurst D.F. (1991) Stomatal response to humidity in air and helox. *Plant, Cell and Environment* **14**, 509-515.
- Mott K.A. & O'Leary J.W. (1984) Stomatal behaviour and CO₂ exchange characteristics in amphistomatous leaves. *Plant Physiology* **74**, 47-51.
- Napp-Zinn K. (1984) Anatomie des Blattes. Gebrüder Bornträger, Berlin.

- Neger F. (1912) Spaltöffnungsschluß und künstliche Turgorsteigerung. *Berichte der Deutschen Botanischen Gesellschaft* **30**, 179-194.
- Neger F. (1918) Wegsamkeit der Laubblätter für Gase. *Flora* **111**, 152-161.
- Nikolopoulos D., Liakopoulos G., Drossopoulos I. & Karabourniotis G. (2002) The relationship between anatomy and photosynthetic performance of heterobaric leaves. *Plant Physiology* **129**, 235-243.
- Niinemets U. (1998) Adjustment of foliage structure and function to a canopy light gradient in two co-existing deciduous trees. Variability in leaf inclination angles in relation to petiole morphology. *Trees* **12**, 446-451.
- Niklas K.J. (2000) The evolution of leaf form and function. In: Leaf Development and Canopy Growth (eds B.Marshall & J.A.Roberts), Sheffield Academic Press, Sheffield.
- Nobel P.S. (1991) Physiochemical and Environmental Plant Physiology. Academic press Inc. Hardcourt Brace Jovanovich, San Diego.
- Nobel P.S., Forseth I.N. & Long S.P. (1993) Canopy structure and light interception. In: Photosynthesis and Production in a Changing Environment (eds D.O.Hall et al.), Chapman and Hall, London.
- Norby R.J., Kobayashi K. & Kimball B.A. (2001) Rising CO₂ - future ecosystems. *New Phytologist* **150**, 215-221.
- Omasa K. & Takayama K. (2003) Simultaneous measurement of stomatal conductance, non-photochemical quenching, and photochemical yield of photosystem II in intact leaves by thermal and chlorophyll fluorescence imaging. *Plant, Cell and Environment* **44**, 1290-1300.
- Ort D.R. (2001) When there is too much light. *Plant Physiology* **125**, 29-32.
- Ort D.R. & Baker N.R. (2002) A photoprotective role for O₂ as an alternative electron sink in photosynthesis? *Current Opinion in Plant Biology* **5**, 193-198.
- Osmond C.B., Badger M.R., Maxwell K., Björkman O. & Leegood R.C. (1997) Too many photons: photo-respiration, photoinhibition and photooxidation. *Trends in Plant Science* **2**, 119-121.
- Panković D., Sakač Z., Kevrešan, S. & Plesničar M. (1999) Acclimation to long-term water deficit in the leaves of two sunflower hybrids: photosynthesis, electron transport and carbon metabolism. *Journal of Experimental Botany* **50**, 127-138.
- Parkhurst D.F. (1994) Transley review no. 65 diffusion of CO₂ and other gases inside leaves. *New Phytologist* **126**, 449-479.
- Parry M.A.J., Andralojic P.J., Khan S., Lea P.J. & Keys A.J. (2002) Rubisco activity: Effects of drought stress. *Annals of Botany* **89**, 833-839.
- Pearcy R.W., Chazdon R.L., Gross L.J. & Mott K.A. (1994) Photosynthetic utilisation of sunfleck: A temporarily patchy resource on a time scale of second to minutes. In: Exploitation of Environmental Heterogeneity by Plants (eds M.M.Caldwell & R.W.Pearcy), Academic Press, San Diego.
- Pearcy R.W., Gross L.J. & He D. (1997) An improved dynamic model of photosynthesis for estimation of carbon gain in sunfleck light regimes. *Plant, Cell and Environment* **20**, 411-424.
- Pearcy R.W. & Krall J.P. (1996) Photosynthesis in fluctuating light environment. In: Photosynthesis and the Environment (ed N.R.Baker), Kluwer Academic Press, Dordrecht.
- Pearcy W., Valladares F., Wright J. & de Paulis E.L. (2004) A functional analysis of the crown architecture of tropical forest *Psychotria* species: do species vary in light capture efficiency and consequently in carbon gain and growth? *Oecologia* **139**, 163-177.

References

- Peña-Rojas K., Aranda X., Joffre R. & Fleck I. (2005) Leaf morphology, photochemistry and water status in changes in resprouting *Quercus ilex* during drought. *Functional Plant Biology* **32**, 117-130.
- Penning De Vries F.W.T. (1975) The cost of maintenance processes in plant cells. *Annals of Botany* **39**, 77-92.
- Pfitsch W.A. & Pearcy R.W. (1989) Daily carbon gain by *Adenocaulon bicolor* (Asteraceae), a redwood understory forest herb, in relation to its light environment. *Oecologia* **80**, 465-470.
- Pieruschka R., Schurr U. & Jahnke S. (2005) Lateral gas diffusion inside leaves. *Journal of Experimental Botany* **56**, 857-864.
- Pinelli P. & Loreto F. (2003) ¹²CO₂ emission from different metabolic pathways measured in illuminated and darkened C₃ and C₄ leaves at low, atmospheric and elevated CO₂ concentration. *Journal of Experimental Botany* **54**, 1761-1769.
- Pons T.L. & Pearcy R.W. (1992) Photosynthesis in flashing light in soybean leaves grown in different conditions. II. Lightfleck utilization efficiency. *Plant, Cell and Environment* **15**, 577-584.
- Pons T.L. & Welschen R.A.M. (2002) Overestimation of respiration rates in commercially available clamp-on leaf chambers. Complications with measurements of net photosynthesis. *Plant, Cell and Environment* **25**, 1367-1372.
- Pons T.L. & Westbeek M.H.M. (2004) Analysis of differences in photosynthetic nitrogen-use efficiency between four contrasting species. *Physiologia Plantarum* **122**, 68-78.
- Pooter H. & Evans J.R. (1998) Photosynthetic nitrogen-use efficiency of species that differ inherently in specific leaf area. *Oecologia* **116**, 26-37.
- Proff, B. (2003) Automationssystem zur Untersuchung von Gaswechsel- und Transportprozessen an Pflanzen. Universität Duisburg-Essen, Thesis.
- Rogers A., Allen D.J., Davey P.A., Morgan P.B., Ainsworth E.A., Bernacchi C.J., Cornic G., Dermody O., Dohleman F.G., Heaton E.A., Mahoney J., Zhu X.G., DeLucia E.H., Ort D.R. & Long S.P. (2004) Leaf photosynthesis and carbohydrate dynamics of soybeans grown throughout their life-cycle under Free-Air Carbon dioxide Enrichment. *Plant, Cell and Environment* **27**, 449-458.
- Sage R.F. (2002) Variation in the k_{cat} of Rubisco in C₃ and C₄ plants and some implications for photosynthetic performance at high and low temperature. *Journal of Experimental Botany* **53**, 609-620.
- Sage R.F., Sharkey T.D. & Seemann J.R. (1990) Regulation of ribulase-1,5-bisphosphate carboxylase activity in response to light intensity and CO₂ in C₃ annuals *Chenopodium album* L. and *Phaseolus vulgaris* L. *Plant Physiology* **94**, 1735-1742.
- Schulte M., Offer C. & Hansen U. (2003) Induction of CO₂-gas exchange and electron transport: comparison of dynamic and steady-state responses in *Fagus sylvatica* leaves. *Trees* **17**, 153-163.
- Sellers P.J., Berry J.A., Collatz G.J., Field C.B. & Hall F.G. (1992) Canopy reflectance, photosynthesis, and transpiration. III. A reanalysis using improved leaf models and a new canopy integration scheme. *Remote Sensing of Environment* **42**, 187-216.
- Shapiro J.B., Griffin K.L., Lewis J.D. & Tissue D.T. (2004) Response of *Xanthium strumarium* leaf respiration in the light to elevated CO₂ concentration, nitrogen availability and temperature. *New Phytologist* **162**, 377-386.
- Sharkey T.D. (1985) Photosynthesis in intact leaves of C₃ plants: physics, physiology and rate limitations. *The Botanical Review* **51**, 53-105.

- Souza R.P., Machado E.C., Silva J.A.B., Lagôa A.M.M.A. & Silveira J.A.G. (2004) Photosynthetic gas exchange, chlorophyll fluorescence and some associated metabolic changes in cowpea (*Vigna unguiculata*) during water stress and recovery. *Environmental and Experimental Botany* **51**, 45-56.
- Talbott L.D., Rahveh E. & Zeiger E. (2003) Relative humidity is a key factor in the acclimation of the stomatal response to CO₂. *Journal of Experimental Botany* **54**, 2141-2147.
- Terashima I. (1992) Anatomy of non-uniform photosynthesis. *Photosynthesis Research* **31**, 195-212.
- Terashima I., Ishibashi M., Ono K. & Hikosaka K. (1996) Three resistances to CO₂ diffusion: leaf-surface water, intercellular space and mesophyll cells. In: *Photosynthesis: From Light to Biosphere: Proceedings of the Xth International Photosynthesis Congress*, Montpellier, France, 20-25 August 1995 (ed P.Mathis), pp. 537-542. Kluwer Academic Publishers.
- Terashima I., Masuzawa T., Ohba H. & Yokoi Y. (1995) Is photosynthesis suppressed at higher elevations due to low CO₂ pressure. *Ecology* **76**, 2663-2668.
- Terashima I., Wong S-C., Osmond C.B. & Farquhar G.D. (1988) Characterisation of non-uniform photosynthesis by abscisic acid in leaves having different mesophyll anatomies. *Plant and Cell Physiology* **29**, 385-394.
- Tezara W., Mitchell V., Driscoll S.P. & Lawlor D.W. (2002) Effects of water deficit and its interaction with CO₂ supply on the biochemistry and physiology of photosynthesis in sunflower. *Journal of Experimental Botany* **53**, 1781-1791.
- Tezara W., Mitchell V., Driscoll S.P. & Lawlor D.W. (1999) Water stress inhibits plant photosynthesis by decreasing coupling factor and ATP. *Nature* **401**, 914-917.
- Tognetti R., Johnson J.D. & Michelozzi M. (1997) Ecophysiological responses of *Fagus sylvatica* seedlings to changing light conditions. I. Interactions between photosynthetic acclimation and photoinhibition during simulated canopy gap formation. *Physiologia Plantarum* **101**, 115-123.
- Valentini R., Epron D., De Angelis P., Matteucci G. & Dryer E. (1995) In situ estimation of net CO₂ assimilation, photosynthetic electron flow and photorespiration in Turkey oak (*Quercus cerris* L.) leaves - diurnal cycle under different levels of water-supply. *Plant, Cell and Environment* **18**, 631-640.
- Valladares F., Allen M.T. & Pearcy R.W. (1997) Photosynthetic responses to dynamic light under field conditions in six tropical rainforest shrubs occurring along a light gradient. *Oecologia* **111**, 505-514.
- von Caemmerer S. (2000) *Biochemical Models of Photosynthesis*. Commonwealth Scientific and Industrial Research Organisation Publications, Victoria, Australia.
- von Caemmerer S. & Farquhar G.D. (1981) Some relation between the biochemistry of photosynthesis and the gas exchange of leaves. *Planta* **153**, 376-387.
- von Willert J., Matysek R., & Herppich W. (1995) *Experimentelle Pflanzenökologie*. Georg Thieme Verlag, Stuttgart.
- Walz H. (2003) IMAGING-PAM Chlorophyll Fluorometer. Instrument Description and Information for Users. Walz, H. <http://www.walz.com/support/downloads/downloads/pdfs/Ipam3e.pdf> (3. Edition).
- Watling J.R., Robinson S.A., Woodrow I.E. & Osmond C.B. (1997) Responses of rainforest understory plants to excess light during sunflecks. *Australian Journal of Plant Physiology* **24**, 17-25.
- Weis E. & Berry J.A. (1987) Quantum efficiency of Photosystem II in relation to 'energy'-dependent quenching of chlorophyll fluorescence. *Biochimica et Biophysica Acta* **894**, 198-208.
- Williams W.T. (1948) The continuity of intercellular spaces in the leaf of *Pelargonium zonale*, and its bearing in the recent stomatal investigation. *Annals of Botany* **12**, 411-420.

References

- Wingler A., Quick W.P., Bungard R.A., Bailey K.J., Lea P.J. & Leegood R.C. (1999) The role of photorespiration during drought stress: an analysis utilizing barley mutants with reduced activities of photorespiratory enzymes. *Plant, Cell and Environment* **22**, 361-373.
- Wulfschleger S.D. (1993) Biochemical limitations to carbon assimilation in C₃ plants - a retrospective analysis of the A/C_i curves from 109 species. *Journal of Experimental Botany*, **44**, 907-920.
- Wylie R.B. (1952) The bundle sheath extension in leaves of dicotyledons. *American Journal of Botany* **39**, 645-651.
- Xue X., Gauthier D.A., Turpin D.H. & Weger, H.G. (1996) Interactions between photosynthesis and respiration in the green alga *Chlamydomonas reinhardtii* (Characterization of light-enhanced dark respiration). *Plant Physiology* **112**, 1005-1014.

Abbreviations

A/c_i	CO ₂ assimilation as a function of leaf internal [CO ₂]
AE_{CO_2}	Apparent effect of CO ₂ on $NCER$, %
$AE_{\Delta c}$	Apparent effect of a CO ₂ gradient on $NCER$, %
$AE_{I'}$	Apparent effect of CO ₂ on I' , %
$AE_{J_{max}}$	Apparent effect of CO ₂ on J_{max} , %
AE_{RD}	Apparent effect of CO ₂ on R_D , %
AE_{shade}	Apparent effect of shade on assimilation, %
$AE_{V_{cmax}}$	Apparent effect of CO ₂ on V_{cmax} , %
$A_{leaf,s}$ and $A_{leaf,l}$	Net CO ₂ uptake of the whole leaf under illumination with a small and large spot, respectively, $\mu\text{mol m}^{-2} \text{s}^{-1}$
$AR_{ias,l}$	Area of intercellular air space open for lateral diffusion, m^2
A_S and A_L	Gross assimilation rates of the small and large illuminated spot, respectively, $\mu\text{mol m}^{-2} \text{s}^{-1}$
c_a	Atmospheric [CO ₂], $\mu\text{L L}^{-1}$
$c_{a,i}$	Atmospheric [CO ₂] inside the leaf chamber, $\mu\text{L L}^{-1}$
$c_{a,o}$	Atmospheric [CO ₂] outside the leaf chamber, $\mu\text{L L}^{-1}$
c_i	Intercellular [CO ₂], $\mu\text{L L}^{-1}$
$c_{i,i}$	Intercellular [CO ₂] inside the leaf chamber, $\mu\text{L L}^{-1}$
$c_{i,o}$	Intercellular [CO ₂] outside the leaf chamber, $\mu\text{L L}^{-1}$
D	Diffusion coefficient of CO ₂ in air, $\text{m}^2 \text{s}^{-1}$
DP	Dewpoint trap
ΔP	Air pressure difference between the leaf chamber and atmosphere, kPa
E	Transpiration rate, $\text{mmol m}^{-2} \text{s}^{-1}$
e/A	Electron requirement for assimilated CO ₂
E_{calc}	Calculated transpiration rate, $\text{mmol m}^{-2} \text{s}^{-1}$; $E_{calc} = g_{leaf} \bullet \frac{VPD_{LA}}{P_{LC}}$
ETR	Linear electron transport rate, $ETR = \phi_{PSII} \bullet PFD_a \bullet 0.5$
F_m'	Maximum fluorescence in the light
F_m	Maximal chlorophyll fluorescence
F_o	Minimum chlorophyll fluorescence
ϕ_{PSII}	Effective quantum yield of photosystem, $\phi_{PSII} = \frac{F_m' - F_o'}{F_o'}$
F_t	Steady state fluorescence prior to the saturating flash
F_v/F_m	Maximum quantum yield of dark adapted plants
G	Leaf chamber gaskets
g	Conductance, $\text{mmol m}^{-2} \text{s}^{-1}$
I'	CO ₂ compensation point, $\mu\text{L L}^{-1}$

g^*	Conductivity, $\text{mmol m}^{-1} \text{s}^{-1}$
I^*	CO_2 compensation point in absence of respiration, $\mu\text{L L}^{-1}$
$g_{\text{leaf},l}^*$	Leaf gas conductivity in lateral direction, $\text{mmol m}^{-1} \text{s}^{-1}$
$g_{\text{leaf},v}^*$	Leaf gas conductivity in vertical direction, $\text{mmol m}^{-1} \text{s}^{-1}$
GC	Growth cabinet
G_i	Inner leaf chamber gaskets
g_{leaf}	Leaf gas conductance, $\text{mmol m}^{-2} \text{s}^{-1}$
$g_{\text{leaf},l}$	Leaf gas conductance in lateral direction, $\text{mmol m}^{-2} \text{s}^{-1}$
$g_{\text{leaf},v}$	Leaf gas conductance in vertical direction, $\text{mmol m}^{-2} \text{s}^{-1}$
G_o	Outer leaf chamber gaskets
GP	Pump
H	Humidity sensor, rel. humidity, %
h_{leaf}	Thickness (height) of the leaf blade, m
HM	Humidifier
IRGA	Infrared gas analyser
J_{max}	Maximum rate of carboxylation limited by electron transport, $\mu\text{mol m}^{-2} \text{s}^{-1}$
K_c	Michaelis-Menten constant for carboxylation of RubisCO
K_o	Michaelis-Menten constant for oxygenation of RubisCO
LA_{leaf}	Leaf area, m
LA_S and LA_L	Illuminated leaf area of the small and large spot, respectively, m
LC	Double-gasket leaf chamber
LC_i	Inner leaf chamber of LC
LC_o	Outer leaf chamber of LC
LEDR	Light enhanced dark respiration
L_{gasket}	Circumference of the leaf chamber gasket, m
LLC	Large, single gasket leaf chamber
LSB	Light-shade borderline
MFC	Mass flow controller
MFM	Mass flow meter, $\text{cm}^3 \text{s}^{-1}$
MV	Solenoid valve
$NCER$	Net CO_2 exchange rate, $\mu\text{mol m}^{-2} \text{s}^{-1}$
NPQ	Non-photochemical quenching, $NPQ = \frac{F_m - F_m'}{F_m'}$
NV	Needle valve
P_{air}	Atmospheric air pressure, kPa
PD	Differential pressure transducer, kPa
PFD	Photon flux density, $\mu\text{mol m}^{-2} \text{s}^{-1}$
PIB	Post-illumination burst
P_{LC}	Air pressure in the leaf chamber, kPa
porosity	Fraction of the volume of intercellular air space

Abbreviations

<i>PR</i>	Fraction of photorespiration, %
<i>PSI</i>	Photosystem I
<i>PSII</i>	Photosystem II
<i>r</i>	Diffusion resistance, $\text{m}^2 \text{s mmol}^{-1}$
<i>R_D</i>	Respiration rate in the presence of light, $\mu\text{mol m}^{-2} \text{s}^{-1}$
<i>R_N</i>	Dark respiration, $\mu\text{mol m}^{-2} \text{s}^{-1}$
ROI	Region of interest
RubisCO	Ribulose-1,5-Bisphosphate Carboxylase/Oxygenase
RubP	Ribulose-1-5-bisphosphate
<i>SD</i>	Standard deviation
<i>SEM</i>	Standard error of the mean
T	Thermocouples
τ	Tortuosity, estimated correction for the diffusion pathways inside leaves
V	Valve
<i>V_{cm}</i>	Maximum rate of RubisCO mediated carboxylation, $\mu\text{mol m}^{-2} \text{s}^{-1}$
<i>VP_{air}</i>	Vapour pressure of the air, kPa
<i>VPD_{LA}</i>	Vapour pressure deficit between leaf and air, kPa
<i>VP_{leaf}</i>	Vapour pressure inside the leaf, kPa
<i>w_{gasket}</i>	Width of the leaf chamber gasket, m
<i>WUE_L</i> and <i>WUE_S</i>	Water use efficiency when the leaf is illuminated with the large and small spot respectively, $WUE=A/E$
<i>WVP</i>	Water vapour pressure, kPa
XLC	Large whole-leaf chamber

Appendix

Geometrical correction of conductance and conductivity

The circular leaf chamber (LLC) with the concentric-cylinder geometry of the gaskets should be considered when regarding diffusion fluxes (Crank, 1975).

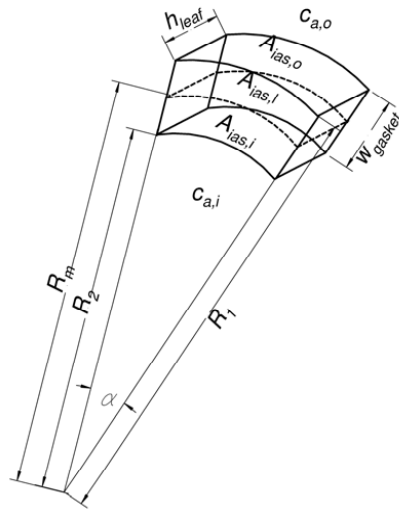


Figure 38. A section of a leaf with an angle α enclosed in a leaf chamber. R_1 , R_2 and R_m define the radii of the circular leaf chamber. The difference between the radii R_2 and $R_1 = w_{gasket}$ corresponds to the width of the leaf chamber sealing; $A_{ias,i}$, $A_{ias,l}$ and $A_{ias,o}$ are the potential leaf areas open for diffusion at R_1 , R_2 and R_m respectively; $c_{a,i}$ and $c_{a,o}$ describe the CO_2 concentration on both sides of the leaf chamber sealing; h_{leaf} depicts the leaf thickness.

Steady state diffusion across a hollow cylinder with an inner and outer radius R_1 and R_2 respectively is described by following equation (cf. Crank 1975):

$$\frac{d}{dR} \left(R \cdot \frac{dc}{dR} \right) = 0 \quad \text{Eqn. 11}$$

with $R_1 < R < R_2$. The general solution of this equation is $C = A + B \cdot \ln(R)$ where A and B are constants to be determined from the boundary conditions at $R=R_1$ and $R=R_2$. In this case $c_{a,o} = A + B \ln R_1$ and $c_{a,i} = A + B \ln R_2$ with B resulting in:

$$B = \frac{c_{a,i} - c_{a,o}}{\ln\left(\frac{R_2}{R_1}\right)} \quad \text{Eqn. 12}$$

According to the laws of mass maintenance the mass flow through the area $A_{ias,o}$ is identical with the flow through $A_{ias,i}$ (assuming only radial and not vertical gradients). Thus a constant χ can be defined:

$$A_{ias,i} \bullet J_{ias,i} = A_{ias,o} \bullet J_{ias,o} = A_{ias,l} \bullet J_{ias,l} = const = \chi \quad \text{Eqn. 13}$$

with $J_{ias,i}$ as the diffusion flux rate through the area $A_{ias,i}$, $J_{ias,o}$ as the diffusion flux rate through the area $A_{ias,o}$ and $J_{ias,l}$ as the diffusion flux rate through the area $A_{ias,l}$ respectively (cf. Fig. 4; page 18). The diffusion area can be described as $A_{ias} = \alpha \bullet R \bullet h_{leaf}$ and Fick's first law of diffusion is defined as $J = D \bullet \frac{dc}{dR}$. Thus, the term χ can be written as:

$$\chi = D \bullet \frac{dc}{dR} \bullet \alpha \bullet R \bullet h_{leaf} \quad \text{Eqn. 14}$$

From equations 11 and 12, $\frac{dc}{dR}$ can be defined as $\frac{dc}{dR} = \frac{B}{R}$ and combining this equation with equation 14 (page 118) D can be solved as:

$$D = \frac{\chi}{B \bullet \alpha \bullet h_{leaf}} \quad \text{Eqn. 15}$$

Combination of equation 12 and 15 results in:

$$D = \frac{\chi \bullet \ln\left(\frac{R_2}{R_1}\right)}{\alpha \bullet h_{leaf} \bullet (c_{a,i} - c_{a,o})} \quad \text{Eqn. 16}$$

In this case, the diffusion flux was measured regarding the mean circumference of the leaf chamber sealing i.e. $\frac{R_2 + R_1}{2} = R_m$. Thus, the term $\chi = A_{ias,l} \bullet J_{ias,l}$ and D can be defined as:

$$D = \frac{A_{ias,l}}{\alpha \cdot h_{leaf}} \cdot \ln\left(\frac{R_2}{R_1}\right) \cdot \frac{J_{ias,l}}{(c_{a,i} - c_{a,o})} = R_m \cdot \ln\left(\frac{R_2}{R_1}\right) \cdot \frac{J_{ias,l}}{(c_{a,i} - c_{a,o})} \quad \text{Eqn. 17}$$

Because conductance is defined as: $g = \frac{D}{\Delta R}$ (cf. Nobel 1991) conductance for a circular leaf chamber can be calculated according to the following equation:

$$g_{ias,l} = \frac{R_m}{\Delta R} \cdot \ln\left(\frac{R_2}{R_1}\right) \cdot \frac{J_{ias,l}}{(c_{a,i} - c_{a,o})} \quad \text{Eqn. 18}$$

The term $\frac{J_{ias,l}}{(c_{a,i} - c_{a,o})}$ is constant under steady state conditions and the correction for conductance is defined by:

$$\beta = \frac{R_m}{\Delta R} \cdot \ln\left(\frac{R_2}{R_1}\right) \quad \text{Eqn. 19}$$

When inserting the radii of the leaf chamber into equation 19 ($R_1=0.035\text{m}$, $R_2=0.043\text{m}$, $R_m=0.039\text{m}$) the numeric value for the geometrical correction can be calculated as 1.0035. Thus, the conductance for the circular leaf chamber should be corrected by 0.35%, which can be neglected. This uncertainty was so much below the variability of different measurements (cf. Tab. 3; page 37) that it was not regarded here. Calculation of $A_{ias,l}$ by using L_{gasket} as defined in equation 1 (page 20) is a simplification of the real situation.

1. **Energiemodelle in der Bundesrepublik Deutschland. Stand der Entwicklung**
IKARUS-Workshop vom 24. bis 25. Januar 1996
herausgegeben von S. Molt, U. Fahl (1997), 292 Seiten
ISBN: 3-89336-205-3
2. **Ausbau erneuerbarer Energiequellen in der Stromwirtschaft**
Ein Beitrag zum Klimaschutz
Workshop am 19. Februar 1997, veranstaltet von der Forschungszentrum Jülich GmbH und der Deutschen Physikalischen Gesellschaft
herausgegeben von J.-Fr. Hake, K. Schultze (1997), 138 Seiten
ISBN: 3-89336-206-1
3. **Modellinstrumente für CO₂-Minderungsstrategien**
IKARUS-Workshop vom 14. bis 15. April 1997
herausgegeben von J.-Fr. Hake, P. Markewitz (1997), 284 Seiten
ISBN: 3-89336-207-X
4. **IKARUS-Datenbank - Ein Informationssystem zur technischen, wirtschaftlichen und umweltrelevanten Bewertung von Energietechniken**
IKARUS. Instrumente für Klimagas-Reduktionsstrategien
Abschlußbericht Teilprojekt 2 „Datenbank“
H.-J. Laue, K.-H. Weber, J. W. Tepel (1997), 90 Seiten
ISBN: 3-89336-214-2
5. **Politiksznarien für den Klimaschutz**
Untersuchungen im Auftrag des Umweltbundesamtes
Band 1. Szenarien und Maßnahmen zur Minderung von CO₂-Emissionen in Deutschland bis zum Jahre 2005
herausgegeben von G. Stein, B. Strobel (1997), 410 Seiten
ISBN: 3-89336-215-0
6. **Politiksznarien für den Klimaschutz**
Untersuchungen im Auftrag des Umweltbundesamtes
Band 2. Emissionsminderungsmaßnahmen für Treibhausgase, ausgenommen energiebedingtes CO₂
herausgegeben von G. Stein, B. Strobel (1997), 110 Seiten
ISBN: 3-89336-216-9
7. **Modelle für die Analyse energiebedingter Klimagasreduktionsstrategien**
IKARUS. Instrumente für Klimagas-Reduktionsstrategien
Abschlußbericht Teilprojekt 1 „Modelle“
P. Markewitz, R. Heckler, Ch. Holzapfel, W. Kuckshinrichs, D. Martinsen, M. Walbeck, J.-Fr. Hake (1998), VI, 276 Seiten
ISBN: 3-89336-220-7

8. **Politiksszenarien für den Klimaschutz**
Untersuchungen im Auftrag des Umweltbundesamtes
Band 3. Methodik-Leitfaden für die Wirkungsabschätzung von Maßnahmen zur Emissionsminderung
herausgegeben von G. Stein, B. Strobel (1998), VIII, 95 Seiten
ISBN: 3-89336-222-3
9. **Horizonte 2000**
6. Wolfgang-Ostwald-Kolloquium der Kolloid-Gesellschaft
3. Nachwuchstage der Kolloid- und Grenzflächenforschung
Kurzfassungen der Vorträge und Poster
zusammengestellt von F.-H. Haegel, H. Lewandowski, B. KrahI-Urban (1998),
150 Seiten
ISBN: 3-89336-223-1
10. **Windenergieanlagen - Nutzung, Akzeptanz und Entsorgung**
von M. Kleemann, F. van Erp, R. Kehrbaum (1998), 59 Seiten
ISBN: 3-89336-224-X
11. **Policy Scenarios for Climate Protection**
Study on Behalf of the Federal Environmental Agency
Volume 4. Methodological Guideline for Assessing the Impact of Measures for Emission Mitigation
edited by G. Stein, B. Strobel (1998), 103 pages
ISBN: 3-89336-232-0
12. **Der Landschaftswasserhaushalt im Flußeinzugsgebiet der Elbe**
Verfahren, Datengrundlagen und Bilanzgrößen
Analyse von Wasserhaushalt, Verweilzeiten und Grundwassermilieu im
Flußeinzugsgebiet der Elbe (Deutscher Teil). Abschlußbericht Teil 1.
von R. Kunkel, F. Wendland (1998), 110 Seiten
ISBN: 3-89336-233-9
13. **Das Nitratabbauvermögen im Grundwasser des Elbeeinzugsgebietes**
Analyse von Wasserhaushalt, Verweilzeiten und Grundwassermilieu im
Flußeinzugsgebiet der Elbe (Deutscher Teil). Abschlußbericht Teil 2.
von F. Wendland, R. Kunkel (1999), 166 Seiten
ISBN: 3-89336-236-3
14. **Treibhausgasminderung in Deutschland zwischen nationalen Zielen und internationalen Verpflichtungen**
IKARUS-Workshop am 27.05.1998, Wissenschaftszentrum Bonn-Bad
Godesberg. Proceedings
herausgegeben von E. Läge, P. Schaumann, U. Fahl (1999), ii, VI, 146 Seiten
ISBN: 3-89336-237-1

15. **Satellitenbildauswertung mit künstlichen Neuronalen Netzen zur Umweltüberwachung**
Vergleichende Bewertung konventioneller und Neuronaler Netzwerkalgorithmen und Entwicklung eines integrierten Verfahrens
von D. Klaus, M. J. Canty, A. Poth, M. Voß, I. Niemeyer und G. Stein (1999), VI, 160 Seiten
ISBN: 3-89336-242-8
16. **Volatile Organic Compounds in the Troposphere**
Proceedings of the Workshop on Volatile Organic Compounds in the Troposphere held in Jülich (Germany) from 27 – 31 October 1997
edited by R. Koppmann, D. H. Ehhalt (1999), 208 pages
ISBN: 3-89336-243-6
17. **CO₂-Reduktion und Beschäftigungseffekte im Wohnungssektor durch das CO₂-Minderungsprogramm der KfW**
Eine modellgestützte Wirkungsanalyse
von M. Kleemann, W. Kuckshinrichs, R. Heckler (1999), 29 Seiten
ISBN: 3-89336-244-4
18. **Symposium über die Nutzung der erneuerbaren Energiequellen Sonne und Wind auf Fischereischiffen und in Aquakulturbetrieben**
Symposium und Podiumsdiskussion, Izmir, Türkei, 28.-30.05.1998.
Konferenzbericht
herausgegeben von A. Özdamar, H.-G. Groehn, K. Ülgen (1999), IX, 245 Seiten
ISBN: 3-89336-247-9
19. **Das Weg-, Zeitverhalten des grundwasserbürtigen Abflusses im Elbeeinzugsgebiet**
Analyse von Wasserhaushalt, Verweilzeiten und Grundwassermilieu im Flußeinzugsgebiet der Elbe (Deutscher Teil). Abschlußbericht Teil 3.
von R. Kunkel, F. Wendland (1999), 122 Seiten
ISBN: 3-89336-249-5
20. **Politiksznarien für den Klimaschutz**
Untersuchungen im Auftrag des Umweltbundesamtes
Band 5. Szenarien und Maßnahmen zur Minderung von CO₂-Emissionen in Deutschland bis 2020
herausgegeben von G. Stein, B. Strobel (1999), XII, 201 Seiten
ISBN: 3-89336-251-7
21. **Klimaschutz durch energetische Sanierung von Gebäuden. Band 1**
von J.-F. Hake, M. Kleemann, G. Kolb (1999), 216 Seiten
ISBN: 3-89336-252-2

22. **Electroanalysis**
Abstracts of the 8th International Conference held from 11 to 15 June 2000 at the University of Bonn, Germany
edited by H. Emons, P. Ostapczuk (2000), ca. 300 pages
ISBN: 3-89336-261-4
23. **Die Entwicklung des Wärmemarktes für den Gebäudesektor bis 2050**
von M. Kleemann, R. Heckler, G. Kolb, M. Hille (2000), II, 94 Seiten
ISBN: 3-89336-262-2
24. **Grundlegende Entwicklungstendenzen im weltweiten Stoffstrom des Primäraluminiums**
von H.-G. Schwarz (2000), XIV, 127 Seiten
ISBN: 3-89336-264-9
25. **Klimawirkungsforschung auf dem Prüfstand**
Beiträge zur Formulierung eines Förderprogramms des BMBF
Tagungsband des Workshop „Klimaforschung“, Jülich, vom 02. bis 03.12.1999
von J.-Fr. Hake, W. Fischer (2000), 150 Seiten
ISBN: 3-89336-270-3
26. **Energiezukunft 2030**
Schlüsseltechnologien und Techniklinien
Beiträge zum IKARUS-Workshop 2000 am 2./3. Mai 2000
herausgegeben von U. Wagner, G. Stein (2000), 201 Seiten
ISBN: 3-89336-271-1
27. **Der globale Wasserkreislauf und seine Beeinflussung durch den Menschen**
Möglichkeiten zur Fernerkundungs-Detektion und -Verifikation
von D. Klaus und G. Stein (2000), 183 Seiten
ISBN: 3-89336-274-6
28. **Satelliten und nukleare Kontrolle**
Änderungsdetektion und objektorientierte, wissensbasierte Klassifikation von Multispektralaufnahmen zur Unterstützung der nuklearen Verifikation
von I. Niemeyer (2001), XIV, 206 Seiten
ISBN: 3-89336-281-9
29. **Das hydrologische Modellsystem J2000**
Beschreibung und Anwendung in großen Flußgebieten
von P. Krause (2001), XIV, 247 Seiten
ISBN: 3-89336-283-5
30. **Aufwands- und ergebnisrelevante Probleme der Sachbilanzierung**
von G. Fleischer, J.-Fr. Hake (2002), IV, 64 Blatt
ISBN: 3-89336-293-2

31. **Nachhaltiges Management metallischer Stoffströme**
Indikatoren und deren Anwendung
Workshop, 27.-28.06.2001 im Congresscentrum Rolduc, Kerkrade (NL)
herausgegeben von W. Kuckshinrichs, K.-L. Hüttner (2001), 216 Seiten
ISBN: 3-89336-296-7
32. **Ansätze zur Kopplung von Energie- und Wirtschaftsmodellen zur Bewertung zukünftiger Strategien**
IKARUS-Workshop am 28. Februar 2002, BMWi, Bonn. Proceedings
herausgegeben von S. Briem, U. Fahl (2003), IV, 184 Seiten
ISBN: 3-89336-321-1
33. **TRACE. Tree Rings in Archaeology, Climatology and Ecology**
Volume 1: Proceedings of the Dendrosymposium 2002,
April 11th – 13th 2002, Bonn/Jülich, Germany
edited by G. Schleser, M. Winiger, A. Bräuning et al., (2003), 135 pages, many
partly coloured illustrations
ISBN: 3-89336-323-8
34. **Klimaschutz und Beschäftigung durch das KfW-Programm zur CO₂-Minderung und das KfW-CO₂-Gebäudesanierungsprogramm**
von M. Kleemann, R. Heckler, A. Kraft u. a., (2003), 53 Seiten
ISBN: 3-89336-326-2
35. **Klimaschutz und Klimapolitik: Herausforderungen und Chancen**
Beiträge aus der Forschung
herausgegeben von J.-Fr. Hake, K. L. Hüttner (2003), III, 231 Seiten
ISBN: 3-89336-327-0
36. **Umweltschutz und Arbeitsplätze, angestoßen durch die Tätigkeiten des Schornsteinfegerhandwerks**
Auswertung von Schornsteinfeger-Daten
von M. Kleemann, R. Heckler, B. Krüger (2003), VII, 66 Seiten
ISBN: 3-89336-328-9
37. **Die Grundwasserneubildung in Nordrhein-Westfalen**
von H. Bogen, R. Kunkel, T. Schöbel, H. P. Schrey, F. Wendland (2003), 148
Seiten
ISBN: 3-89336-329-7
38. **Dendro-Isotope und Jahrringbreiten als Klimaproxy der letzten 1200 Jahre im Karakorumgebirge/Pakistan**
von K. S. Treydte (2003), XII, 167 Seiten
ISBN: 3-89336-330-0
39. **Das IKARUS-Projekt: Energietechnische Perspektiven für Deutschland**
herausgegeben von P. Markewitz, G. Stein (2003), IV, 274 Seiten
ISBN: 3-89336-333-5

40. **Umweltverhalten von MTBE nach Grundwasserkontamination**
von V. Linnemann (2003), XIV, 179 Seiten
ISBN: 3-89336-339-4
41. **Climate Change Mitigation and Adaptation: Identifying Options for Developing Countries**
Proceedings of the Summer School on Climate Change, 7-17 September 2003, Bad Münstereifel, Germany
edited by K. L. Hüttner, J.-Fr. Hake, W. Fischer (2003), XVI, 341 pages
ISBN: 3-89336-341-6
42. **Mobilfunk und Gesundheit: Risikobewertung im wissenschaftlichen Dialog**
von P. M. Wiedemann, H. Schütz, A. T. Thalmann (2003), 111 Seiten
ISBN: 3-89336-343-2
43. **Chemical Ozone Loss in the Arctic Polar Stratosphere: An Analysis of Twelve Years of Satellite Observations**
by S. Tilmes (2004), V, 162 pages
ISBN: 3-89336-347-5
44. **TRACE. Tree Rings in Archaeology, Climatology and Ecology**
Volume 2: Proceedings of the Dendrosymposium 2003, May 1st – 3rd 2003, Utrecht, The Netherlands
edited by E. Jansma, A. Bräuning, H. Gärtner, G. Schleser (2004), 174 pages
ISBN: 3-89336-349-1
45. **Vergleichende Risikobewertung: Konzepte, Probleme und Anwendungsmöglichkeiten**
von H. Schütz, P. M. Wiedemann, W. Hennings et al. (2004), 231 Seiten
ISBN: 3-89336-350-5
46. **Grundlagen für eine nachhaltige Bewirtschaftung von Grundwasserressourcen in der Metropolregion Hamburg**
von B. Tetzlaff, R. Kunkel, R. Taug, F. Wendland (2004), 87 Seiten
ISBN: 3-89336-352-1
47. **Die natürliche, ubiquitär überprägte Grundwasserbeschaffenheit in Deutschland**
von R. Kunkel, H.-J. Voigt, F. Wendland, S. Hannappel (2004), 207 Seiten
ISBN: 3-89336-353-X
48. **Water and Sustainable Development**
edited by H. Bogen, J.-Fr. Hake, H. Vereecken (2004), 199 pages
ISBN: 3-89336-357-2
49. **Geo- and Biodynamic Evolution during Late Silurian / Early Devonian Time (Hazro Area, SE Turkey)**
by O. Kranendonck (2004), XV, 268 pages
ISBN: 3-89336-359-9

50. **Politiksszenarien für den Umweltschutz**
Untersuchungen im Auftrag des Umweltbundesamtes
Langfristszenarien und Handlungsempfehlungen ab 2012 (Politiksszenarien III)
herausgegeben von P. Markewitz u. H.-J. Ziesing (2004), XVIII, 502 Seiten
ISBN: 3-89336-370-X
51. **Die Sauerstoffisotopenverhältnisse des biogenen Opals lakustriner Sedimente als mögliches Paläothermometer**
von R. Moschen (2004), XV, 130 Seiten
ISBN: 3-89336-371-8
52. **MOSYRUR: Water balance analysis in the Rur basin**
von Heye Bogena, Michael Herbst, Jürgen-Friedrich Hake, Ralf Kunkel, Carsten Montzka, Thomas Pütz, Harry Vereecken, Frank Wendland (2005), 155 Seiten
ISBN: 3-89336-385-8
53. **TRACE. Tree Rings in Archaeology, Climatology and Ecology**
Volume 3: Proceedings of the Dendrosymposium 2004, April 22nd – 24th 2004, Birmensdorf, Switzerland
edited by Holger Gärtner, Jan Esper, Gerhard H. Schleser (2005), 176 pages
ISBN: 3-89336-386-6
54. **Risikobewertung Mobilfunk: Ergebnisse eines wissenschaftlichen Dialogs**
herausgegeben von P. M. Wiedemann, H. Schütz, A. Spangenberg (2005), ca. 380 Seiten
ISBN: 3-89336-399-8
55. **Comparison of Different Soil Water Extraction Systems for the Prognoses of Solute Transport at the Field Scale using Numerical Simulations, Field and Lysimeter Experiments**
by L. Weihermüller (2005), ca. 170 Seiten
ISBN: 3-89336-402-1
56. **Effect of internal leaf structures on gas exchange of leaves**
by R. Pieruschka (2005), 120 Seiten
ISBN: 3-89336-403-X

Forschungszentrum Jülich
in der Helmholtz-Gemeinschaft



Band/Volume 56
ISBN 3-89336-403-X

Umwelt
Environment